Camila de Carvalho Almança Lopes

Caracterização química e morfológica da cárie relacionada à radiação

Chemical and morphological characterization of radiation related caries

Tese apresentada à Faculdade de Odontologia da Universidade Federal de Uberlândia, como requisito parcial para obtenção do Título de Doutor em Odontologia na Área de Clínica Odontológica Integrada.

Uberlândia, 2019

Camila de Carvalho Almança Lopes

Caracterização química e morfológica da cárie relacionada à radiação

Chemical and morphological characterization of radiation related caries

Tese apresentada à Faculdade de Odontologia da Universidade Federal de Uberlândia, como requisito parcial para obtenção do Título de Doutor em Odontologia na Área de Clínica Odontológica Integrada.

Orientadora: Profa. Dra. Veridiana Resende Novais

Banca Examinadora:

Profª. Drª. Veridiana Resende Novais Simamoto – Faculdade de Odontologia –Universidade Federal de Uberlândia

Prof. Dra. Fabiana Sodré de Oliveira

Profa. Dra. Marina Guimarães Roscoe

Profa. Dra. Paula Dechichi

Profa. Dra. Ynara Bosco de Oliveira Lima Arsati

Uberlândia, 2019

UNIVERSIDADE FEDERAL DE UBERLÂNDIA
Coordenação do Programa de Pós-Graduação em Odontologia
Av. Pará, 1720, Bloco 4L, Anexo B, Sala 35 - Bairro Umuarama, Uberlândia-MG, CEP 38400-902
Telefone: (34) 3225-8115/8108 - www.ppgoufu.com - copod@umuarama.ufu.br

ATA

Ata da defesa de TESE DE DOUTORADO junto ao Programa de Pós-graduação em Odontologia da Faculdade de Odontologia da Universidade Federal de Uberlândia.

Defesa de: Tese de Doutorado COPOD

Data: 15/03/2019

Discente: **Camila de Carvalho Almança Lopes (11613ODO006)**

Título do Trabalho: Caracterização da cárie relacionada a radiação

Área de concentração: Clínica Odontológica Integrada.

Linha de pesquisa: **Propriedades físicas e biológicas dos materiais odontológicos e das estruturas dentais**

Projeto de Pesquisa de vinculação: Propriedades físicas e biológicas dos materiais odontológicos e das estruturas dentais

As **oito horas e trinta minutos** do dia **quinze de março de 2019** no Anfiteatro Bloco 4L Anexo A, sala 23 Campus Umuarama da Universidade Federal de Uberlândia, reuniu-se a Banca Examinadora, designada pelo Colegiado do Programa de Pós-graduação em fevereiro de 2019, assim composta: Professores Doutores: Fabiana Sodré de Oliveira (UFU); Paula Dechichi (UFU); Ynara Bosco de Oliveira Lima Arsati (UEFS); Marina Guimarães Roscoe (UNG);) orientador(a) do(a) candidato(a) Veridiana Resende Novais Simamoto**.**

Iniciando os trabalhos o(a) presidente da mesa Dra. Veridiana Resende Novais Simamoto apresentou a Comissão Examinadora e o candidato(a), agradeceu a presença do público, e concedeu ao Discente a palavra para a exposição do seu trabalho. A duração da apresentação do Discente e o tempo de argüição e resposta foram conforme as normas do Programa.

A seguir o senhor(a) presidente concedeu a palavra, pela ordem sucessivamente, aos (às) examinadore (as), que passaram a argüir o(a) candidato(a). Finalizada a argüição, que se desenvolveu dentro dos termos regimentais, a Banca, em sessão secreta, atribuiu os conceitos finais.

Em face do resultado obtido, a Banca Examinadora considerou o(a) candidato(a) (A)provado(a).

Esta defesa de Tese de Doutorado é parte dos requisitos necessários à obtenção do título de Doutor. O competente diploma será expedido após cumprimento dos demais requisitos, conforme as normas do Programa, a legislação pertinente e a regulamentação interna da UFU.

Nada mais havendo a tratar foram encerrados os trabalhos às 13 horas e 15 minutos. Foi lavrada a presente ata que após lida e achada conforme foi assinada eletronicamente pela Banca Examinadora.

Documento assinado eletronicamente por **Veridiana Resende Novais**, **Professor(a) do Magistério Superior**, em 18/03/2019, às 15:24, conforme horário oficial de Brasília, com fundamento no art. 6º, § 1º, do Decreto nº 8.539, de 8 de outubro de 2015.

Documento assinado eletronicamente por **Paula Dechichi Barbar**, **Professor(a) do Magistério Superior**, em 18/03/2019, às 15:42, conforme horário oficial de Brasília, com fundamento no art. 6º, § 1º, do Decreto nº 8.539, de 8 de outubro de 2015.

Documento assinado eletronicamente por **Fabiana Sodre de Oliveira**, **Professor(a) do Magistério Superior**, em 19/03/2019, às 09:03, conforme horário oficial de Brasília, com fundamento no art. 6º, § 1º, do Decreto nº 8.539, de 8 de outubro de 2015.

Documento assinado eletronicamente por **YNARA BOSCO DE OLIVEIRA LIMA ARSATI**, **Usuário Externo**, em 19/03/2019, às 10:13, conforme horário oficial de Brasília, com fundamento no art. 6º, § 1º, do Decreto nº 8.539, de 8 de outubro de 2015.

Documento assinado eletronicamente por **Marina Guimarães Roscoe**, **Usuário Externo**, em 19/03/2019, às 15:19, conforme horário oficial de Brasília, com fundamento no art. 6º, § 1º, do Decreto nº 8.539, de 8 de outubro de 2015.

A autenticidade deste documento pode ser conferida no site https://www.sei.ufu.br/sei/controlador_externo.php?acao=documento_conferir&id_orgao_acesso_externo=0, informando o código verificador **1094867** e o código CRC **34086D3A**.

Dados Internacionais de Catalogação na Publicação (CIP)
Sistema de Bibliotecas da UFU, MG, Brasil.

L864c
2019

Lopes, Camila de Carvalho Almanca, 1991-
Caracterização química e morfológica da cárie relacionada a radiação [recurso eletrônico] / Camila de Carvalho Almanca Lopes. - 2019.

Orientadora: Veridiana Resende Novais.
Tese (Doutorado) - Universidade Federal de Uberlândia, Programa de Pós-Graduação em Odontologia.
Modo de acesso: Internet.
Disponível em: http://dx.doi.org/10.14393/ufu.te.2019.1502
Inclui bibliografia.
Inclui ilustrações.

1. Odontologia. 2. Espectroscopia de infravermelho. 3. Desmineralização do dente. 4. Radioterapia. I. Novais, Veridiana Resende, 1979-. II. Universidade Federal de Uberlândia. Programa de Pós-Graduação em Odontologia. III. Título.

CDU: 619

Isabella de Brito Alves - CRB-6/3045

DEDICATÓRIA

A Deus, aos meus pais Mara e Ronan,

às minhas irmãs Isabela e Gabriela e

ao meu namorado Pedro Henrique.

.

AGRADECIMENTOS ESPECIAIS

*À **Professora Dra. Veridiana Resende Novais Simamoto,*** por ter acreditado em mim desde a graduação e aberto tantas portas. Muito obrigada pela paciência, cuidado, carinho e disposição com os quais você sempre conduz seus trabalhos. Obrigada por me fazer buscar o conhecimento e me motivar nesta carreira. Admiro muito a pessoa que você é, humana, carinhosa, excelente professora, dedicada à família e amiga. Acima de tudo obrigada pelo acolhimento em sua casa e por me permitir ser além de ser sua orientada, sua amiga! Sou eternamente grata a você por todo esse tempo de amizade e orientação.

AGRADECIMENTOS

A ***Deus***, pelo dom da vida, por me presentear com cada amanhecer. Obrigada por me dar sabedoria, paciência e força e por me guiar até aqui.

Aos ***meus pais, Ronan e Mara,*** agradeço pelo amor incondicional, por todos os ensinamentos, pelo seu caráter, sua verdade, respeito, companheirismo, compreensão, cumplicidade, força e por não me deixar esquecer que Deus tem um propósito para a nossa vida. Agradeço sobremaneira por acreditarem nos meus sonhos, me incentivarem e não medir esforços para realizá-los. Esta conquista também é de vocês! Serei eternamente grata por sempre fazerem questão de estarem perto, unidos, participando da minha vida e pelo esforço que fazem diariamente para proporcionar o melhor para as suas filhas. Vocês são o meu equilíbrio. Amo vocês!

Às ***minhas irmãs, Isabela e Gabriela,*** que mais do que irmãs, são minhas melhores amigas! Obrigada pelo companheirismo, cumplicidade e amizade em todos os momentos da minha vida. Obrigada pelo carinho, cuidado, apoio, paciência e compreensão. Dividir com vocês cada momento dessa trajetória tornou-a mais leve e prazerosa. Amo muito vocês!

Ao ***meu namorado, Pedro Henrique,*** pelo amor, companheirismo, incentivo, força, paciência e cuidado! Obrigada por me trazer paz... por torcer pelo meu sucesso. Você foi nesta fase um grande exemplo de força, perseverança e dedicação. Você é muito importante para mim! Te amo muito!

À ***toda minha família***, em especial a minhas ***avós Meire e Olivertina*** pelo amor, pelas orações e torcida constantes. Amo vocês!

À ***Natália Carvalho e Carine Schumacher*** pela amizade de tantos anos, por sempre me acompanharem mesmo que a distância e torcerem pelo meu crescimento. Obrigada pela partilha de tantos bons momentos vividos juntas, por serem tão especiais. Sinto-me privilegiada em tê-las como amigas. E obrigada por me darem dois grandes amigos, **Leopoldo e William**.

À ***Eliane, Pedro, João Pedro, Roseni, Eder e Lorraine*** pelo convívio, amizade, por me acolherem tão bem na família de vocês. Obrigada pelos momentos compartilhados, pelas conversas e por sempre se preocuparem comigo.

Aos meus queridos amigos ***Alessandra, Rodrigo, Mário, Renato, Diego, Bernardo*** por me acolherem, pelo companheirismo e por todos os bons momentos.

Aos amigos ***Renata Borges e Rafael Resende***, pela amizade e companheirismo. Obrigada por toda conversa, puxão de orelha, discussão e troca de experiências. Foi muito bom poder trabalhar com vocês! Obrigada por serem tão importantes nesta jornada! Obrigada pela torcida e auxílio. Podem contar comigo sempre!

Aos amigos do grupo de pesquisa ***Novais VR***, obrigada a cada um pela amizade e pela agradável convivência nos laboratórios, clínicas e aulas. Obrigada por toda troca de experiências, conhecimentos e ajuda. Obrigada a todos aqueles que tive a oportunidade de co-orientar (Carol, Marden, Renatinha, Allyne, Brenda), acho que mais aprendi com vocês, do que vocês comigo. Levarei boas recordações e muito aprendizado.

Aos ***amigos do mestrado,*** agradeço pela convivência, amizade, conhecimentos compartilhados e por tornar mais fácil e agradável essa etapa.

Aos ***amigos do doutorado***, que apesar de não nos encontrarmos tão frequentemente, sempre foi muito bom todas as conversas pelos corredores, no laboratório, pela companhia nas matérias compartilhadas. Desejo a cada um de vocês um caminho de muitas realizações e sucesso!

Ao ***Prof. Dr. Paulo Simamoto***, muito obrigada pela amizade, por todos os ensinamentos e por sempre me acolher tão bem na sua casa. E por sempre abrir portas para mim.

Ao ***Prof. Dr. Carlos José Soares***, pelo carinho e cuidado com que você sempre conduziu o programa de pós-graduação. Você além de exemplo, é um grande motivador de todos os seus alunos! Muitas vezes fui inspirada por suas aulas e conselhos.

À ***Profª. Dra. Paula Dechichi,*** pela paciência, aprendizado e cuidado durante a condução da revisão de literatura sobre o FTIR. Obrigada por ser tão solicita sempre que precisei de sua ajuda!

A ***amiga e Prof. Dra. Morgana*** pela amizade, por todo o aprendizado, pelo seu jeito de conduzir sua extensão e por me fazer apaixonar ainda mais por prótese total. Obrigada por ser tão cuidadosa e carinhosa com todos que a cercam.

Ao ***Prof. Dr. Maximiliano Sergio Cenci***, pela disponibilidade, por me receber tão bem em Pelotas e pela realização de parte experimental da minha tese Faculdade de Odontologia de Pelotas - Universidade Federal de Pelotas.

A querida ***Juliana L. Stolfo Uehara*** que me recebeu tão bem em Pelotas, que me fez sentir em casa desde o primeiro dia que cheguei. Que não me deixou desanimar em meio a tantas coisas dando errado. Sorrimos e choramos, foi tudo muito intenso. Apesar de toda a distância e a correria de nossas vidas, sempre vou levar você no coração com todo o carinho do mundo. O que você fez por mim, pouquíssimas pessoas o fariam de tal forma. Te desejo muito sucesso!

A ***Tamires Maske***, que mesmo na reta final de sua tese, auxiliou no uso do da MOCS e por atender as ligações e responder as mensagens de duas meninas desesperadas.

Ao ***Setor de Radioterapia do Hospital de Clínicas da Universidade Federal do Triângulo Mineiro,*** pela parceria.

Às ***Professoras da banca***, Prof. Dra. Fabiana Sodré de Oliveira, Profa. Dra. Marina Guimarães Roscoe e Profa. Dra. Ynara Bosco de Oliveira Lima Arsati obrigada por terem aceito o convite, contribuírem com o trabalho e participarem desse momento.

Aos professores da banca de qualificação, ***Prof. Dr. Lucas Zago Naves, Prof. Dr. João Paulo Silva Servato*** muito obrigada pelas considerações e contribuições que fizeram para o meu trabalho.

Aos ***amigos Cid, Maria Paula, Poliana e Tamis***, muito obrigada pela amizade e por todos os momentos alegres vividos juntos!

Ao ***pessoal do Programa de Cuidados Específicos à Doenças Estomatológicas (PROCEDE)***, Maria Auxiliadora, Célia Márcia, Keller Carvalho, Dhiancarlo Macedo,

Cizelene Faleiros e Dalva, obrigado por todo o apoio e suporte durante esse tempo que estive com vocês, foi uma experiência muito boa e somou muito à minha formação pessoal e profissional.

Aos **técnicos do Centro de Pesquisa de Biomecânica, Biomateriais e Biologia Celular (CPBio)*, Jonh Douglas, Bruno e Eliete***, obrigada por cada bom-dia ao chegar no laboratório, pela amizade e ajuda!

À ***Mariani,*** técnica do laboratório de Histologia do Instituto de Ciências Biomédicas da Universidade Federal de Uberlândia, pela amizade e por todo esforço em fazer com que a microscopia desse certo e toda a paciência durante as nossas tentativas!

Aos **professores da Faculdade de Odontologia da Universidade Federal de Uberlândia (FOUFU)** pela dedicação, amizade e ensinamentos transmitidos a mim na graduação e pós-graduação. Vocês são espelhos para mim!

Aos ***funcionários da FOUFU,*** em especial à Camila, Daniele, Graça, Brenda e Advaldo. Muito obrigada pela amizade e ajuda sempre que precisei.

Às amigas da especialização, ***Emmelyne, Rafaela, Bruna, Mábia, Renata,*** pelos bons momentos vividos juntos e pela amizade de todas. Por se fazerem sempre presentes mesmo com toda essa distância. Tenho certeza que nossa amizade será para sempre!!! Muito obrigada por tudo!!

À ***Universidade Federal de Uberlândia*** e ***Faculdade de Odontologia – FOUFU***, obrigada pela oportunidade de cursar minha graduação, mestrado e doutorado. Por mais que o mundo de voltas, sempre lembrarei de mencionar de onde vim, e o farei com muito orgulho.

Ao ***Centro de Pesquisas Odontológico Biomecânica, Biomateriais e Biologia Celular*** (CPBiO).

À ***Coordenação de Aperfeiçoamento de Pessoal de Nível Superior*** (CAPES), pelo apoio financeiro por meio da bolsa de Doutorado.

À ***Fundação de Amparo à Pesquisa do estado de Minas Gerais*** (FAPEMIG), pelo apoio financeiro.

Ao ***Conselho Nacional de Desenvolvimento Científico e Tecnológico*** (CNPq), pelo apoio financeiro.

A todos que torceram por mim e que de alguma forma contribuíram para a realização deste trabalho!!!

“Lembre-se de olhar para as estrelas e não para baixo, para os seus pés. Tente achar sentido no que você vê e pergunte sobre o que faz o Universo existir. Seja curioso. E por mais difícil que a vida possa parecer, há sempre algo que você pode fazer e ter sucesso. É importante que você não desista! ”

Stephen Hawking

SUMÁRIO

RESUMO

Entre os efeitos adversos da radioterapia no tratamento de neoplasias malignas na região de cabeça e pescoço, a cárie relacionada à radiação é considerada uma das mais preocupantes, pois configura uma forma de cárie com grande potencial destrutivo e de rápida progressão, podendo levar à amputação total da coroa e completa perda da dentição, interferindo na qualidade de vida desses pacientes. Possui como etiologia a combinação de efeitos indiretos da radioterapia (hipossalivação, alterações na composição e no pH da saliva, mucosites, mudanças na dieta e nos hábitos de higiene oral), somados aos efeitos diretos na estrutura dentária. Sabendo disso, trabalhos devem ser realizados com o intuito de entender melhor essa alteração, prevenir e tratá-la. Este trabalho envolveu 3 objetivos. **Objetivo 1:** avaliar a literatura buscando condensar informações sobre o emprego do FTIR na caracterização química do esmalte, dentina e osso. Identificando assim, picos do espectro e suas atribuições relacionados ao diagnóstico das alterações e patologias dos tecidos mineralizados. **Objetivo 2:** investigar o efeito da radiação ionizante e do fluxo salivar na susceptibilidade da dentina a cárie por meio de um modelo de biofilme microcosmo. **Objetivo 3:** comparar uma dentina sadia a uma dentina cariada de pacientes pré-radioterapia e de pacientes submetidos a radioterapia de cabeça e pescoço. Por meio da revisão de literatura, realizada no objetivo 1, pode-se concluir que a espectroscopia de infravermelho por transformada de Fourier (FTIR) pode fornecer informações fundamentais sobre a estrutura molecular de componentes orgânicos e inorgânicos do esmalte, dentina e osso. Além de ser uma das técnicas analíticas mais versáteis para a caracterização química não destrutiva de amostras, é capaz de detectar alterações e patologias dos tecidos mineralizados, como por exemplo a cárie dentária. O objetivo 2 mostrou que o modelo de biofilme microcosmo promoveu uma desmineralização, expôs e alterou a matriz orgânica da dentina. Com o fluxo salivar reduzido, as alterações minerais foram mais detectáveis. A radiação ionizante também promoveu alterações na matriz inorgânica e orgânica e na densidade mineral da dentina. E por último, com o objetivo 3, verificou-se que a cárie e a radiação ionizante levaram à desmineralização da hidroxiapatita e à degradação proteica. No entanto, cáries relacionadas à radiação exibiram mudanças mais pronunciadas, com um padrão de desmineralização difuso.

Palavras chave: Espectroscopia, Desmineralização dental, Radioterapia.

ABSTRACT

Among the adverse effects of radiotherapy in the treatment of malignant neoplasms in the head and neck region, radiation-related caries is considered one of the most worrying, since it constitutes a form of caries with great destructive potential and rapid progression, which can lead to total amputation of the crown and complete loss of the dentition, interfering in the quality of life of these patients. It has as its etiology the combination of indirect effects of radiotherapy (hyposalivation, changes in the composition and pH of saliva, mucositis, changes in diet and oral hygiene habits), together with the direct effects on dental structure. Knowing this, studies should be done in order to better understand this change, prevent and treat it. This work involved 3 objectives. **Objective 1:** to evaluate the literature seeking to condense information on the use of FTIR in the chemical characterization of enamel, dentin and bone. Identifying in this way, spectrum peaks and their attributions related to the diagnosis of alterations and pathologies of mineralized tissues. **Objective 2:** to investigate the effect of ionizing radiation and salivary flow rateon dentin susceptibility to caries by means of a microcosm biofilm model. **Objective 3:** to compare a sound dentin to a carious affected dentin of pre-radiotherapy patients and patients submitted to head and neck radiotherapy. Through the literature review, carried out in objective 1, it can be concluded that Fourier transform infrared spectroscopy (FTIR) can provide fundamental information on the molecular structure of organic and inorganic of dental enamel, dentin and bone. It is one of the most versatile analytical techniques for the non-destructive, chemical characterization of samples. Moreover, it is able to detect alterations and pathologies of mineralized tissues, such as dental caries. Objective 2 showed that the microcosm biofilm model promoted demineralization, exposed and altered the organic matrix of dentin. With reduced salivary flow, the mineral alterations were more detectable. Ionizing radiation also promoted changes in the inorganic and organic matrix and the mineral density of dentin. Finally, in the objective 3, dental caries and ionizing radiation led to a hydroxyapatite demineralization and protein degradation. However, caries related to radiation exhibited more pronounced changes, with a diffuse demineralization pattern.

Keywords: Spectrum Analysis, Tooth Demineralization, Radiotherapy.

INTRODUÇÃO E REFERENCIAL TEÓRICO

1 - INTRODUÇÃO E REFERENCIAL TEÓRICO

De acordo com o Instituto Nacional do Câncer, neoplasias malignas é um termo dado a um conjunto de mais de cem doenças que têm em comum o crescimento desordenado de células, que invadem tecidos e órgãos, com possibilidade de ocasionar metástase para outras regiões do corpo (Instituto Nacional do Câncer José Alencar Gomes da Silva - INCA) e são popularmente conhecidas como câncer. O câncer de cabeça e pescoço constitui um grupo heterogêneo de neoplasias malignas, constituído por vários sítios anatômicos. O câncer da cavidade oral é um deles, afetando lábios, estruturas da boca, como gengivas, bochechas, céu da boca, língua e a região embaixo da língua, segundo o INCA (INCA, 2018). O câncer de cabeça e pescoço tem sido reconhecido como um dos cânceres com mais alta taxa de prevalência (Jemal et al., 2008), responsável por uma incidência de 900.000 casos novos por ano no mundo (Silveira et al., 2012), sendo a sexta causa de morte por câncer em todo o mundo (Warnakulasuriya, 2009). Estima-se, para o Brasil, biênio 2018-2019, a ocorrência de 600 mil casos novos de câncer, para cada ano. 1,2 milhão de novos casos de câncer devem surgir no Brasil até 2019 (INCA, 2018). Sendo estes, 11.200 novos casos de câncer da cavidade oral em homens e 3.500 em mulheres para cada ano do biênio 2018-2019. Esses valores correspondem a um risco estimado de 10,86 casos novos a cada 100 mil homens, ocupando a quinta posição dos cânceres que mais acometem os homens; e de 3,28 para cada 100 mil mulheres, sendo o 12º mais frequente entre todos os cânceres que acometem as mulheres (INCA, 2018). O carcinoma espinocelular é a histologia predominante, representando mais de 90% dos casos (Tribius e Bergelt, 2011; Marur et al., 2016). Os fatores de risco mais comuns para o desenvolvimento de cânceres da cavidade oral são uso de cigarro e de álcool e, no caso dos cânceres orofaríngeos, a infecção pelo papiloma vírus humano (Tribius e Bergelt, 2011).

Os cânceres de cabeça e pescoço são frequentemente tratados com radioterapia, uma técnica que utiliza radiação ionizante e danifica de forma semi-seletiva material genético de células malignas vulneráveis, ou através da produção de radicais livres, levando a morte celular (de Felice et al., 2018). A radioterapia pode ser utilizada de forma exclusiva ou associada à cirurgia e à quimioterapia (Kielbassa et al., 2006; Lazarus et al., 2007; de Felice et al., 2018). A localização, o tipo e a extensão do tumor que determinam como o tratamento é conduzido, se a radiação é usada isoladamente ou em combinação

com outras modalidades de tratamento, bem como a dose de radiação necessária. A unidade empregada para medir a quantidade de radiação é o Gray (Gy), que informa a dose de radiação absorvida por qualquer material ou tecido humano (INCA, 2018). No geral, a dose total de radiação para tratamento de câncer de cabeça e pescoço varia de 30 a 72 Gy, sendo muito comum o esquema de fracionamento, com aplicação de 2 Gy diários, 5 dias por semanas até atingir a totalidade de Gy planejados (Jham & Freire, 2006; Epstein et al., 2012).

Apesar de ser um tratamento altamente eficaz para o controle do câncer e ter a vantagem de não ser invasiva, a radioterapia provoca muitas reações adversas que afetam significativamente a qualidade de vida dos pacientes (Vissink et al., 2003; Kielbassa, 2006; Ray-Chaudhuri et al., 2013; Lieshout & Bots, 2014; Deng et al., 2015; Buglione et al., 2016). Nos últimos anos, a consciência das sequelas de radioterapia tem crescido, e esforços têm sido feitos para limitar a exposição à radioterapia de estruturas essenciais para funções como deglutição, mastigação e salivação (Buglione et al., 2016). Nas últimas duas décadas, a distribuição de radiação evoluiu de um tratamento bidimensional de feixe externo convencional (2DRT) para um tridimensional conformada (3DCRT). E mais recentemente, a técnica foi aprimorada para radioterapia de intensidade modulada (IMRT). Esta técnica usa planejamento baseado em tomografia computadorizada e entrega de radiação, auxiliado pela otimização computadorizada das intensidades do feixe de radiação, com o objetivo de melhorar a conformação da dose em 3 dimensões, maximizando o controle da doença e minimizando a morbidade e toxicidade para tecidos saudáveis em torno do volume de tratamento direcionado (Tribius & Bergelt, 2011; Marta et al., 2014). No entanto, essa não é a realidade de muitos centros de tratamento oncológico no Brasil, pois se trata de um equipamento de alto custo.

A radioterapia está tipicamente associada a toxicidades agudas e tardias aos tecidos saudáveis localizados no campo da radiação. As toxicidades agudas mais comuns da cavidade oral incluem mucosite, disfagia, hipossalivação, tecidos moles sensíveis ou dolorosos, infecções por fungos (Vissink et al., 2003; Jham & Freire, 2006). Outras consequências têm um caráter mais tardio como o trismo, a hipossalivação, a osteorradionecrose da mandíbula, as alterações nas estruturas dentárias e a cárie relacionada à radiação (Jham & Freire, 2006; Kielbassa et al., 2006; Tolentino et al., 2011;

Jawad et al., 2015; Hong et al., 2017). Por isso, é tão importante e necessário o acompanhamento clínico odontológico de pacientes submetidos à radioterapia na região de cabeça e pescoço antes, durante e após o tratamento (Vissink et al., 2003; Beech et al., 2014; Devi & Singh, 2014; Jawad et al., 2015).

A radiação pode causar alterações nas propriedades mecânicas e químicas, na microestrutura/morfologia, na estrutura cristalina, na solubilidade do esmalte e da dentina (Vissink et al., 2003; Soares et al., 2010; Gonçalves et al., 2014; Lieshout & Bots 2014; Qing et al., 2015; Reed et al., 2015; Liang et al., 2016; Novais et al., 2016; Qing et al., 2016; Thiagarajan et al., 2017; Campi et al. 2018; de Miranda et al., 2018; Lopes et al., 2018; Queiroz et al., 2018; Rodrigues et al., 2018; Seyedmahmoud et al., 2018; Velo et ., 2018; Lu et al., 2019).

A gravidade e a extensão dos efeitos da radiação dependem do conteúdo mineral e orgânico das estruturas do dente, sendo que a dentina pode ser mais vulnerável aos efeitos da radiação (Gonçalves et al., 2014). Dessa forma, o conhecimento sobre a estrutura dentinária é importante para melhor compreender os efeitos da radioterapia. A dentina é um tecido de origem mesenquimal, constitui o corpo do dente e tem como funções principais proteger a polpa e dar suporte para o esmalte sobrejacente. A dentina madura é composta de aproximadamente 70% mineral, 20% matriz orgânica e 10% de água (Tjaderhane, 2016). Seu componente inorgânico consiste em hidroxiapatita e a parte orgânica é fundamentalmente composta de colágeno (principalmente tipo I com pequenas quantidades dos tipos III e IV), que proporciona a resiliência necessária para a coroa suportar o ato mastigatório. Ela apresenta menor conteúdo mineral do que o esmalte e maior incorporação de magnésio e carbonato, o que leva ao aumento da sua solubilidade (Hoppenbrouwers, Driessens & Borggreven, 1987). Em relação à parte orgânica, o colágeno tipo I age como suporte que acomoda e mantêm juntos os cristais de apatita nos orifícios e poros das fibrilas, alguns dos quais estão precipitados dentro da fina estrutura de hélice de colágeno. Com essa estrutura há sinergia entre matriz e apatita (Nanci & Ten Cate, 2008).

A literatura mostra que a radioterapia é capaz de produzir radicais livres a partir da radiólise de moléculas diferentes, como a água que produz os íons H + e OH−, e os últimos são altamente instáveis e reativos. Esses íons se ligarão a outras moléculas, que

serão danificadas e perderão a função, ou produzirão mais radicais livres. Esse mecanismo de radiação sustenta o consenso na literatura de que a radioterapia dos tecidos dentais tem maiores efeitos deletérios quando maiores concentrações de conteúdo orgânico estão presentes no tecido (Pioch, Golfels, & Staehle, 1992; Soares et al., 2010). Este processo também pode causar desnaturação dos componentes orgânicos das estruturas dentárias alterando sua estrutura e causando a fragmentação das fibras colágenas (Pioch et al., 1992; Gonçalves et al., 2014; de Miranda et al., 2018; Velo et al., 2018; Lu et al., 2019). A degeneração dos componentes orgânicos enfraquece a sua interação com os cristais de hidroxiapatita, levando à diminuição da cristalinidade da apatita e maior solubilidade na saliva em pH baixo (Lu et al., 2019).

Vários estudos in vitro e in situ, com dentina bovina e humana, mostraram uma diminuição da microdureza entre a dentina irradiada e não irradiada (Markitziu, 1986, Kielbassa 1997; Kielbassa et al., 2002; Franzel et al., 2006; Gonçalves et al., 2014; Liang et al. 2016; Novais et al. 2016; Qing et al. 2016; Velo et al. 2018); alteração do comportamento de desgaste (Qing et al. 2016); diminuição da solubilidade da dentina irradiada (Markitziu, 1986); diminuição da resistência a tração (Soares et al., 2010; Soares et al., 2011); aumento da rigidez próximo a junção amelo-dentinária, o que pode levar a delaminação do esmalte (Reed et al. 2015); alterações morfológicas, como a obliteração dos túbulos dentinários, precedida de degeneração dos processos odontoblásticos (Grötz et al., 1997, Soares et al., 2011; de Siqueira Mellara et al., 2014; Gonçalves et al., 2014; Velo et al. 2018; Lu et al., 2019); alterações químicas (Reed et al. 2015; Qing et al. 2016; Campi et al. 2018; de Miranda et al. 2018; Rodrigues et al., 2018; Velo et al. 2018), aumento da atividade das metaloproteinases (Queiroz et al., 2018). Sendo que o aumento das doses cumulativas de radiação resulta em alterações micro-morfológicas progressivas das estruturas de esmalte e dentina (Gonçalves et al., 2014; Liang et al., 2016).

Os primeiros sinais de deterioração do tecido duro dos dentes podem ser vistos dentro de três meses após a finalização da radioterapia (Vissink et al., 2003). Esses sinais são áreas de porosidade do esmalte, formação de cavitações com a exposição do esmalte subsuperficial, ou até mesmo da dentina subjacente. À esta deterioração dá se o nome de cárie relacionada à radiação (Vissink et al., 2003; Kielbassa et al., 2006). Assim como a cárie convencional, a cárie relacionada à radiação possui etiologia multifatorial e é

resultante do desequilíbrio no balanço entre o mineral do dente e o fluido do biofilme. A produção de ácido por meio da metabolização de nutrientes pelas bactérias do biofilme e consequente baixa do pH são os fatores responsáveis pela desmineralização do tecido dentário que pode resultar na formação da lesão de cárie, com a perda de cálcio e fosfato dos tecidos dentais mineralizados para o meio bucal (Maltz, 2016).

No entanto, a cárie relacionada à radiação se diferencia da cárie convencional pois se desenvolve rapidamente, é altamente destrutiva e na maior parte manifesta-se sem dor (Jansma et al., 1993; Walker et al., 2001; Kielbassa et al., 2006, Abdalla et al., 2018). Quanto à localização, as cáries relacionadas à radiação tendem a ocorrer na região cervical (próximo à junção entre a coroa e a raiz), podendo se estender para mesial e distal (Jawad et al., 2015). Ela também se difere em relação à sua aparência. Na maioria das vezes, essas lesões de cáries relacionadas à radiação apresentam-se com uma coloração marrom e com alteração da translucidez da estrutura dentária. É muito comum observar uma área de desmineralização circunferencial na cervical do dente, afetando superfícies lisas do esmalte que normalmente são resistentes à cárie dentária, bem como superfícies expostas de cemento (Abdalla et al., 2017). Podendo até mesmo levar a fratura da coroa nesta região, afetando severamente a mastigação e a estética desses pacientes (Andrews et al., 2001; Franzel et al., 2006).

Os efeitos da radioterapia no início e na progressão de uma lesão de cárie podem ser de origem direta, alterando os tecidos dentários, ou de origem indireta (de Siqueira Mellara et al., 2014). Os efeitos diretos sobre os tecidos duros dentais já foram discutidos acima. Dentre os efeitos indiretos, pode-se citar as alterações nas glândulas salivares, como por exemplo a hipossalivação (diminuição do fluxo salivar), reduzindo assim a efetividade da saliva em promover suas atividades tampão e de limpeza nos dentes e mucosa (Jensen et al., 2010), além de mudanças na sua composição, no pH e da microbiota bucal (Gaetti-Jardin et al., 2018). Somado a isso, modificações induzidas no meio oral pela radiação, como alterações gustatórias e dietéticas levando a preferência por alimentos macios e ricos em carboidratos, e o aparecimento de mucosites, gerando dor e sensibilidade nas mucosas, dificultando a higienização, tornam o meio oral desses pacientes altamente cariogênicos (Kielbassa et al., 2000; Vissink et al., 2003; Kielbassa et al., 2006; Walker et al., 2011; Jawad et al., 2015).

A cárie relacionada à radiação representa um desafio para o dentista, porque o acesso às lesões cervicais é freqüentemente restrito, a escavação da cárie pode se dar de forma incompleta, as margens da preparação da cavidade podem ser difíceis de definir e os preparos podem fornecer pouca retenção mecânica para as restaurações (Hu et al., 2005). Além disso, a restauração fica comprometida pelo efeito prejudicial da radiação ionizante na resistência de união ao esmalte e à dentina humanos, quando o procedimento restaurador adesivo é realizado após a radioterapia (Naves et al., 2012; Rodrigues et al., 2018). Assim, algumas das medidas recomendadas incluem higiene bucal rigorosa, auto-aplicação diária tópica de gel de fluoreto de sódio (NaF) a 1,0% (Jansma et al., 1989), limitação de alimentos cariogênicos, enxáguante bucal remineralizador e preparações de saliva artificial. Este regime preventivo, no entanto, é muitas vezes dificultado pela má adesão nesta categoria de pacientes (Vissink et al., 2003).

Diante desse cenário, uso de métodos capazes de detectar mínimas alterações, torna-se de grande relevância para a compreensão de como a radioterapia altera os tecidos dentais, de como a cárie relacionada à radiação se inicia e progride, e de como ela se difere da cárie convencional. A espectroscopia de infravermelho por transformada de Fourier (FTIR) tem se mostrado uma ferramenta muito importante na detecção de alteração da composição química tecidos dentários, uma vez que quando associado a técnica de reflectância total atenuada (ATR) nenhum ou pouco preparo da amostra é necessário, e pelo fato de que componentes como água, fosfato, carbonato e colágeno absorvem fortemente na região do infra-vermelho (Lopes et al., 2018).

OBJETIVOS

2. OBJETIVOS

Objetivo geral

O objetivo geral deste trabalho foi revisar a literatura quanto a composição química dos tecidos mineralizados (esmalte, dentina e osso) por meio do FTIR e caracterizar química e morfologicamente a cárie relacionada à radiação.

Objetivos específicos

Objetivo específico 1

Capítulo 1 - Fourier transform infrared spectroscopy (FTIR) application chemical characterization of enamel, dentin and bone

Este objetivo específico avaliou a literatura buscando condensar informações sobre o emprego do FTIR na caracterização química do esmalte, dentina e osso. Identificando picos e/ou bandas do espectro e suas atribuições relacionados ao diagnóstico das alterações e patologias dos tecidos mineralizados.

Objetivo específico 2

Capítulo 2 - Effect of radiotherapy and salivary flow rate on root dentin caries susceptibility

Este objetivo específico investigou o efeito da radiação ionizante e do fluxo salivar na susceptibilidade da dentina radicular à cárie por meio de um modelo de biofilme microcosmo.

Objetivo específico 3

Capítulo 3 - Chemical and morphological characterization of radiation related caries

Este objetivo específico comparou dentina sadia à dentina cariada de pacientes não irradiados e de pacientes submetidos à radioterapia de cabeça e pescoço.

CAPÍTULOS

3. CAPÍTULOS

3.1 Capítulo 1

Camila de Carvalho Almança Lopes, Pedro Henrique Justino Oliveira Limirio, Veridiana Resende Novais & Paula Dechichi

DOI: 10.1080/05704928.2018.1431923

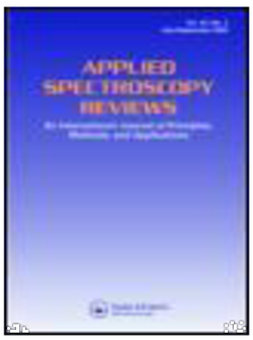

Applied Spectroscopy Reviews

ISSN: 0570-4928 (Print) 1520-569X (Online) Journal homepage: http://www.tandfonline.com/loi/laps20

Fourier transform infrared spectroscopy (FTIR) application chemical characterization of enamel, dentin and bone

Camila de Carvalho Almança Lopes, Pedro Henrique Justino Oliveira Limirio, Veridiana Resende Novais & Paula Dechichi

To cite this article: Camila de Carvalho Almança Lopes, Pedro Henrique Justino Oliveira Limirio, Veridiana Resende Novais & Paula Dechichi (2018): Fourier transform infrared spectroscopy (FTIR) application chemical characterization of enamel, dentin and bone, Applied Spectroscopy Reviews, DOI: 10.1080/05704928.2018.1431923

To link to this article: https://doi.org/10.1080/05704928.2018.1431923

Published online: 06 Feb 2018.

APPLIED SPECTROSCOPY REVIEWS
https://doi.org/10.1080/05704928.2018.1431923

Fourier transform infrared spectroscopy (FTIR) application chemical characterization of enamel, dentin and bone

Camila de Carvalho Almanca¸ Lopes[a], Pedro Henrique Justino Oliveira Limirio[a], Veridiana Resende Novais[a], and Paula Dechichi [b]

[a]Faculty of Dentistry, Federal University of Uberlândia, Uberlândia, Minas Gerais, Brazil; [b]Biomedical Science Institute, Federal University of Uberlâdia, Uberlândia, Minas Gerais, Brazil

ABSTRACT

Fourier transform infrared spectroscopy (FTIR) has been used extensively for chemical characterization of mineralized tissues in the past few decades. FTIR is an ideal technique to analyze chemical structural properties of natural materials, since the frequencies of several vibrational modes of organic and inorganic molecules are active in the infrared. This review discusses the use of FTIR methodology, highlighting the attenuated total reflection (ATR) sampling mode, particularly for characterization of enamel, dentin and bone tissues. Enamel, dentin and bone, are composed of an organic and a mineral phase. The mineral phase is characterized essentially as nonstoichiometric substituted apatite, being the carbonate and phosphate spectral peaks the main representative of these phase. Organic matrix of the post-eruptive enamel is small (»1% weight (wt)). The dentin and bone organic phases are mainly composed of type I collagen that appears as spectral bands of amide I, amide II, amide III bands. Furthermore, synthetic apatite materials are being designed for total or partial replacement, restoration or augmentation of these biological tissues with FTIR assistance.

KEYWORDS

Spectroscopy, fourier transform infrared; dental enamel; dentin; bone and bones; dentistry

1. Introduction

Enamel, dentin and bone are considered mineralized tissues that are widely studied in medi-cine and dentistry. Their characterization is based on experimental methods, which leads to the dissemination of relevant scientific knowledge. The most frequently analyzed character-istics of these tissues are their mechanical properties, morphology, structure and chemical analysis. Among the methods that determine the chemical composition of enamel, dentin and bone are energy dispersive X-ray (EDX/EDS) (1–6), Raman spectroscopy (7–12) and Fourier transform infrared (FTIR) spectroscopy (8, 13–57).

Energy dispersive X-ray (EDX) spectroscopy is a surface analysis method that provides semi-quantitative chemical analysis of the sample. This method relies on the radiation of samples with high-energy electrons and observation of X-ray emissions resulting from the core-hole via de-excitation of electrons. The X-ray energies emitted will generally differ

CONTACT Paula Dechichi pauladechichi@ufu.br Histology Department, Federal University of Uberl^andia, Avenida Para 1720, Campus Umuarama, Bloco 2B, Bairro Umuarama, Uberl^andia, 38.400-902 Minas Gerais, Brazil.

Color versions of one or more of the figures in the article can be found online at www.tandfonline.com/laps.

from element to element considering that each element has a unique atomic structure. Some limitations, for example, are relatively poor spectral resolution and high detection limits (58).

Raman and FTIR are complementary vibrational spectroscopic techniques. In Raman spectroscopy, a change is observed in the polarization of molecules; that is, a visible or ultra-violet photons interacts with the vibrating molecular bonds, gaining or losing part of their energy, thereby generating the spectrum. An advantage of Raman spectroscopy is that the spectral analysis is carried out in reflection mode, so tissues can be probed in their native state without any, or minimal preparation.

Fourier transform infrared spectroscopy is a widely used vibrational spectroscopic technique for chemical analysis in biomedical samples (59), since most inorganic and organic components in the environment are active in infrared (IR) radiation because they have dipole moments (60). This spectroscopic technique refers to absorption of IR radiation and relies on the absorption of energy from a photon that subsequently promotes the transition from a lower-energy state to a higher-energy, or an excited state (61). The excited states result in vibrations of molecular bonds (i.e., stretching, bending, twisting, rocking, wagging, and out-of-plane deformation) occurring at varying wavenumbers (or frequencies) in the IR region of light spectrum (59). The wavenumber of each IR absorbance peak is determined by the intrinsic physicochemical properties of the corresponding molecule. Therefore, this is diagnosed as a fingerprint of that particular functional group (e.g., C–H, O–H, C=O, etc.) (62).

FTIR spectra can be acquired by means of different techniques: transmission, specular reflectance, diffuse reflectance, photoacoustic infrared spectroscopy and attenuated total reflectance (ATR) (63, 64). Transmission has been widely used for biological samples. In this approach, a pellet has to be prepared and the sample has to be deposited on infrared trans-parent windows, such as calcium fluoride or barium fluoride windows, or potassium bromide (KBr). The pellet is processed by preparing a homogenous mixture of KBr with a pulverized sample, under high pressure until the pellet becomes transparent (62). One issue with this technique is to estimate the right proportion of the sample material in the pellet, so the resulting peak absorbance is not too weak or too intense (preferably between 0.2 to 0.7 absorbance units) (62). The advances in FTIR spectroscopy allowed the development of diffuse reflectance, photoacoustic infrared spectroscopy and attenuated total reflectance (ATR), requiring little or almost no sample preparation.

In specular reflection, IR spectra are generated based on the IR specular reflection light from a polished surface, thereby eliminating the need for thin specimens as in the case of the transmission mode (65). This technique is seldom used, because biological material polish-ing is not easy or desirable and the samples are often non-reflective (63). Diffuse reflectance refers to the light that has been reflected from within the object, rather than from its surface (66). This reflectance mode is often used for heterogeneous samples or powders and solids that have a rough surface, used in mid (MIR) and near infrared (NIR) spectroscopy. When using MIR, powders have to be diluted with KBr.

A photo-acoustic signal is generated when infrared radiation absorbed by a sample is con-verted into heat within the sample. This heat diffuses to the sample surface and into the adja-cent atmosphere, and the thermal expansion of gas produces a photo-acoustic signal. Samples can be analyzed in their physiological condition and also in different depths (64).
ATR is a form of internal reflection spectroscopy, in which a sample is placed in contact with an internal reflection element (IRE) with a high refractive index, for example, a diamond

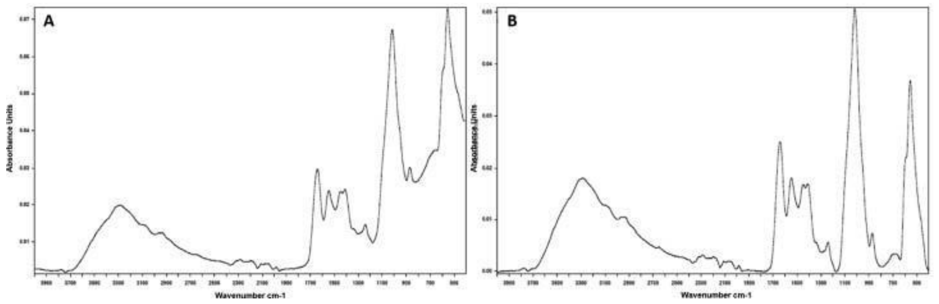

Figure 1. Baseline correction: (A) Original spectrum; (B) Spectrum after baseline subtraction.

crystal. A complete internal reflection occurs at the sample–IRE interface and after this, infra-red radiation is directed to a detector. Since infrared light is transmitted through the sample, little or almost no preparation is needed (62), thus it is considered a non-destructive method (59). Moreover, the presence of the ATR crystal allows IR spectra to be obtained with improved signal-to-noise ratios. An additional advantage is that it enables the collection of quality data of aqueous systems at crystal interfaces (63). ATR also has a small and well controlled depth of penetration, which implies it measures a relatively thin layer of the sample that is in contact with the ATR element surface (59). Because of the small depth of penetration, some contact pressure is necessary on samples that do not self-adhere to the ATR crystal to obtain a quality spectrum (63).

Infrared radiation is located between visible light and microwaves in the spectrum, and can be divided into three regions: near infrared 12800–4000 cm^{-1}, medium infrared 4000– 200 cm^{-1} and far infrared 200–100 cm^{-1} (67). The majority of articles in the dental literature have evaluated the samples in the middle of the infrared region (approximately 4000 to 400 cm^{-1}) (62). The absorbance units of molecular vibrations under IR radiation are proportional to the abundance of the functional groups. To calculate the absorbance units after spectrum generation, a baseline correction must be made to make the base level value constant (68). Several baseline algorithms are available, but in general, a constant value is only found by joining the points of lowest absorbance on a peak, preferably in reproducibly flat parts of the absorption line (Figure 1). The absorbance of each vibrational band is often measured by the maximum height or the integrated area between the peaks (Figure 2) (62). This article reviews FTIR spectroscopy applications in dentistry and identifies important peaks and the related assignments in the spectrum of FTIR spectroscopy to diagnose

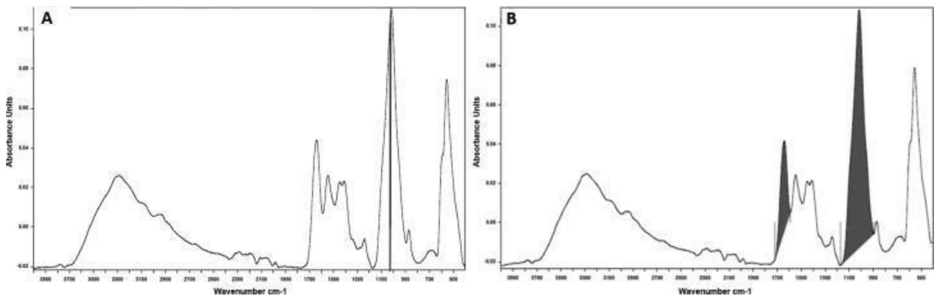

Figure 2. Calculation of the absorbance. (A) By the maximum height (absorbance intensity) (gray line) and (B) By integrated area (gray region).

mineralized tissue alterations and pathologies. By identifying the relevant peaks, this article serves as a guide for further studies with mineralized tissues using FTIR spectroscopy.

2. FTIR dentistry applications

2.1. Mineralized tissues characterization

Enamel, dentin and bone tissues are composed of water, organic and a mineral phase. The mineral matrix of these hard tissues is mainly composed of phosphate and calcium ions that form hydroxyapatite crystals – $Ca_{10}(PO_4)_5(OH)_2$, in addition to bicarbonate, magnesium, potassium, sodium, and citrate ions in small amounts. These crystals differ in size and quantity for each mineralized tissue (69). Bone and dentin organic matrix is mainly composed of type I collagen, and small quantities of other components (70). However, the enamel organic matrix in post-eruptive tissue is small (~1% weight (wt)), containing proteolyzed fragments and an insoluble protein matrix distributed along the dentin enamel junction (71). Differences in chemical composition between the depth and surface can occur in the same tissue (72, 73) or between different individuals and animals (69).

The chemical components present in these hard tissues such as water, phosphate, carbonate and collagen components strongly absorb IR region (Figure 3). The precise identification of chemical components depends on some details, such as sample preparation or the age of the subject/animal from which the sample is withdrawn, but despite these variables, the values remain very similar (72).

The water is present in two forms, adsorbed water, that is weakly bound to the structure, and structural water, that is strongly bound to the tissue (74). The most intense band can be observed at 3398 cm^{-1}, assigned to the v_1, $2v_2$ and v_3 vibrational modes. Another band can be observed at 1643 cm^{-1}, associated to v_2 mode, however in dentin and bone, this band shifts its position to 1660 cm^{-1} because it overlaps with the collagen band (69). Masked with the broad H_2O absorptions, the stretching vibration of the structural hydroxyl group of hydroxyapatite can be observed at 3569 cm^{-1} in the carbonated apatites (64).

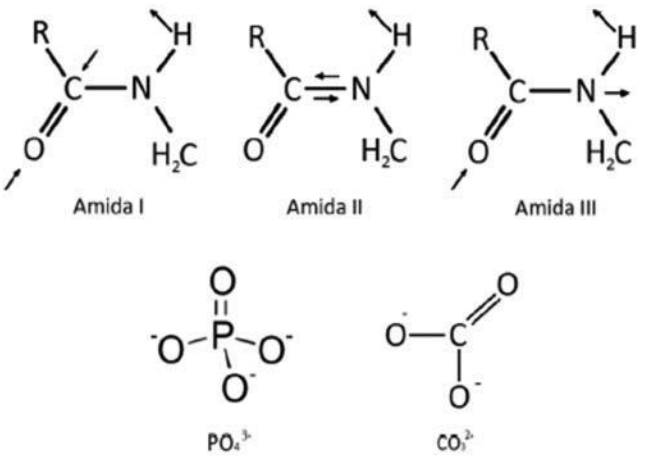

Figure 3. Structural formula with the vibrational modes of amide I, amide II, amide III, phosphate and carbonate.

Phosphate ions have four vibrational modes, v_1, v_2, v_3 and v_4. All these modes are IR active and observed in enamel, dentin and bone tissues. A singles intense v_3 band is present at about 1046 cm^{-1}. The v_3 band overlaps with the v_1 band, being the first one of greater intensity (75). Phosphate v_1 band is present at 960 cm^{-1}. The phosphate v_4 band in present in the region of 660 cm^{-1} and 520 cm^{-1} and is a sharp well-defined band (64). Lastly, the weak phosphate v_2 band is observed in the region of 470 cm^{-1} (69).

Carbonate ions also have four vibrational modes, three of which are observed in infrared spectrum (v_2, v_3 and v_4) and two of which are observed in the Raman spectrum (v_1 and v_4) (64). The carbonate v_4 bands are seldom seen in the infrared spectrum and beyond that have very low intensity (22, 64). The v_3 vibrational mode corresponds to the bands assigned in the region of 1650 to 1300 cm^{-1} and the peak at 873 cm^{-1} is due to the v_2 vibrational mode. The bands raised from v_3 vibrational mode are assigned to surface carbonate ions, rather than to carbonate ions in the lattice of phosphate ions.

Below, further information will be presented about each tissue, in addition to a representative spectrum and tables with the vibrational bands in the infrared region for enamel, den-tin and bone tissues functional groups. A brief description of synthetic analogue materials to the mineral phase of these tissues will also be addressed.

2.2. Enamel chemical characterization

Enamel is the hardest tissue covering on the tooth crown surface. It consists of 96% (wt) inorganic mineralized material, 1% (wt) organic material, and 3% (wt) water by weight (76). Hydroxyapatite (HA) crystals form the large part of the inorganic structure. The remaining parts consist of water, lipids, and proteins. Histologically, the enamel tissue shows a prismatic structure. The prisms have a cylindrical shape and stretch from the enamel dentin junction through to the tooth surface. Proteins, lipids and carbohydrates are located in the interprismatic area, and so is water (76).

Enamel studies using FTIR have investigated various pathologies, such as, enamel erosion, hypomaturation and hypomineralization (20, 23, 24, 27). Enamel erosion caused by acids originating from acidic foods or beverages, promotes enamel demineralization (77). FTIR was found to be highly sensitive for detecting changes in enamel erosion, in which the phos-phate content was changed and its peak was shifted (20, 24). Amelogenesis imperfecta (Hypomaturation) is a hereditary enamel disorder with a wide spectrum of clinical manifestations, including a discolored appearance; radiodensity similar to that of dentin; a soft tex-ture, and it is highly vulnerable to dental caries (78). Sa et al. (23) attributed the change in the crystallinity, crystal size and solubility of hydroxyapatite crystals to the high carbonate content in hypomaturation enamel. Molar Incisor Hypomineralization (MIH) is a developmental disturbance of the enamel in permanent first molars and incisors. This pathology is associated with a number of subjective and objective problems and complications, such as dental fear and anxiety, severe enamel loss, hypersensitivity, increased treatment need and problems in performing proper filling therapy (79). Hypomineralization was characterized by FTIR as a decrease in mineral phase and larger amide bands (27).

Substances for prevention of enamel demineralization and for enamel remineralization have been investigated by FTIR (15, 21). These substances (asparagine–serine–serine peptide and zinc) commonly act predominantly on enamel surfaces at phosphate sites in the hydroxyapatite lattice reducing enamel demineralization or improving its remineralization.

Lasers for increasing enamel acid resistance with the purpose of preventing dental caries also have been investigated by FTIR (13, 16–18, 22). CO_2, Nad:YAG and Er,Cr:YSGG lasers promoted water and carbonate loss, and were proved to be effective for controlling dental caries.

One of the most investigated subjects using FTIR is tooth whitening. Studies noted a decrease in the amount of phosphate and carbonate mineral content and in protein concentrations, proportional to treatment time and peroxide concentration (8, 14, 19, 25, 26, 45).

IR absorption frequencies of fundamental organic and inorganic functional groups in enamel are listed in Table 1, and typical ATR-FTIR enamel spectra are shown in Figure 4. The organic matrix bands are weak in comparison with mineral bands, especially relative to their lower content.

2.3. Chemical characterization of dentin

Comprising the greatest part of the dental tissue, dentin is a hard, elastic, avascular mineralized tissue supporting enamel and enclosing the central pulp chamber (80). It contains approximately (by weight) 70% mineral, 20% organic matrix, and 10% fluids (32). The major component of dentin organic matrix is heterotrimeric fibrillar type I collagen (90%) that serves as an oriented scaffold for mineral crystal deposition and packing of noncollagenous matrix (81). The deposition of minerals into and between collagen fibrils leads to the construction of a hard, resilient and resistant matrix. The histologic dentin architecture shows dentinal tubules, peritubular dentin and intertubular dentin (80). Dentinal tubules have an S-shaped path observed in a cross section of the long axis, from the outer surface of the den-tin to the area nearest the pulp chamber. The density and diameter of the tubules are greatest near the pulp. Peritubular dentin is found around the lumen of the tubules thus, in a cross-section the structures appear to be ring-like (82). Intertubular dentin that comprises the main body of dentin, is less mineralized than peritubular dentin (80, 82).

Dentin can be changed by physiological and pathological processes that cause modifications in its structure and biological behavior (83). Knowledge about dentin molecular structure associated with its histological, microscopic and mechanical aspects is important for full understanding of its properties and role (36). In this respect, FTIR is a powerful methodology for generating direct information about the chemical composition of dentin samples and indirectly, about their molecular structure.

Studies have used FTIR spectroscopy to investigate the influence of lasers and plasma on dentin (28, 31–34, 39, 41). The studies showed collagen structure loss (31–33, 39, 41), and that this loss after plasma/ laser treatment enhanced adhesive/dentin interface bonding (31, 33, 39). After erbium laser irradiation, loss of water, change in collagen structure and composition, and increase in the OH^- radicals were observed (28). Lin et al. (34) investigated whether it would be possible to fuse a root fracture by Nd:YAG laser. In this study, FTIR detected two different absorption bands at 2200 cm^{-1} and 2015 cm^{-1} in the spectrum, which suggested that a reaction had occurred in the organic matrix or between the organic matrix and minerals. Furthermore, FTIR showed that radiotherapy changed the absorption bands of dentin, with increased bands of amide I (18.8%), amide II (1.51%), amide III (38%), phosphate (20%), and proline and hydroxyproline (4.94%), suggesting changes in dentin properties (40).

Moreover, in endodontic research, Yassen et al. and Yassen et al. (46, 47) showed a superficial collagen degradation or demineralization of radicular dentin caused by calcium hydroxide $Ca(OH)_2$, or antibiotic pastes, medicaments used in endodontic regeneration.

Table 1. Absorption bands and/or range of chemical components presented in human enamel.

Assignment	Absorption peaks and/or bands (cm^{-1})
PO_4^{3-} v_2	470 (25)
Symmetric angular deformation	469 (69)
PO_4^{3-} v_4	568 e 602 (27)
Antisymmetric angular deformation	450–700 (23)
	500–650 (19)
	500–650 (26)
	582 (45)
	568 and 603 (25)
	520–650 (69)
	604, 564 (600–560) (13)
PO_4^{3-} v_1	958 (27)
Symmetric stretching	958 (25)
	960 (13)
PO_4^{3-} v_3	1040 (27)
Antisymmetric stretching	1100 and 1042 (45)
	1040 (25)
	1030–1160 (1035) (13)
	1100–1000/1220–900 (69)
CO_3^{2-} v_2	875 (22)
Symmetric angular deformation	
	872 (27)
	845–890 (23)
	850–890 (19)
	850–890 (26)
	890 e 860 (69)
	879 type A (69)
	873 type B (69)
	870–960, 872 (13)
CO_3^{2-} v_3	1415, 1460 (22)
Antisymmetric stretching	1420 (27)
	1350–1520 (23)
	1405 (19)
	1540 (25)
	1415, 1450–1550 (13)
	1544, 1530 (69)
CO_3^{2-} v_4	1560 (22)
Structural OH	3448, 3569 (22)
Stretching mode	3565 (27)
	749, 3570 (69)
	3793–2652 (17, 18)
	3800–3000 (15)
	3450–3570 (26)
	3570; 3500–2900 (69)
	3600–2400 (13)
Amide III	1202 (27)
Carbonate + Amide II	1540 A site (27)
N-H bending	1453 B site (27)
C-N stretching vibrations	1540 (27)
	1540 (26)
	1550 (45)
	1453 (25)
	1544, 1530–1380 (69)
	1640–1600 (69)
	1450–1425- Carbonate; 1550 – Amide II (13)
H_2O + Amide I	1646 (15)
	1642 (69)
	1630 (13)
	1638 (22)
	1653 (27)
	1575–1730 (23)

(Continued on next page)

Table 1. (Continued)

Assignment	Absorption peaks and/or bands (cm^{-1})
	1660 (1400–1700) (19) 1700–1600 (26)
	1650 (45) 1673 (25) 1690–1650 (69) 1660 (13)

Neelakantan et al. (38) investigated the influence of irrigation on the chemical interaction between root canal sealers and dentin by means of FTIR. They observed a new peak formed at 1735 cm^{-1} (C D O stretch) suggesting a chemical interaction between AH Plus root canal sealer and collagen when 3% NaOCl, 17% EDTA, water and 3% NaOCl, QMix, water were used as irrigation solutions.

Dental caries has been characterized by Liu et al. and Maske et al. in their studies (36, 37). Liu et al. (36) analyzed dentin transitions from the transparent zone (TZ) into the normal zone (NZ) regarding structural changes in collagen and hydroxyapatite, by using FTIR imaging system. They showed that collagen in TZ is hardly altered. Moreover, the resemblance between the STZ and NZ in terms of carbonate-rich A-type carbonate content, suggested that the mineral that initially occluded dentin tubules was hydroxyapatite. Maske et al. (37) developed a biofilm cariogenic challenge model and showed carries-affected dentin had lower mineral and amide I content. This was in agreement with Ramakrishnaiah et al. (84)

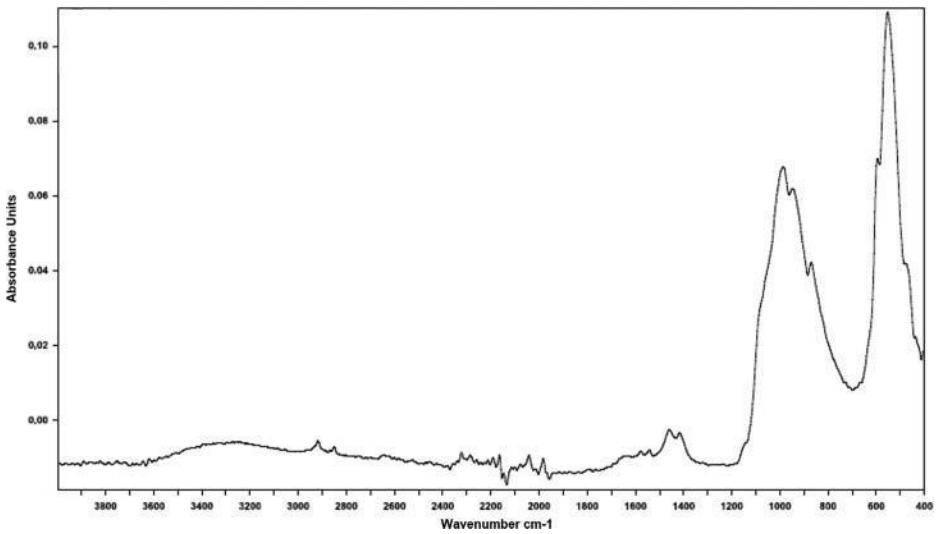

Figure 4. Typical ATR-FTIR spectrum of dental enamel.

who described dental caries as the demineralization of inorganic substances (hydroxyapatite crystals) and destruction of organic substance (collagen matter).

FTIR spectroscopy is also useful in demonstrating reduced mineral and organic content in tooth whitening (25, 45). Moreover, it can be used to evaluate dentin collagen for various other reasons, such as heated and rehydrated dentin; demineralized dentin and deproteinized dentin; and substances against collagen degradation (29, 30, 35, 42– 44, 85).

IR absorption frequencies of fundamental organic and inorganic functional groups in dentin are listed in Table 2, and typical ATR-FTIR dentin spectra are shown in Figure 5.

2.4. Bone

Bone tissue is a connective tissue with mineralized extracellular matrix that provides bone with hardness and resistance. The biomechanical properties of bone result from a complex structural arrangement between organic and inorganic components (86). Bone organic matrix is composed of collagen, noncollagenous proteins, and lipids, with 85–90% of the total bone protein being type I collagen (87). The hydroxyapatite crystal is the main inorganic matrix component. In bone, the hydroxyapatite has a structure similar to the mineral calcium hydroxyapatite, $Ca_{10}(PO_4)_6(OH)_2$, however, it is considered a carbonated and poorly crystalline hydroxyapatite (55). This is due to substitution and aggregation of small amounts of other ions, such as magnesium (Mg^{2+}), potassium (K^+), and/or sodium (Na^+) by Ca^{2+}, acidic phosphate (HPO_4^{2-}) for PO_4, and carbonate (CO_3^{2-}), which can actually substitute either OH^- (type A), or PO_4^{3-} (type B), or be loosely bound on the crystal surface (55). The type and extent of substitutions influence the crystal solubility as well as the size and shape, usually referred to as crystallinity (55). The carbonate is predominantly present as B-type carbonate, which increases the crystal solubility (88).

Understanding the physical and chemical properties of bone is important to enable researchers and practitioners to fully exploit this vital material. However, since bone is a complex heterogeneous material, analysis of these properties becomes somewhat problematic (89). ATR-FTIR spectroscopy has been successfully used, because in this technique, there is no need for sample preparation and spatial variation is not lost (90).

The first bone analyses using FTIR spectroscopy were performed to confirm the x-ray diffraction findings, in which a similar microstructure was observed between the bone mineral matrix and the mineral hydroxyapatite (90, 91). At present, this technique is being used to investigate different conditions that can change bone composition and structure, and thus affect its mechanical properties.

FTIR studies revealed increased mineral crystal sizes and decreased carbonate content for diabetic femur and tibia, suggestive of osteoporosis (92). Gong et al. (51) conducted a review that described new technologies for their diagnosis and treatment, including postmeno-pausal osteoporosis fracture risk (51). FTIR is an important methodology, because it helps to understand bone quality and fracture risk in osteoporotic patients by calculating parameters related to bone quality, such as mineral-to-matrix ratios, carbonate-to-phosphate ratios, mineral crystallinity, and/or collagen maturity (55). Higher collagen maturity and lower mineral-to-matrix ratio and ratio heterogeneity have been found in women with femoral fractures than in women without these (50). Lower carbonate-to-phosphate heterogeneity and crystallinity variability have also been found in fracture cases (51).

Table 2. Absorption bands and/or range of chemical components present in human dentin.

Components	Absorption (cm^{-1})
PO_4^{3-} v_2	470 (25)
PO_4^{3-} v_4	568 and 603 (25)
PO_4^{3-} v_1	958 (25)
	960 (37)
	961 (46)
PO_4^{3-} v_3	1005 (35)
	1013 (46)
	1025 (39)
	1035 (36, 37, 41)
	1040 (25)
	1042 and 1100 (45)
	1000–1100 (34)
CO_3^{2-} v_2	870 (34, 39, 46)
	872 (35, 36)
	875 (41)
	820–920 (36)
CO_3^{2-} v_3 overlapped with collagen	1410 (36)
	1411–1451(46)
	1410–1560 (41)
	1425–1450 (34)
	1540–1453 (25)
	1450–1640 (43)
Amide III	1230 (39, 45)
N-H deformation	1232 (30)
C-N stretching	1235 (32, 35, 36, 85, 86)
	1240 (41)
	1046 (46)
Scissoring CH_2	1450 (35, 36, 85)
	1460 (45)
Carbonate + Amide II:	1540 (33)
N-H bending	1542 (32)
C-N stretching	1544 (35, 85)
CNH	1550 (33, 34, 41, 45, 86)
	1551 (30, 46)
	1500–1600 (39)
H_2O + Amide I	1600–1700 (37)
C = O stretching	1630 (30, 39)
	1633 (35)
	1643 (33)
	1645 (46)
	1650 (33, 45)
	1653 (32)
	1655 (36)
	1660 (41)
	1673 (25)
H_2O v_2 overlap by the collagen band	1660 (69)
Structural OH	634 (34) and 2400–3600 (41)
Adsorbed H_2O (v_2)	1643 (69)
H_2O v_1, v_2, v_3	3398 (69)
Free OH	3596 (32)
hydroxyapatite, and amide N–H stretch	3433 (43)
H-bonded OH	3443 (32)
Amide A and amine N-H	3260; 3309 (30)
Amide B: COH	2930 (30)
CO_3	2300–2400 (43)
A-type carbonate	897 (36)
B-type carbonate	872 (36)

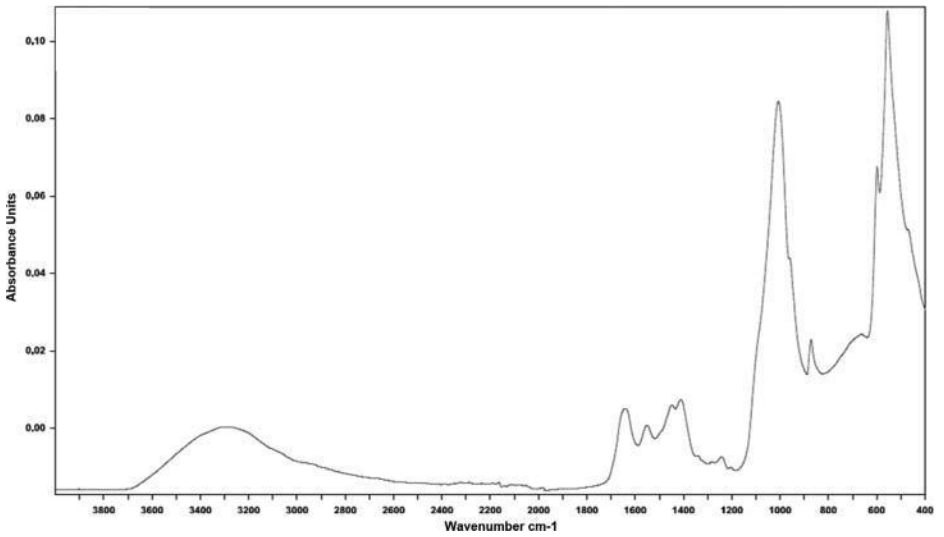

Figure 5. Typical ATR-FTIR dentin spectrum.

FTIR has been used to assess the effect of irradiation on bone, arising from medical therapy or bone-allograft sterilization causing loss and damage of bone collagen (87). FTIR showed increased glycosaminoglycan bands and decreased hydroxyapatite bands in bone and cartilage tissues. This possibly occurred because of glycosidic bond disruption, H_2O radiolysis and formation of amyloid-like proteins due to oxidative stress and free radical reactions.

Ellingham et al. (93) conducted a methodological review to estimate the temperature to which burnt bone was exposed. FTIR was used to assess bone crystallinity and the authors found that the crystallinity index increased with increasing temperature up to 800 C. From which point onwards, however, the values decreased due to the fusion of crystals as an effect of sintering (89). This topic is especially important to forensic anthropologists.

Another topic addressed in the studies with FTIR was sample preparation – longitudinal or cross-sections of human bone and compositional mapping of the cartilage-to-bone interface considering tissue region and age (53, 72). Gu et al. (53) showed stoichiometric changes resulting from mineral-collagen interactions in the two orientations. Furthermore, Khanarian et al. (72) observed tissue-dependent and age-related changes at the cartilage-to-bone interface, with relative increase in collagen content from cartilage to bone, whereas proteoglycan peaked within the deep zone of cartilage. In addition, irrespective of age, mineral content increased exponentially across the calcified cartilage interface.

Literature studies have also investigated the thermal effects on bone produced by the laser irradiation. Benetti et al. (48) showed by FTIR analysis that Er,Cr:YSGG laser promoted changes in bone tissue in both the mineral and organic components depending on the laser energy density. The carbonate to phosphate ratio showed a decreasing trend with a rise in energy density; however, there was no change in mineral crystallinity (48). Organic components significantly decreased with the increase in the energy density used, possibly due to the increase in the temperature of the tissue (48).

IR absorption frequencies of fundamental organic and inorganic functional groups in bone are listed in Table 3, and typical ATR-FTIR bone spectra are shown in Figure 6.

Table 3 – Absorption bands and/or range of chemical components present in bone tissue.

Components	Absorption (cm^{-1})
PO_4^{3-} v_2	470 (53)
Symmetric bending	
PO_4^{3-} v_4	480–770 (87)
Antisymmetric bending	565 and 605 (90)
	500–660 (93)
	606, 567 (53)
PO_4^{3-} v_1	960 (90)
	960 (53)
PO_4^{3-} v_3	1035 (94)
Antisymmetric stretching	1028–1100 (90)
	1100–1180 (53)
PO_4^{3-} v_1 C PO_4^{3-} v_3	900–1200 (87)
	916–1180 (52)
	900–1200 (93)
	900–1200 (72)
CO_3^{2-} v_2	900 (94)
	874 (90)
	840–892 (52)
	850–890 (93)
	850–890 (72)
	875 (53)
CO_3^{2-} v_3	1415(94)
	1400–1550 (90)
Amide III	1210–1280 (48)
CO_3^{2-} + Amide II	1550(94)
protein N-H bending C C-N stretching	1492–1590 (72)
	1546–1506 (53)
H_2O + Amide I	1585–1720 (87)
protein C = O stretch	1592–1712 (52)
	1650 (94)
	1590 – 1720 (72)
	1654 (53)
	1630–1660 (90)
Amide I	1660 (88)
Pyridinoline collagen crosslinks	1660 (52)
Amide I	1690 (88)
DHLNL collagen crosslinks	1690 (52)
OH	573, 632–650, 3400 (90)
	~2100, 3328, 3570 (53)

2.4.1. Synthetic analogue materials

Synthetic calcium phosphate bioceramics are common alternatives to autogeneous bone, xenograft or allograft materials due to their biocompatibility and chemical similarity to the inorganic matrix of bone, and of tooth enamel and dentine (94). They have gained acceptance for various dental or medical applications that include, e.g., fillers for periodontal defects, alveolar ridge augmentation, maxillofacial reconstruction, and coatings for metallic implants (95–97). Different phases and forms of calcium phosphates, including b-tricalcium phosphate (β-TCP), α-tricalcium phosphate, hydroxyapatite (HA), biphasic calcium phos-phate and monocalcium phosphate monohydrate are commonly used as blocks, cements, pastes, powders or granules (98). The biological performance of a synthetic material depends on fundamental parameters: chemical composition, morphology and biodegradability (99).

The tricalcium phosphate (TCP) has received great attention as grafts for bone regeneration applications due to its excellent biocompatibility and biodegradability (100, 101). Its capacity for dissolution and adsorption in biological tissues is 12 times higher than HA, since

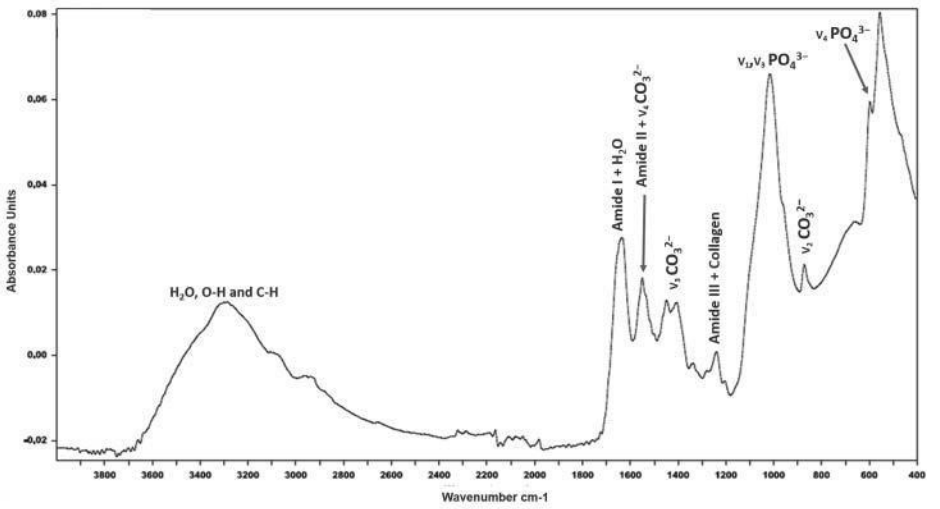

Figure 6. Typical ATR-FTIR bone spectrum.

it is not stable in aqueous solution or in the presence of humidity. Naturally, TCP is found in pathological calcifications, such as dental and urinary calculi, besides being the main inorganic constituent in dental caries lesions. Due to its biodegradable behavior, TCP in allotropic forms α and β has become an object of interest in the area of biomaterials, being used in dentistry as filling material in cavities, regions with bone defects and fixation of soft tissues (102). FTIR spectra of commercially available β -TCP ceramics are shown in Figure 7, identifying the calcium phosphate bands.

HA is an ideal phase of calcium-phosphate for application in the human body due to its biocompatibility, osteoconductivity, bioactivity and minimal risks of allergic reactions (103). In Figure 8, the spectra of a synthetic hydroxyapatite powder shows a number of spectral details indicating some similarities with the carbonated apatite.

The FT-IR assay has been most frequently used for the assignment of the substitution types of ions in synthetic apatite products (103–106) and in the structural modifications

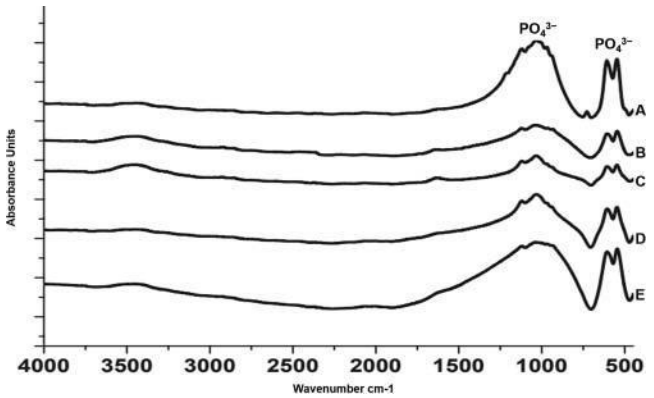

Figure 7. FTIR spectra of commercially available TCP ceramics. A - Vitoss , B - Cerasorb , C - Ceros , D - Chronos , E - Bioresorb .

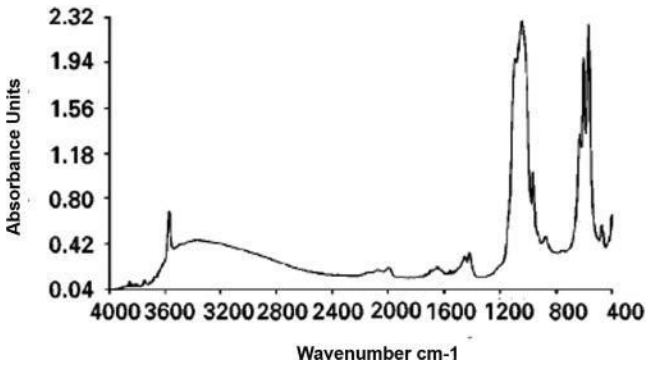

Figure 8. FTIR spectrum of synthetic hydroxyapatite powder.

related processing of HA-based materials (107). Doping of the original sites of HA can induce improved biological responses, adding new characteristics and properties, capable of increasing the degree of biocompatibility of these materials. Substitutions within the HA lattice are observed both for naturally occurring and synthetic HA (108). HA can be substituted by numerous ions such as cations Na^{+}, Mg^{2+}, Mn^{2+}, Zn^{2+} and anions CO_3^{2-}, Cl^{-}, F^{-}. The most common are substitutions involving fluoride and carbonate ions (109). When F^{-} substitutes for the hydroxyl (OH^{-}) group, makes the structure more hexagonal and less soluble than pure hydroxyapatite at pH= 5–7 (108). The presence of CO_3^{2-} in the structure is a para-mount importance because it is the main source of distortion of the crystalline network, cre-ating micro-stresses and defects in its vicinity, greatly influencing its solubility (110). The $C03^{-}$ ion can substitute for either the hydroxyl groups (type A) or the phosphate (type B) of HA (103). Type A causes augmentation of the a-exis and decrease of the c-axis in the HA unit cell. The incorporation of type B carbonate can cause the following effects: decrease in the a-axis and increase of the c-axis in the unit cell, decrease in crystal size, change in crystal morphology and decrease of crystallinity and increase of solubility of the material (97).

2.4.2. Parameters that are commonly assessed for enamel, dentin and bone and their importance

In FTIR spectroscopy, the area under a band is directly proportional to the concentration of the chemical species that gives rise to the specific band. However, it is sometimes preferable to use ratios between reference areas or peak heights, since the comparison parameters resulting from single bands are subject to uncertainties arising from sample to sample variations (54).

2.4.3. Mineral to matrix ratio

This ratio directly measures the amount of organic matrix in the volume analyzed (50, 86). The division of the integrated areas of the v_1,v_3 PO_4^{3-} (stretching and bending vibrations) to amide I (mainly from the peptide bond C = O stretching vibration with minor contribu-tions from the out of phase CN stretching vibration, the CCN deformation and the NH in-plane bend) provides what is commonly reported as mineral/matrix ratio or phosphate to amide I ratio (Figure 9) (86). A further way of obtaining the mineral/matrix ratio is by divid-ing v_1,v_3 PO_4^{3-} by amide II (out of phase combination of the NH in-plane bend and the CC

and NC stretching vibration with smaller contributions from the CO in-plane bend and the CC and NC stretching vibrations) (48, 50), either v_1,v_3 PO_4^{3-} by amide III (48).

2.4.4. Carbonate to phosphate ratio or carbonate to mineral ratio

Carbonate to phosphate ratio indicates the extent of carbonate incorporation into the hydroxyapatite lattice. In FTIR, two bands are assigned to carbonate, nonetheless they are overlap with acidic phosphate peaks (850–890 cm^{-1}) or noncollagenous protein peaks (1400–1500 cm^{-1}). Therefore, it is necessary to perform second derivative spectroscopy (Figure 10) followed by curve-fitting routines to gain information on the extent and the type of carbonate substitution (54). Curve-fitting of the carbonate band reveals two types of sub-stitution, A-type and B-type, which is designated to carbonate ions occupying the positions of hydroxide whereas the latter designates phosphate ions, respectively (36, 56). A-type carbonate (878 cm^{-1}) occurs at a significant level in dental enamel and B-type carbonate (871 cm^{-1}), and represents the major substitution site in bone and dentin (54). This sub-stitution causes deformations in the crystalline lattice and results in less stable phases that are more soluble in acid (111).

2.4.5. Mineral maturity/crystallinity

The crystallinity index (CI) is defined as the crystallinity volume fraction of one phase in a given sample and represents a measure of the average crystallite size, perfection, and order-ing (91). In biologic mineralized tissues, the hydroxyapatite crystals are poorly crystalline since they contain impurities (50, 112). As a result, efforts have been made to extrapolate these values from the direct measure of FTIR spectroscopy, which is the mineral maturity to mineral crystallinity ratio. This is measured by the ratio of the peak height intensities of the 1030 and 1020 cm^{-1} (Figure 11). Mineral crystallinity correlates linearly with HA crystal size and perfection in the c-axis direction is determined by X-ray diffraction analyses (57).

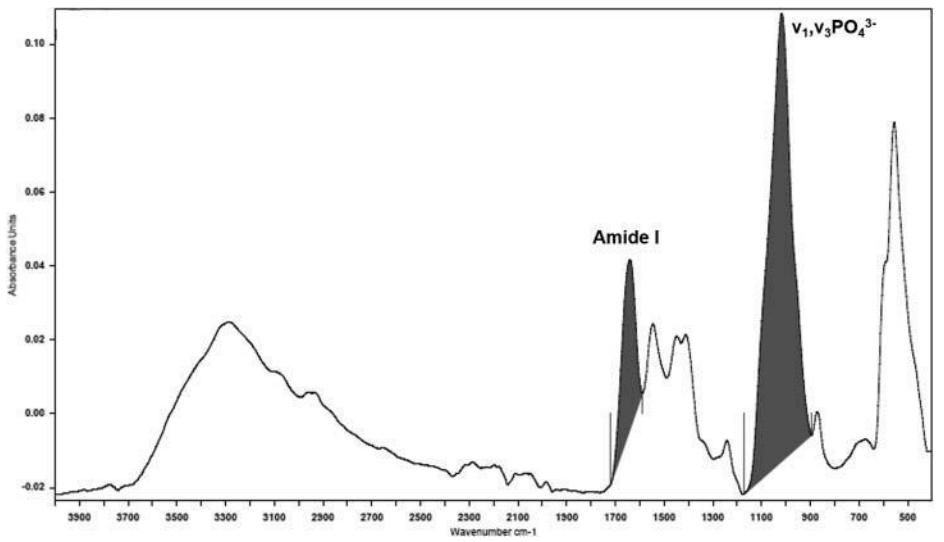

Figure 9. Calculation of the Mineral to Matrix Ratio by the integrated areas from v1,v3 PO43- and amide I (gray region).

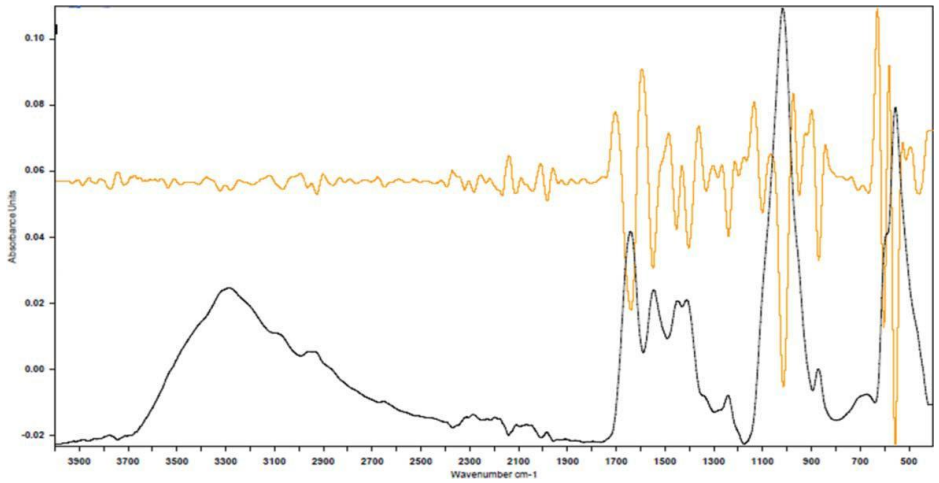

Figure 10. Example of the second derivative of a spectrum: Absorption spectrum (black); Second deriva-tive of the spectrum (orange line).

2.4.6. Collagen cross-links

One of the most abundant proteins in mineralized connective tissues is type I collagen. A distinct feature of collagen is its cross-linking chemistry and molecular packing structure (113). This arrangement is responsible for mechanical properties such as tensile strength and viscoelasticity of the fibrillar matrix. To date, seven major collagen cross-links have been established as naturally occurring intermolecular cross-links (112). Vibrational spectroscopic analysis is able to describe the spatial distribution of two types of the collagen cross-links, namely pyridinoline and divalent cross-links (50, 112). In FTIR this parameter is determined through the resolution and quantification of the amide I peak (peptide C = O stretch, 1650 cm^{-1}) by means of second derivative spectroscopy and curve-fitting routines (112,

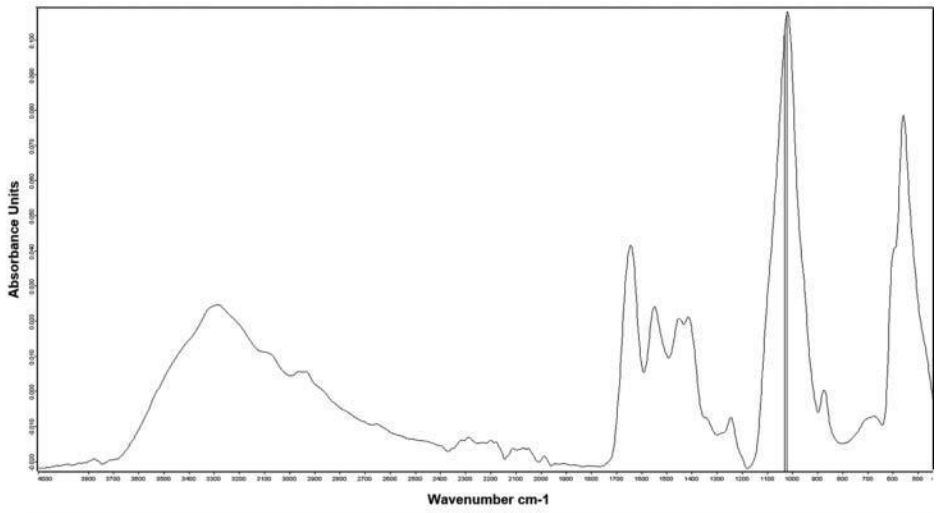

Figure 11. Calculation of the Mineral Maturity by peak height intensities of the 1030 and 1020 cm-1 (gray lines).

114). Two sub-bands of amide I are of particular interest in collagen denaturation: one at 1660 cm^{-1} and one at 1690 cm^{-1}, corresponding to the nonreducible and reducible collagen, respectively (112). Cross-linking is important for the development of the underlying matrix, which in turn is essential for initial mineral formation and crystal growth in mineralized connective tissue (52). Changes in this network can result in severe dysfunction of the tissue and may be associated with the age-related increase in fracture and diseases (115–117). Furthermore, the ratio of amide I to amide II band areas can be used to determine collagen fiber orientation (118).

3. Conclusion

FTIR spectroscopy has been shown to be an advantageous technique since it provides a fast, convenient, and accurate quantitative approach to investigating mineralized tissues and its synthetic analogues. Moreover, it provides insightful information on the chemical structure at the molecular scale. At present, this technique has been used to investigate different conditions that can change enamel, dentin and bone chemical composition and structure. FTIR can be utilized in hard dental tissue research for the investigation of development disturbances (such as amelogenesis imperfect, hypomineralization); diseases that lead to tooth structure loss (erosion, dental caries); tooth whitening; the mechanism of action of lasers and plasma on enamel and dentin, among others. In the same way, FTIR can be used in bone studies to examine diseases that affect bone remodeling (diabetes and osteoporosis), the action of lasers and raio-x, and age-related changes, etc. In addition, several studies have used FTIR in the analysis of ionic substitution types and of the structural modifications related to the processing of synthetic apatite products applied in dental or medical areas.

ORCID

Paula Dechichi http://orcid.org/0000-0001-5509-8138

References

1. Soares, L. E., and De Carvalho Filho, A. C. (2015) Protective effect of fluoride varnish and fluoride gel on enamel erosion: roughness, SEM-EDS, and micro-EDXRF studies. Microsc Res Tech, 78(3):240–248.
2. Gjorgievska, E. S., Nicholson, J. W., Slipper, I. J., and Stevanovic, M. M. (2013) Remineralization of demineralized enamel by toothpastes: a scanning electron microscopy, energy dispersive X-ray analysis, and three-dimensional stereo-micrographic study. Microsc Microanal, 19 (3):587–595.
3. de Morais, R. C., Silveira, R. E., Chinelatti, M., Geraldeli, S., de Carvalho Panzeri Pires-de-Souza, F. (2017) Bond strength of adhesive systems to sound and demineralized dentin treated with bio-active glass ceramic suspension. Clin Oral Investig.
4. Rodrigues, R. V., Giannini, M., Pascon, F. M., Panwar, P., Bromme, D., Manso, A. P., et al. (2017) Effect of conditioning solutions containing ferric chloride on dentin bond strength and collagen degradation. Dent Mater, 33(10):1093–1102.
5. Camilo, C. C., Silveira, C.A.E., Faeda, R. S., de Almeida Rollo, J.M.D., Purquerio, B. M., and Fortulan, C. A. (2017) Bone response to porous alumina implants coated with bioactive

materials, observed using different characterization techniques. J Appl Biomater Funct Mater, 15 (3):e223–e235.
6. Neufurth, M., Wang, X., Wang, S., Steffen, R., Ackermann, M., Haep, N. D., et al. (2017) 3D printing of hybrid biomaterials for bone tissue engineering: Calcium-polyphosphate microparticles encapsulated by polycaprolactone. Acta Biomater, 64:377–388.
7. Reed, R., Xu, C., Liu, Y., Gorski, J. P., Wang, Y., and Walker, M. P. (2015) Radiotherapy effect on nano-mechanical properties and chemical composition of enamel and dentine. Arch Oral Biol, 60(5):690–697.
8. Sun, L., Liang, S., Sa, Y., Wang, Z., Ma, X., Jiang, T., et al. (2011) Surface alteration of human tooth enamel subjected to acidic and neutral 30% hydrogen peroxide. J Dent, 39(10):686–692.
9. Lopes, F. C., Roperto, R., Akkus, A., Akkus, O., Palma-Dibb, R. G., de Sousa-Neto, M. D. (2017) Effect of laser activated bleaching on the chemical stability and morphology of intracoronal den-tin. Arch Oral Biol, 86:40–45.
10. Toledano, M., Perez-Alvarez, M. C., Aguilera, F. S., Osorio, E., Cabello, I., Toledano-Osorio, M., et al. (2017) A zinc oxide-modified hydroxyapatite-based cement facilitated new crystalline-stoichiometric and amorphous apatite precipitation on dentine. Int Endod J, 50(Suppl 2):e109–e119.
11. Shi, C., Mandair, G. S., Zhang, H., Vanrenterghem, G. G., Ridella, R., Takahashi, A., et al. (2017) Bone morphogenetic protein signaling through ACVR1 and BMPR1A negatively regulates bone mass along with alterations in bone composition. J Struct Biol.
12. Tanaka, Y. K., Yajima, N., Okada, M., Matsumoto, T., Higuchi, Y., Miyazaki, S., et al. (2017) The effect of Mg and Sr on the crystallinity of bones evaluated through Raman spectroscopy and laser ablation-ICPMS analysis. Analyst, 142(22):4265–4278.
13. Antunes, A., Rossi, W., and Zezell, D. M. (2006) Spectroscopic alterations on enamel and dentin after nanosecond Nd:YAG laser irradiation. Spectrochimica Acta Part A, 1142–1146.
14. Bistey, T., Nagy, I. P., Simo, A., and Hegedus, C. (2007) In vitro FT-IR study of the effects of hydrogen peroxide on superficial tooth enamel. J Dent, 35(4):325–330.
15. Chung, H. Y., and Li, C. C. (2013) Microstructure and nanomechanical properties of enamel remineralized with asparagine-serine-serine peptide. Mater Sci Eng C Mater Biol Appl, 33 (2):969–973.
16. Cohen, J., Featherstone, J. D., Le, C. Q., Steinberg, D., and Feuerstein, O. (2014) Effects of CO2 laser irradiation on tooth enamel coated with biofilm. Lasers Surg Med, 46(3):216–223.
17. Correa-Afonso, A. M., Bachmann, L., Almeida, C. G., Corona, S. A., and Borsatto, M. C. (2012) FTIR and SEM analysis of CO2 laser irradiated human enamel. Arch Oral Biol, 57 (9):1153–1158.
18. Correa-Afonso, A. M., Bachmann, L., de Almeida, C. G., Dibb, R. G., and Borsatto, M. C. (2015) Loss of structural water and carbonate of Nd:YAG laser-irradiated human enamel. Lasers Med Sci, 30(4):1183–1187.
19. Gonzalez-Lopez, S., Torres-Rodriguez, C., Bolanos-Carmona, V., Sanchez-Sanchez, P., Rodriguez-Navarro, A., Alvarez-Lloret, P., et al. (2016) Effect of 30% hydrogen peroxide on mineral chemical composition and surface morphology of bovine enamel. Odontology, 104 (1):44–52.
20. Kim, I. H., Son, J. S., Min, B. K., Kim, Y. K., Kim, K. H., and Kwon, T. Y. (2016) A simple, sensi-tive and non-destructive technique for characterizing bovine dental enamel erosion: attenuated total reflection Fourier transform infrared spectroscopy. Int J Oral Sci, 8(1):54–60.
21. [illegible] Anderson, P. (9):1096–1104.
22. Rabelo, J. S., Ana, P. A., Benetti, C., Valerio, M.E.G., and Zezell, D. M. (2006) Changes in Dental Enamel Oven Heated or Irradiated with Er,Cr:YSGG Laser. Analysis by FTIR. Laser Physics, 20:871–875.
23. Sa, Y., Liang, S., Ma, X., Lu, S., Wang, Z., Jiang, T., et al. (2014) Compositional, structural and mechanical comparisons of normal enamel and hypomaturation enamel. Acta Biomater, 10 (12):5169–5177.

24. Sari, M. E., Erturk, A. G., Koyuturk, A. E., and Bekdemir, Y. (2014) Evaluation of the effect of food and beverages on enamel and restorative materials by SEM and Fourier transform infrared spectroscopy. Microsc Res Tech, 77(1):79–90.
25. Sato, C., Rodrigues, F. A., Garcia, D. M., Vidal, C. M., Pashley, D. H., Tjaderhane, L., et al. (2013) Tooth bleaching increases dentinal protease activity. J Dent Res, 92(2):187–192.
26. Severcan, F., Gokduman, K., Dogan, A., Bolay, S., and Gokalp, S. (2008) Effects of in-office and at-home bleaching on human enamel and dentin: an in vitro application of Fourier transform infrared study. Appl Spectrosc, 62(11):1274–1279.
27. Taube, F., Marczewski, M., and Noren, J. G. (2015) Deviations of inorganic and organic carbon content in hypomineralised enamel. J Dent, 43(2):269–278.
28. Bachmann, L., Diebolder, R., Hibst, R., and Zezell, D. M. (2005) Changes in chemical composition and collagen structure of dentine tissue after erbium laser irradiation. Spectrochim Acta A Mol Biomol Spectrosc, 61(11–12):2634–2639.
29. Bachmann, L., Gomes, A. S., and Zezell, D. M. (2005) Collagen absorption bands in heated and rehydrated dentine. Spectrochim Acta A Mol Biomol Spectrosc, 62(4–5):1045–1049.
30. Botta, S. B., Ana, P. A., Santos, M. O., Zezell, D. M., and Matos, A. B. (2012) Effect of dental tissue conditioners and matrix metalloproteinase inhibitors on type I collagen microstructure ana-lyzed by Fourier transform infrared spectroscopy. J Biomed Mater Res B Appl Biomater, 100 (4):1009–1016.
31. Chen, M., Zhang, Y., Dusevich, V., Liu, Y., Yu, Q., and Wang, Y. (2014) Non-thermal atmospheric plasma brush induces HEMA grafting onto dentin collagen. Dent Mater, 30(12):1369–1377.
32. Deng, M., Dong, X., Zhou, X., Wang, L., Li, H., and Xu, X. (2013) Characterization of dentin matrix biomodified by Galla chinensis extract. J Endod, 39(4):542–547.
33. Gan, J., Liu, S., Zhou, L., Wang, Y., Guo, J., and Huang, C. (2017) Effect of Nd:YAG Laser Irradi-ation Pretreatment on the Long-Term Bond Strength of Etch-and-Rinse Adhesive to Dentin. Oper Dent, 42(1):62–72.
34. Lin, C. P., Lee, B. S., Lin, F. H., Kok, S. H., and Lan, W. H. (2001) Phase, compositional, and morphological changes of human dentin after Nd:YAG laser treatment. J Endod, 27(6):389–393.
35. Liu, Y., and Wang, Y. (2013) Proanthocyanidins' efficacy in stabilizing dentin collagen against enzymatic degradation: MALDI-TOF and FTIR analyses. J Dent, 41(6):535–542.
36. Liu, Y., Yao, X., Liu, Y. W., and Wang, Y. (2014) A Fourier transform infrared spectroscopy analysis of carious dentin from transparent zone to normal zone. Caries Res, 48(4):320–329.
37. Maske, T. T., Isolan, C. P., van de Sande, F. H., Peixoto, A. C., Faria, E.S.A.L., Cenci, M. S., et al. (2015) A biofilm cariogenic challenge model for dentin demineralization and dentin bonding analysis. Clin Oral Investig, 19(5):1047–1053.
38. Neelakantan, P., Sharma, S., Shemesh, H., and Wesselink, P. R. (2015) Influence of Irrigation Sequence on the Adhesion of Root Canal Sealers to Dentin: A Fourier Transform Infrared Spectroscopy and Push-out Bond Strength Analysis. J Endod, 41(7):1108–1111.
39. Prado, M., Roizenblit, R. N., Pacheco, L. V., Barbosa, C. A., Lima, C. O., and Simao, R. A. (2016) Effect of Argon Plasma on Root Dentin after Use of 6% NaOCl. Braz Dent J, 27(1):41–45.
40. Rodrigues, R. B., Soares, C. J., Junior, P.C.S., Lara, V. C., Arana-Chavez, V. E., and Novais, V. R. (2017) Influence of radiotherapy on the dentin properties and bond strength. Clin Oral Investig.
41. Sasaki, K. M., Aoki, A., Masuno, H., Ichinose, S., Yamada, S., and Ishikawa, I. (2002) Compositional analysis of root cementum and dentin after Er:YAG laser irradiation compared with CO2 lased and intact roots using Fourier transformed infrared spectroscopy. J Periodontal Res, 37 (1):50–59.
42. Silva Junior, Z. S., Botta, S. B., Ana, P. A., Franca, C. M., Fernandes, K. P., Mesquita-Ferrari, R. A., et al. (2015) Effect of papain-based gel on type I collagen–spectroscopy applied for microstructural analysis. Sci Rep, 5:11448.
43. Tabatabaei, F. S., Tatari, S., Samadi, R., and Torshabi, M. (2016) Surface characterization and biological properties of regular dentin, demineralized dentin, and deproteinized dentin. J Mater Sci Mater Med, 27(11):164.

44. Tezvergil-Mutluay, A., Seseogullari-Dirihan, R., Feitosa, V. P., Tay, F. R., Watson, T. F., Pashley, D. H., et al. (2014) Zoledronate and ion-releasing resins impair dentin collagen degradation. J Dent Res, 93(10):999–1004.
45. Ubaldini, A. L., Baesso, M. L., Medina Neto, A., Sato, F., Bento, A. C., and Pascotto, R. C. (2013) Hydrogen peroxide diffusion dynamics in dental tissues. J Dent Res, 92(7):661–665.
46. Yassen, G. H., Chu, T. M., Eckert, G., and Platt, J. A. (2013) Effect of medicaments used in endodontic regeneration technique on the chemical structure of human immature radicular dentin: an in vitro study. J Endod, 39(2):269–273.
47. Yassen, G. H., Eckert, G. J., and Platt, J. A. (2015) Effect of intracanal medicaments used in end-odontic regeneration procedures on microhardness and chemical structure of dentin. Restor Dent Endod, 40(2):104–112.
48. Benetti, C., Ana, P. A., Bachmann, L., and Zezell, D. M. (2015) Mid-Infrared Spectroscopy Analysis of the Effects of Erbium, Chromium:Yattrium-Scandium-Gallium-Garnet (Er,Cr: YSGG) Laser Irradiation on Bone Mineral and Organic Components. Appl Spectrosc, 69 (12):1496–1504.
49. Gamsjaeger, S., Brozek, W., Recker, R., Klaushofer, K., and Paschalis, E. P. (2014) Transmeno-pausal changes in trabecular bone quality. J Bone Miner Res, 29(3):608–617.
50. Gamsjaeger, S., Mendelsohn, R., Boskey, A. L., Gourion-Arsiquaud, S., Klaushofer, K., and Paschalis, E. P. (2014) Vibrational spectroscopic imaging for the evaluation of matrix and mineral chemistry. Curr Osteoporos Rep, 12(4):454–464.
51. Gong, B., Mandair, G. S., Wehrli, F. W., and Morris, M. D. (2014) Novel assessment tools for osteoporosis diagnosis and treatment. Curr Osteoporos Rep, 12(3):357–365.
52. Gourion-Arsiquaud, S., Faibish, D., Myers, E., Spevak, L., Compston, J., Hodsman, A., et al. (2009) Use of FTIR spectroscopic imaging to identify parameters associated with fragility fracture. J Bone Miner Res, 24(9):1565–1571.
53. Gu, C., Katti, D. R., and Katti, K. S. (2013) Photoacoustic FTIR spectroscopic study of undisturbed human cortical bone. Spectrochim Acta A Mol Biomol Spectrosc, 103:25–37.
54. Ou-Yang, H., Paschalis, E. P., Mayo, W. E., Boskey, A. L., and Mendelsohn, R. (2001) Infrared microscopic imaging of bone: spatial distribution of CO3(2-). J Bone Miner Res, 16(5):893–900.
55. Paschalis, E. P., Gamsjaeger, S., and Klaushofer, K. (2017) Vibrational spectroscopic techniques to assess bone quality. Osteoporos Int, 28(8):2275–2291.
56. Rey, C., Collins, B., Goehl, T., Dickson, I. R., and Glimcher, M. J. (1989) The carbonate environ-ment in bone mineral: a resolution-enhanced Fourier Transform Infrared Spectroscopy Study. Calcif Tissue Int, 45(3):157–164.
57. Reyes-Gasga, J., Martinez-Pineiro, E. L., Rodriguez-Alvarez, G., Tiznado-Orozco, G. E., Garcia-Garcia, R., and Bres, E. F. (2013) XRD and FTIR crystallinity indices in sound human tooth enamel and synthetic hydroxyapatite. Mater Sci Eng C Mater Biol Appl, 33(8):4568–4574.
58. Mitic, Z., Stolic, A., Stojanovic, S., Najman, S., Ignjatovic, N., Nikolic, G., et al. (2017) Instrumen-tal methods and techniques for structural and physicochemical characterization of biomaterials and bone tissue: A review. Mater Sci Eng C Mater Biol Appl, 79:930–949.
59. Andrew Chan, K. L., and Kazarian, S. G. (2016) Attenuated total reflection Fourier-transform infrared (ATR-FTIR) imaging of tissues and live cells. Chem Soc Rev, 45(7):1850–1864.
60. Griffiths, P. R., de Haseth, J. A. Fourier Transform Infrared Spectrometry. 2nd ed. New York, NY, USA: John Wiley & Sons; 2007. p. 560.
61. Parikh, S. J., and Chorover, J. (2005) FTIR spectroscopic study of biogenic Mn-oxide formation by Pseudomonas putida GB-1. Geomicrobiology Journal, 22:207–218.
62. Chen, Y., Zou, C., Mastalerz, M., Hu, S., Gasaway, C., and Tao, X. (2015) Applications of Micro-Fourier Transform Infrared Spectroscopy (FTIR) in the Geological Sciences–A Review. Int J Mol Sci, 16(12):30223–30250.
63. Kazarian, S. G., and Chan, K. L. (2013) ATR-FTIR spectroscopic imaging: recent advances and applications to biological systems. Analyst, 138(7):1940–1951.
64. Rehman, I., and Bonfield, W. (1997) Characterization of hydroxyapatite and carbonated apatite by photo acoustic FTIR spectroscopy. J Mater Sci Mater Med, 8(1):1–4.

65. Acerbo, A. S., Carr, G. L., Judex, S., and Miller, L. M. (2012) Imaging the material properties of bone specimens using reflection-based infrared microspectroscopy. Anal Chem, 84(8):3607–3613.
66. Ruohonen, M., Palo, K., and Alander, J. (2013) Spectroscopic Detection of Caries Lesions. J Med Eng, 2013:161090.
67. Skoog, D. A., Holler, F. J., and Nieman, T. A. (1998) Principles on instrumental analysis. 5th Phil-adelphia: Saunders College Pub. Orlando, Fla.
68. Stuart, B. H. (2004) Infrared Spectroscopy: Fundamentals and Applications. 1 John Wiley & Sons.
69. Bachmann, L., Diebolder, R., Hibst, R., and Zezell, D. M. (2003) Infrared Absorption Bands of Enamel and Dentin Tissues from Human and Bovine Teeth. Applied Spectroscopy Reviews, 38:1–14.
70. Palmer, L. C., Newcomb, C. J., Kaltz, S. R., Spoerke, E. D., and Stupp, S. I. (2008) Biomimetic sys-tems for hydroxyapatite mineralization inspired by bone and enamel. Chem Rev, 108(11):4754– 4783.
71. Paine, M. L., White, S. N., Luo, W., Fong, H., Sarikaya, M., and Snead, M. L. (2001) Regu-lated gene expression dictates enamel structure and tooth function. Matrix Biol, 20(5– 6):273–292.
72. Khanarian, N. T., Boushell, M. K., Spalazzi, J. P., Pleshko, N., Boskey, A. L., and Lu, H. H. (2014) FTIR-I compositional mapping of the cartilage-to-bone interface as a function of tissue region and age. J Bone Miner Res, 29(12):2643–2652.
73. Donnelly, E., Meredith, D. S., Nguyen, J. T., and Boskey, A. L. (2012) Bone tissue composi-tion varies across anatomic sites in the proximal femur and the iliac crest. J Orthop Res, 30 (5):700–706.
74. LeGeros, R. Z., Bonel, G., and Legros, R. (1978) Types of "H2O" in human enamel and in precip-itated apatites. Calcif Tissue Res, 26(2):111–118.
75. Nelson, D. G., and Featherstone, J. D. (1982) Preparation, analysis, and characterization of car-bonated apatites. Calcif Tissue Int, 34(Suppl 2):S69–81.
76. Duverger, O., Beniash, E., and Morasso, M. I. (2016) Keratins as components of the enamel organic matrix. Matrix Biol, 52–54:260–265.
77. Grippo, J. O., Simring, M., and Schreiner, S. (2004) Attrition, abrasion, corrosion and abfraction revisited: a new perspective on tooth surface lesions. J Am Dent Assoc, 135(8):1109–1118; quiz 1163–1105.
78. Gadhia, K., McDonald, S., Arkutu, N., and Malik, K. (2012) Amelogenesis imperfecta: an intro-duction. Br Dent J, 212(8):377–379.
79. Willmott, N. S., Bryan, R. A., and Duggal, M. S. (2008) Molar-incisor-hypomineralisation: a lit-erature review. Eur Arch Paediatr Dent, 9(4):172–179.
80. Xu, C., and Wang, Y. (2012) Chemical composition and structure of peritubular and intertubular human dentine revisited. Arch Oral Biol, 57(4):383–391.
81. Beniash, E., Traub, W., Veis, A., and Weiner, S. (2000) A transmission electron microscope study using vitrified ice sections of predentin: structural changes in the dentin collagenous matrix prior to mineralization. J Struct Biol, 132(3):212–225.
82. Goldberg, M., Kulkarni, A. B., Young, M., and Boskey, A. (2011) Dentin: structure, composition and mineralization. Front Biosci (Elite Ed), 3:711–735.
83. Marshall, G. W., Habelitz, S., Gallagher, R., Balooch, M., Balooch, G., and Marshall, S. J. (2001) Nanomechanical properties of hydrated carious human dentin. J Dent Res, 80(8):1768–1771.
84. Ramakrishnaiah, R., Rehman, G. u., Basavarajappa, S., Khuraif, A.A.A., Durgesh, B. H., Khan, A. S., et al. (2015) Applications of Raman Spectroscopy in Dentistry: Analysis of Tooth Structure. Applied Spectroscopy Reviews, 50:332–350.
85. Liu, Y., Bai, X., Li, S., Liu, Y., Keightley, A., and Wang, Y. (2015) Molecular weight and galloyla-tion affect grape seed extract constituents' ability to cross-link dentin collagen in clinically rele-vant time. Dent Mater, 31(7):814–821.
86. Fredericks, J. D., Bennett, P., Williams, A., and Rogers, K. D. (2012) FTIR spectroscopy: A new diagnostic tool to aid DNA analysis from heated bone. Forensic Sci Int Genet, 6(3):375–380.

87. Barth, H. D., Zimmermann, E. A., Schaible, E., Tang, S. Y., Alliston, T., and Ritchie, R. O. (2011) Characterization of the effects of x-ray irradiation on the hierarchical structure and mechanical properties of human cortical bone. Biomaterials, 32(34):8892–8904.
88. McElderry, J. D., Zhu, P., Mroue, K. H., Xu, J., Pavan, B., Fang, M., et al. (2013) Crystallinity and compositional changes in carbonated apatites: Evidence from 31P solid-state NMR, Raman, and AFM analysis. J Solid State Chem, 206.
89. Thompson, T. U., Islam, M., and Bonniere, M. (2013) A new statistical approach for determining the crystallinity of heat-altered bone mineral from FTIR spectra. Journal of Archaeological Science, 40(1):416–422.
90. Boskey, A., and Mendelsohn, R. (2005) Infrared analysis of bone in health and disease. J Biomed Opt, 10(3):031102.
91. Termine, J. D., and Posner, A. S. (1966) Infra-red determinaion of the percentage of crystallinity in apatitic calcium phosphates. Nature, 211(5046):268–270.
92. Boyar, H., Turan, B., and Severcan, F. (2003) FTIR Spectroscopic Investigation of Mineral Structure of Streptozotocin Induced Diabetic Rat Femur and Tibia. Spectroscopy, 17:627–633.
93. Ellingham, S. T., Thompson, T. J., Islam, M., and Taylor, G. (2015) Estimating temperature exposure of burnt bone – A methodological review. Sci Justice, 55(3):181–188.
94. Eliaz, N., and Metoki, N. (2017) Calcium Phosphate Bioceramics: A Review of Their History, Structure, Properties, Coating Technologies and Biomedical Applications. Materials (Basel), 10(4).
95. Russo, A., Bianchi, M., Sartori, M., Boi, M., Giavaresi, G., Salter, D. M., et al. (2018) Bone regen-eration in a rabbit critical femoral defect by means of magnetic hydroxyapatite macroporous scaffolds. J Biomed Mater Res B Appl Biomater, 106(2):546–554.
96. Kakar, A., Rao, B.H.S., Hegde, S., Deshpande, N., Lindner, A., Nagursky, H., et al. (2017) Ridge preservation using an in situ hardening biphasic calcium phosphate (beta-TCP/HA) bone graft substitute-a clinical, radiological, and histological study. Int J Implant Dent, 3(1):25.
97. LeGeros, R. Z. (1991) Calcium phosphates in oral biology and medicine. Monogr Oral Sci, 15:1– 201.
98. Cozza, N., Monte, F., Bonani, W., Aswath, P., Motta, A., and Migliaresi, C. (2017) Bioactivity and mineralization of natural hydroxyapatite from cuttlefish bone and Bioglass((R)) co-sintered bioceramics. J Tissue Eng Regen Med.
99. Wang, P., Zhao, L., Liu, J., Weir, M. D., Zhou, X., and Xu, H. H. (2014) Bone tissue engineering via nanostructured calcium phosphate biomaterials and stem cells. Bone Res, 2:14017.
100. Miranda, P., Saiz, E., Gryn, K., and Tomsia, A. P. (2006) Sintering and robocasting of beta-trical-cium phosphate scaffolds for orthopaedic applications. Acta Biomater, 2(4):457–466.
101. Perera, F. H., Martınez-Vazquez, F. J., Miranda, P., Ortiz, A. L., and Pajares, A. (2010) Clarifying the effect of sintering conditions on the microstructure and mechanical properties of b-trical-cium phosphate. Ceramics International, 36(6):1929–1935.
102. Lemons, J. E. (1996) Ceramics: past, present, and future. Bone, 19(1 Suppl):121S–128S.
103. Sroka-Bartnicka, A., Borkowski, L., Ginalska, G., Slosarczyk, A., and Kazarian, S. G. (2017) Structural transformation of synthetic hydroxyapatite under simulated in vivo conditions studied with ATR-FTIR spectroscopic imaging. Spectrochim Acta A Mol Biomol Spectrosc, 171:155– 161.
104. Amaral, J. G., Pessan, J. P., Souza, J.A.S., Moraes, J.C.S., Delbem, A.C.B. (2018) Cyclotriphosphate associated to fluoride increases hydroxyapatite resistance to acid attack. J Biomed Mater Res B Appl Biomater.
105. Baba Ismail, Y. M., Wimpenny, I., Bretcanu, O., Dalgarno, K., El Haj, A. J. (2017) Development of multisubstituted hydroxyapatite nanopowders as biomedical materials for bone tissue engineering applications. J Biomed Mater Res A, 105(6):1775–1785.
106. Bertran, O., del Valle, L. J., Revilla-Lopez, G., Rivas, M., Chaves, G., Casas, M. T., et al. (2015) Synergistic approach to elucidate the incorporation of magnesium ions into hydroxyapatite. Chemistry, 21(6):2537–2546.
107. Sofronia, A. M., Baies, R., Anghel, E. M., Marinescu, C. A., and Tanasescu, S. (2014) Thermal and structural characterization of synthetic and natural nanocrystalline hydroxyapatite. Mater Sci Eng C Mater Biol Appl, 43:153–163.

108. Eslami, H., Solati-Hashjin, M., and Tahriri, M. (2009) The comparison of powder characteristics and physicochemical, mechanical and biological properties between nanostructure ceramics of hydroxyapatite and fluoridated hydroxyapatite. Materials Science and Engineering: C, 29 (4):1387–1398.
109. Rintoul, L., Wentrup-Byrne, E., Suzuki, S., and Grondahl, L. (2007) FT-IR spectroscopy of fluoro-substituted hydroxyapatite: strengths and limitations. J Mater Sci Mater Med, 18 (9):1701–1709.
110. Vallet-Regi, M. (2006) Revisiting ceramics for medical applications. Dalton Trans, (44):5211–5220.
111. Liu, Y., and Hsu, C. Y. (2007) Laser-induced compositional changes on enamel: a FT-Raman study. J Dent, 35(3):226–230.
112. Paschalis, E. P., Verdelis, K., Doty, S. B., Boskey, A. L., Mendelsohn, R., and Yamauchi, M. (2001) Spectroscopic characterization of collagen cross-links in bone. J Bone Miner Res, 16 (10):1821–1828.
113. Knott, L., and Bailey, A. J. (1998) Collagen cross-links in mineralizing tissues: a review of their chemistry, function, and clinical relevance. Bone, 22(3):181–187.
114. Dong, A., Huang, P., and Caughey, W. S. (1990) Protein secondary structures in water from sec-ond-derivative amide I infrared spectra. Biochemistry, 29(13):3303–3308.
115. Cummings, S. R., Black, D. M., Thompson, D. E., Applegate, W. B., Barrett-Connor, E., Musliner, T. A., et al. (1998) Effect of alendronate on risk of fracture in women with low bone density but without vertebral fractures: results from the Fracture Intervention Trial. JAMA, 280 (24):2077–2082.
116. Speiser, P. W., Clarson, C. L., Eugster, E. A., Kemp, S. F., Radovick, S., Rogol, A. D., et al. (2005) Bisphosphonate treatment of pediatric bone disease. Pediatr Endocrinol Rev, 3(2):87–96.
117. Renders, G. A., Mulder, L., Langenbach, G. E., van Ruijven, L. J., van Eijden, T. M. (2008) Bio-mechanical effect of mineral heterogeneity in trabecular bone. J Biomech, 41(13):2793–2798.
118. Bi, X., Li, G., Doty, S. B., and Camacho, N. P. (2005) A novel method for determination of colla-gen orientation in cartilage by Fourier transform infrared imaging spectroscopy (FT-IRIS). Oste-oarthritis Cartilage, 13(12):1050–1058.

3.2 - Capítulo 2

Effect of radiotherapy and salivary flow rateon root dentin caries progression

Artigo a ser submetido para o periódico Clinical Oral Investigation

Title

Effect of radiotherapy and salivary flow rateon root dentin caries progression

Abstract

Objectives: To evaluate the effect of ionizing radiation and salivary flow raterate on the initial development of artificial induced root dentin caries lesions.

Materials and methods: Microcosm biofilms were grown under two different protocols of salivary flow rate (0.06 ml min^{-1} and 0.03 ml min^{-1}, study 1 and 2, respectively) on non-irradiated and irradiated root dentin blocks for up to seven days. Root dentin's vibration modes, matrix/mineral (M/M) and carbonate/mineral (C/M) ratios were evaluated by FTIR. The mineral density was assessed by micro-ct.

Results: In study 1, FTIR revealed an increase in amide III and $v_{1,}\ v_3\ PO_4^{-3}$ values and a decrease in amide II, v_4, $v_2\ PO_4^{-3}$ and C/M ratio in caries affected dentin (CAD). In addition, significantly lower $v_{1,}\ v_3\ PO_4^{-3}$, $v_2\ CO_3^{-2}$ and C/M values were found for irradiated dentin. Differences in mineral density were not significant. In study 2, FTIR also revealed a decrease in amide II and v_4, $v_2\ PO_4^{-3}$, as well as in $v_2\ CO_3^{-2}$ with CAD. Higher $v_{1,}\ v_3\ PO_4^{-3}$ was found for irradiated dentin ($p=0.019$) with no differences between sound and CAD. Irradiated CAD presented higher values of amide III than non-irradiated CAD. Irradiated dentin presented lower mineral density.

Conclusions: Initial caries lesions differed between non-irradiated dentin and irradiated dentin and between normal and reduced salivary flow rate. Alterations in the inorganic and organic matrix and in mineral density was found for irradiated dentin. With reduced salivary flow, mineral alterations were more detectable in the caries lesions.

Clinical relevance: Ionizing radiation and low salivary flow rateenhanced root dentin caries susceptibility.

Key-words: Fourier-transform infrared spectroscopy, ionizing radiation, mineral density, root dentin caries, salivary flow

Introduction

Dental caries is one of the most common oral diseases in humans (1), and its development is associated to a sucrose-rich diet and to an undisturbed microbial biofilm growth on teeth surface (2). Patients with head and neck cancer may have an unusual type of caries among long term effects (3). Radiation-related caries (RRC) have a rapid progression and is highly destructive (4-6). A wide discussion has been made on this topic, whether RRC is originated from a direct or indirect effect of radiation on teeth (5-7). However, other disorders that cause hyposalivation, like diabetes, Sjogren's syndrome, aging, the use of chemotherapy agents, anti-hypertensives and psychiatric agents, do not produce similar lesions to RCC (6, 7). This aspect leads to an understanding that the disease is due to both effects (6, 7). In vitro and in situ studies showed altered morphological, chemical, and mechanical properties of mineralized teeth tissues as well as increased susceptibility of enamel delamination (8-15). Among the indirect effects, it can be mention salivary changes, such as hyposalivation, reducing the effectiveness of saliva in promoting buffer and cleaning activities (16), as well as changes in its composition, pH and oral microbiota (17).

RCC usually presents a circumferential demineralization on the cervical area of the tooth, affecting smooth enamel surfaces that are usually resistant to dental caries, as well as exposed cement surfaces (18). Root dentin caries represents a challenge due to its greater susceptibility to demineralization and treatment when compared to enamel caries (6, 7). Dentin vulnerability to acidic dissolution is because of its higher critical pH for demineralization (6.2 - 6.4) than that of enamel (5.5) (19) and structural morphology (20). The dentin contains a considerable amount of organic material, so the tilt in the balance between demineralization and remineralization towards demineralization process can not explain the dentin caries by itself. The collagen degradation (proteolysis theory) might also play a role in dentin caries development (21).

The development of laboratory models that let biofilm formation for extended periods under controlled conditions have been useful for simulating the oral environment in vitro (22). Dynamic biofilm models presents some advantages, once it allows the manipulation of the variables and the simulation of the physiological and dynamic conditions of the oral environment, such as pH oscillations from the exposure to carbohydrate source, salivary flow rate that might influence bacterial adherence (22).

Bacterial methods approach from reality, the lesions formed mimic the natural morphology of caries lesions, with the presence of an irregular surface, demineralization of intertubular dentin, degradation of collagen fibrils, discreet opening of dentinal tubules (23).

Since the literature shows that there is radiation-induced damage increasing susceptibility to caries, it is expected a different pattern of demineralization in irradiated dentin (24) in vitro. Therefore, the aim of the present study was to compare the initial development of dentin caries in irradiated and non-irradiated dentin by a dynamic microcosm biofilm model and the influence of a normal and a reduced salivary flow rate. The null hypothesis tested was that artificial caries lesion would not differ between non-irradiated dentin and irradiated dentin, neither between normal and reduced salivary flow rate.

Material and Methods

After approval from the Research Ethics Committee (No. 37868814.6.0000.5152), freshly extracted human third molars were collected, cleaned and stored in refrigerated deionized water (4°C), up to 3 months after extraction. Before the experimental procedures, the teeth were examined under a stereoscopic microscope (Leica MS5, Leica Microscopy Systems Ltd; Heerbrugg, Switzerland) to show evidence of caries, enamel hypoplasia and other defects. Forty sound teeth were selected and randomly divided into two studies according to the flow rate of the dynamic microcosm biofilm model: 0.06 ml min^{-1} (normal salivary flow rate) and 0.03 ml min^{-1} (reduced salivary flow rate), simulating a normal and a reduced salivary flow, respectively. For each study, the teeth were divided as follows (n=10): non-irradiated and irradiated.

The teeth of the irradiated group were subjected to fractionated x-ray radiation of 2 Gy per day, applied 5 days per week, during 7 weeks, totalizing 70 Gy. The x-rays source was a linear accelerator (Clinac 600C Varian®— Palo Alto, CA, EUA, Beam 6 MV). Samples were submerged in distilled water during radiotherapy.

Specimen preparation

The teeth were cut at the cementoenamel junction using a water-cooled diamond saw (Isomet, 15HC diamond; Buehler Ltd., Lake Bluff, IL, USA) mounted on a precision saw

(Isomet 1000; Buehler Ltd., Lake Bluff, IL, USA). Another section was made 3 mm below, obtaining a slice of root dentin. The slices were cut into a 2 mm x 4 mm x 2 mm dentin block. Root dentin was wet ground with 600, 1200, 2000 and 2500 grit silicon carbide papers, to obtain a plan surface. Nail varnish (Colorama Maybelline; São Paulo, SP, Brazil) was applied to the sides and bottom of the block, leaving half of the vestibular dentin exposed. Thus, the root dentin blocks were divided into two subgroups (n=10) according to cariogenic challenge: sound (nail varnish protected surface) and caries affected dentin (exposed surface). The blocks were fixed on the removable device placed in the independent units of the culture chamber with high temperature neutral silicone (Wurth do Brazil Peças de Fixação Ltda, São Paulo, SP, Brazil). The culture chamber with the samples inside was sterilized by autoclaving (121 °C for 15 min) (25).

Microcosm Biofilm Model – artificial dentin caries lesions

Fresh whole saliva stimulated by paraffin film chewing was collected from a healthy volunteer (male, aged 24), who had not been under antibiotic therapy at least 6 months. The volunteer abstained from oral hygiene for 24 h and food ingestion for 2 h before saliva collection. The saliva (20 ml) was collected directly into a sterile tube kept on ice and immediately used for baseline analysis (baseline microbial composition – CFU ml^{-1}) and inoculation procedures for biofilm growth (26).

For the inoculation procedures, 12 ml of the saliva was immediately added to 240 ml of sterile defined medium enriched with mucin (DMM) (pH=7.0). The solution was gently homogenized and placed in the culture chamber. Twenty-one ml of DMM/saliva solution were injected into each sample-accommodating independent unit through the specific inoculum-feeding inlet. One hour after initial microbial inoculation, sterile DMM was pumped at a flow-rate of 0.06 ml min^{-1} and 0.03 ml min^{-1}, study1 and study 2, respectively, simulating a normal and a reduced salivary flow. Sucrose pulses started 2 h later (5% sucrose solution, 0.25 ml min^{-1}, 6 min exposure, three times daily with 8 h intervals). The experiments were carried out for up to seven days (26).

Fourier Transform Infrared Spectroscopy (FTIR)

Chemical composition of sound and caries affected dentin was determined for each group using Fourier Transform Infrared Spectroscopy (FTIR Vertex 70 – Bruker; Ettlingen,

Baden-Württemberg, Germany) with an attenuated total reflectance (ATR) accessory. The testing surface was positioned against the diamond crystal of the ATR unit and pressed with a force gauge at constant pressure. Then, the spectra were acquired in the absorbance mode using 32 co-added scans acquired at a frequency range between 400–4,000 cm^{-1} and resolution of 4 cm^{-1}. Spectra were recorded and analyzed by OPUS 6.5 software (Bruker, Ettlingen, Germany). After baseline correction and normalization, the integrated areas of specific bands of organic and inorganic dentin content were calculated: the ν_1 and ν_3 vibration modes of phosphate (PO_4^{-3}) (1300-900 cm^{-1}), amide I (1680-1600 cm^{-1}), the superposition of the carbonate (CO_3^{-2}) + amide II (1580-1480 cm^{-1}), amide III + collagen structure (1200-1300 cm^{-1}), the ν_2 vibration mode of CO_3^{-2} (around 870 cm^{-1}), the superposition of the stretching ν_3 and bending ν_4 vibration mode of CO_3^{-2} (between 1600-1300 cm^{-1}) and the ν_4, ν_2 vibration mode of PO_4^{-3} (617-472 cm^{-1}). The following parameters were also evaluated: (1) mineral/matrix ratio – M/M (the ratio between integrated areas of the C=O stretching of collagen amide I to ν_4, ν_2 PO_4^{-3}); (2) carbonate/mineral ratio C/M (the ratio of the integrated areas of ν_2 CO_3^{-2} to the ν_1, ν_3 PO_4^{-3}) (27, 28).

Micro-ct

Four dentin blocks of each group were scanned using a micro-CT scanner (Skyscan 1272; Skyscan, Kontich, Belgium) to assess mineral density. The following parameters were applied: 70 kV, 142 µA, 5 µm pixel size, 0.5 mm aluminium filter, 0.4° rotation step, and frame averaging of 2. Before the acquisition of the dentin blocks, an acquisition of the HAP phantom of 8mm was done to aid the calculation of mineral density. Further, the specimens were positioned in a closed plastic tube immersed in distilled water and scanned. Scan data for each tooth were reconstructed using the NRecon software (Skyscan). Reconstructed 3-dimensional images were processed and viewed using CTAn data-analyzing software (SkyScan). After generating a correlation between the attenuation coefficient and phantom values (0.75 and 0.25), sound and caries affected dentin were analyzed. The central region of the image of each dentin block was measured, and a square region of interest (ROI) was defined - 1 × 1,5 mm, being analyzed 8 slices below the surface (40µm) (29). Each area of dentin exposed to the biofilm was compared to a corresponding area of sound dentine (covered with nail varnish) in the same block.

Statistical analysis

Data were tested for normal distribution (Shapiro-Wilk, $p > 0.05$) and equality of variances (Levene's test, $p > 0.05$). ATR/FTIR and micro-ct data were analyzed by two-way repeated measurement (RM) ANOVA, considering the factors irradiation and cariogenic challenge, followed by Tukey's post hoc test. Sigma Plot statistical package (version 12.0, Systat Software, Inc., San Jose, CA, USA) was used for analysis and a p value of less than 0.05 was considered to be statistically significant.

Results

Normal salivary flow rate

The spectrum for the studied groups are shown in Figure 1. The mean and standard deviation values for the vibration modes and chemical parameters obtained by ATR/FTIR are shown in Table 1. No statistical differences were found for Amide I, v_3, $v_4\,CO_3^{-2}$ and M/M ratio. For Amide III, Amide II and v_4, $v_2\,PO_4^{-3}$, two-way RM ANOVA showed significant effect only for caries challenge ($p<0.001$). Tukey's post hoc test revealed increased Amide III with caries challenge, although Amide II and v_4, $v_2\,PO_4^{-3}$ decreased. Significantly lower v_1, $v_3\,PO_4^{-3}$ and C/M values were found for irradiated dentin ($p= 0.038$ and 0.042, respectively). Lower C/M values were also found for caries affected dentin ($p=0.026$), whereas higher v_1, $v_3\,PO_4^{-3}$values were found for caries affected dentin. In addition, irradiated dentin showed a significant lower $v_2\,CO_3^{-2}$ ($p=0.026$). The differences in mineral density mean values were not statistically significant for irradiation, caries challenge and for the interaction ($p=0.560$; $p=0.094$; $p=0.392$, respectively) (Figure 2-a).

Reduced salivary flow rate

The spectrum for the studied groups are shown in Figure 3. The mean and standard deviation values for the vibration modes and chemical parameters obtained by ATR/FTIR are shown in Table 2. Regarding the Amide I, v_3, $v_4\,CO_3^{-2}$ and M/M ratio, differences in the mean values were not statistically significant for both variables under analysis. The analysis of Amide II, v_4, $v_2\,PO_4^{-3}$, $v_2\,CO_3^{-2}$ and C/M ratio showed only statistically differences for caries challenge ($p=0.001$, $p<0.001$, $p=0.026$ and $p=0.002$, respectively). Tukey's post hoc test revealed decreased mean values with caries challenge for all these

parameters. Statistically higher $v_{1,}\, v_3\, PO_4^{-3}$ was found for irradiated dentin (p=0.019) with no differences between sound and caries affected dentin. For Amide III, the interaction between the studied factors was significant (p=0.020), with irradiated caries affected dentin presenting higher values than non-irradiated caries affected dentin. Mineral density showed statistical differences between non-irradiated and irradiated dentin (p=0.030), the latter one presenting lower values (Figure 2-b).

Discussion

The null hypothesis was rejected, since the artificial caries lesion differed between non-irradiated dentin and irradiated dentin, neither between normal and reduced salivary flow rate. The methodologies used in this study provide information about dentine, having the benefit from not being destructive. Fourier transform infrared spectroscopy (FTIR) is a fast sampling technique which requires no or minimal preparation of samples (27, 28). The main dental hard tissues constituents can be analyzed by FTIR; phosphate and carbonate, which are related to the inorganic matrix, and the content of amides I, II and III, which are related to the organic matrix, mainly composed by type-I collagen (27, 28). Another important point is that the use of an ATR promotes a small and well controlled depth of penetration (27, 28). In this way, it is possible to evaluate the chemical changes promoted by artificial caries lesion located strictly on the surface of samples, avoiding the analysis from the untreated tissue. While micro-ct is an analytical tool particularly useful in studying mineral changes in dentin. It represents an excellent option due to its tridimensional nature, which allows analyzing the whole bulk of the specimen, obtains volumetric results, and visualizes the internal structure of an object based on a three-dimensional reconstruction (30).

In the present study, artificial caries lesions were produced using a microbial model. Compared to chemically induced artificial caries models, microbial models have the advantage of producing dentin carious lesions with both mineral loss and the destruction of the organic component, which resembles more the clinical situation (31). However, organic acid production by cariogenic bacteria takes more time to demineralize the dental tissue than does the chemical method (32). The dynamic microcosm biofilm

model used has particular advantages over other systems once it allowed independent biofilm growth and artificial caries development from the same mixed oral flora (saliva) within a common environment (26).

Two cariogenic protocols regimens were tested. In study 1, the flow of artificial saliva solution (0.06 ml min^{-1}) represent in vivo unstimulated salivary flow, in which biofilm formation normally occurs (33). In study 2, the flow rate was modified (0.03 ml min^{-1}) in attempt to simulate the hyposalivation conditions usually observed in post radiotherapy patients with head and neck cancer. In both of them, it was observed an initial dentin demineralization by the FTIR, detected by the reduced v_4, $v_2\ PO_4^{-3}$ area and C/M ratio in study 1 and 2, and also reduced $v_2\ CO_3^{-2}$ in study 2. The hydroxiapatite mineral loss was due to bacterial production of acid from sucrose, occurring a drop in the biofilm pH, which results in the outflow of tooth minerals (21).

In case of organic matrix modifications, the bands of amide I and III are the most sensible to protein structural changes (34). The position and the intensity of these bands are sensitive to the molecular conformation/structure of the polypeptide chains of collagen and proteins (34). The amide I is the main and the most intense band in protein and is governed primarily by the stretching vibrations of the C=O (70–85%) e C–N (10–20%) (34). No alteration was detected in amide I, this result may be explained by the fact that the induced dentin caries lesions reached only initial stages, not occurring degradation of the demineralized matrix. Greater exposure of the organic content was detected by the increased amide III areas in study 1 and only in the irradiated group in study 2. The amide III also shift to slightly different wavenumbers with the artificial caries lesion, and this revealed a change in the molecular structural or compositional differences in peptide chain. This complex band originate from the stretching vibration of C–N (appearing at 1243 cm^{-1}) and plane deformation vibration of N–H (appearing at 1267 cm^{-1}) in the peptide chain of collagen/proteins and depends on the details of the force field, the nature of side chains, and hydrogen bonding (34).

The decrease in amide II can be explained by the fact that the $v_3\ CO_3^{-2}$ overlap with the amide II and it was lost in the demineralization process due to its higher solubility (27). The higher v_1 and $v_3\ PO_4^{-3}$ area in study 1 confirms the results of LeGeros and Al-Naimi (35, 36) who showed that in initial caries lesion there is an increase in the subband

hydrogen phosphate (HPO_4^{2-}) located in 1123, 1143, 1003-1005 cm^{-1}. In study 1, there is a tendency for mineral dissolution, but it is not as strong as in study 2, resulting in a slower output of the hydroxyapatite ions, which eventually precipitate on the surface of the dentin (37).

An important aspect of radiation is radiolysis, wherein radiation interacts with water, releasing free radicals of hydrogen and hydrogen peroxide. Since dentin is a tissue with a considerable amount of water, these free radicals acts as a strong oxidant that may cause denaturation of dentin molecular structures and produce new compounds (14, 38). The increase in the v_1 and v_3 PO_4^{-3} in irradiated dentin in the study 2 can be explained by the formation of a new compound. This is in accordance with previous studies that demonstrated that the ions released by water after radiation exposure induced the formation of a secondary non-apatitic calcium phosphate phase, which likely would have made the hydroxiapatite more susceptible to degradation (14, 39).

The low salivary flow rate(study 2) promoted larger dentin demineralization than normal salivary flow rate(study 1) detected by greater loss v_2 CO_3^{-2} (11.76% and 5.5%, respectevely). This finding suggests that the low salivary flow rateand consequently reduced salivary clearance and buffer, lead to a longer time of contact of sucrose with the dentin/biofilm, to a pronounced drop in pH in the biofilm after sucrose release, and to a prolonged duration of the minimum pH phase (37). This is not in accordance with Kielbassa et al. 2000, which have shown no differences between irradiated and nonirradiated initial dentin caries lesions. Probably because the in situ experiment was with participants in good general health and normal salivary flow ratewearing buccal appliances to produce caries lesions (24). Overall, this study strengthens the idea that radiation-related caries occurs also due to hyposalivation. In a normal salivary flow ratethe demineralization-remineralization process occur in a balanced way, which no longer exists with reduced salivary flow rate(37).

In the present study, no differences were observed in mineral density parameter with the induction of caries lesion in the first 40 µm of the dentin. It suggests that the modifications caused by the initial dentin artificial caries lesions occurred superficially, so they were only detected by the ATR/FTIR, which has a small and well controlled penetration depth (27). However, this discrete dentin mineral disruption would not be

detected by the micro-CT resolution. Nonetheless, irradiated dentin presented low mineral density in study 2. Since the whole block was exposed to radiation, the micro-ct was able to detect these changes of mineral density in the analyzed volume, explaining the increase in caries susceptibility of this group.

Thus, the understanding of how radiation-related caries occurs is of the utmost importance since the cure and survival rates of post radiotherapy head and neck cancer patients have increased. This awareness will lead to advances in the prevention and treatment of this injury, ensuring better quality of life of patients. In the meantime, greater efforts are needed to ensure pre-treatment assessment of dentition, adequate oral hygiene techniques, diets to minimize risk of radiation-related caries and daily fluoride use.

Conclusions

Initial caries lesions differed between non-irradiated dentin and irradiated dentin and between normal and reduced salivary flow rate. Alterations in the inorganic and organic matrix and in mineral density was found for irradiated dentin. With reduced salivary flow, mineral alterations were more detectable in the caries lesions.

References

1. Selwitz RH, Ismail AI, Pitts NB (2007) Dental caries. Lancet 369 (9555):51-59. doi:10.1016/S0140-6736(07)60031-2

2. Zero DT, Fontana M, Martinez-Mier EA, Ferreira-Zandona A, Ando M, Gonzalez-Cabezas C, Bayne S (2009) The biology, prevention, diagnosis and treatment of dental caries: scientific advances in the United States. Journal of the American Dental Association 140 Suppl 1:25S-34S

3. Silva AR, Alves FA, Antunes A, Goes MF, Lopes MA (2009) Patterns of demineralization and dentin reactions in radiation-related caries. Caries research 43 (1):43-49. doi:10.1159/000192799

4. Vissink A, Burlage FR, Spijkervet FK, Jansma J, Coppes RP (2003) Prevention and treatment of the consequences of head and neck radiotherapy. Critical reviews in oral

biology and medicine : an official publication of the American Association of Oral Biologists 14 (3):213-225

5. Deng J, Jackson L, Epstein JB, Migliorati CA, Murphy BA (2015) Dental demineralization and caries in patients with head and neck cancer. Oral oncology 51 (9):824-831. doi:10.1016/j.oraloncology.2015.06.009

6. Abdalla R, Omar A, Eid K (2018) Detecting demineralization of enamel and cementum after gamma irradiation using radiographic densitometry. Radiation and environmental biophysics 57 (3):293-299. doi:10.1007/s00411-018-0749-2

7. Abdalla R, Niazy MA, Jamil WE, Hazzaa HA, Elbatouti AA (2017) The role of fluoride and chlorhexidine in preserving hardness and mineralization of enamel and cementum after gamma irradiation. Radiation and environmental biophysics 56 (2):187-192. doi:10.1007/s00411-017-0690-9

8. Goncalves LM, Palma-Dibb RG, Paula-Silva FW, Oliveira HF, Nelson-Filho P, Silva LA, Queiroz AM (2014) Radiation therapy alters microhardness and microstructure of enamel and dentin of permanent human teeth. Journal of dentistry 42 (8):986-992. doi:10.1016/j.jdent.2014.05.011

9. de Siqueira Mellara T, Palma-Dibb RG, de Oliveira HF, Garcia Paula-Silva FW, Nelson-Filho P, da Silva RA, da Silva LA, de Queiroz AM (2014) The effect of radiation therapy on the mechanical and morphological properties of the enamel and dentin of deciduous teeth--an in vitro study. Radiation oncology 9:30. doi:10.1186/1748-717X-9-30

10. Reed R, Xu C, Liu Y, Gorski JP, Wang Y, Walker MP (2015) Radiotherapy effect on nano-mechanical properties and chemical composition of enamel and dentine. Archives of oral biology 60 (5):690-697. doi:10.1016/j.archoralbio.2015.02.020

11. Qing P, Huang S, Gao S, Qian L, Yu H (2015) Effect of gamma irradiation on the wear behaviour of human tooth enamel. Scientific reports 5:11568. doi:10.1038/srep11568

12. de Miranda RR, Silva ACA, Dantas NO, Soares CJ, Novais VR (2018) Chemical analysis of in vivo-irradiated dentine of head and neck cancer patients by ATR-FTIR and Raman spectroscopy. Clinical oral investigations. doi:10.1007/s00784-018-2758-6

13. Rodrigues RB, Soares CJ, Junior PCS, Lara VC, Arana-Chavez VE, Novais VR (2018) Influence of radiotherapy on the dentin properties and bond strength. Clinical oral investigations 22 (2):875-883. doi:10.1007/s00784-017-2165-4

14. Velo M, Farha ALH, da Silva Santos PS, Shiota A, Sansavino SZ, Souza AT, Honorio HM, Wang L (2018) Radiotherapy alters the composition, structural and mechanical properties of root dentin in vitro. Clinical oral investigations 22 (8):2871-2878. doi:10.1007/s00784-018-2373-6

15. Lu H, Zhao Q, Guo J, Zeng B, Yu X, Yu D, Zhao W (2019) Direct radiation-induced effects on dental hard tissue. Radiation oncology 14 (1):5. doi:10.1186/s13014-019-1208-1

16. Jensen SB, Pedersen AM, Vissink A, Andersen E, Brown CG, Davies AN, Dutilh J, Fulton JS, Jankovic L, Lopes NN, Mello AL, Muniz LV, Murdoch-Kinch CA, Nair RG, Napenas JJ, Nogueira-Rodrigues A, Saunders D, Stirling B, von Bultzingslowen I, Weikel DS, Elting LS, Spijkervet FK, Brennan MT, Salivary Gland Hypofunction/Xerostomia Section OCSGMAoSCiCISoOO (2010) A systematic review of salivary gland hypofunction and xerostomia induced by cancer therapies: prevalence, severity and impact on quality of life. Supportive care in cancer : official journal of the Multinational Association of Supportive Care in Cancer 18 (8):1039-1060. doi:10.1007/s00520-010-0827-8

17. Gaetti-Jardim E, Jr., Jardim ECG, Schweitzer CM, da Silva JCL, Oliveira MM, Masocatto DC, Dos Santos CM (2018) Supragingival and subgingival microbiota from patients with poor oral hygiene submitted to radiotherapy for head and neck cancer treatment. Archives of oral biology 90:45-52. doi:10.1016/j.archoralbio.2018.01.003

18. Hu JY, Chen XC, Li YQ, Smales RJ, Yip KH (2005) Radiation-induced root surface caries restored with glass-ionomer cement placed in conventional and ART cavity preparations: results at two years. Australian dental journal 50 (3):186-190

19. Heijnsbroek M, Paraskevas S, Van der Weijden GA (2007) Fluoride interventions for root dentin caries: a review. Oral health & preventive dentistry 5 (2):145-152

20. Kinney JH, Marshall SJ, Marshall GW (2003) The mechanical properties of human dentin: a critical review and re-evaluation of the dental literature. Critical reviews in oral biology and medicine : an official publication of the American Association of Oral Biologists 14 (1):13-29

21. Takahashi N, Nyvad B (2016) Ecological Hypothesis of Dentin and Root dentin caries. Caries research 50 (4):422-431. doi:10.1159/000447309

22. Tang G, Yip HK, Cutress TW, Samaranayake LP (2003) Artificial mouth model systems and their contribution to caries research: a review. Journal of dentistry 31 (3):161-171

23. Marquezan M, Correa FN, Sanabe ME, Rodrigues Filho LE, Hebling J, Guedes-Pinto AC, Mendes FM (2009) Artificial methods of dentine caries induction: A hardness and morphological comparative study. Archives of oral biology 54 (12):1111-1117. doi:10.1016/j.archoralbio.2009.09.007

24. Kielbassa AM, Schendera A, Schulte-Monting J (2000) Microradiographic and microscopic studies on in situ induced initial caries in irradiated and nonirradiated dental enamel. Caries research 34 (1):41-47. doi:10.1159/000016568

25. Cenci MS, Pereira-Cenci T, Cury JA, Ten Cate JM (2009) Relationship between gap size and dentine secondary caries formation assessed in a microcosm biofilm model. Caries research 43 (2):97-102. doi:10.1159/000209341

26. Maske TT, Brauner KV, Nakanishi L, Arthur RA, van de Sande FH, Cenci MS (2016) An in vitro dynamic microcosm biofilm model for caries lesion development and antimicrobial dose-response studies. Biofouling 32 (3):339-348. doi:10.1080/08927014.2015.1130824

27. Lopes CCA, Soares CJ, Lara VC, Arana-Chavez VE, Soares PB, Novais VR (2018) Effect of fluoride application during radiotherapy on enamel demineralization. Journal of applied oral science : revista FOB 27:e20180044. doi:10.1590/1678-7757-2018-0044

28. Zezell DM, Benetti C, Veloso MN, Castroa PAA, Anab PA (2015) FTIR Spectroscopy Revealing the Effects of Laser and Ionizing Radiation on Biological Hard Tissues. J Braz Chem Soc 26 (12):2571-2582. doi:10.5935/0103-5053.20150246

29. Maske TT, Kuper NK, Cenci MS, Huysmans M (2017) Minimal Gap Size and Dentin Wall Lesion Development Next to Resin Composite in a Microcosm Biofilm Model. Caries research 51 (5):475-481. doi:10.1159/000478536

30. Swain MV, Xue J (2009) State of the art of Micro-CT applications in dental research. International journal of oral science 1 (4):177-188. doi:10.4248/IJOS09031

31. Maske TT, Isolan CP, van de Sande FH, Peixoto AC, Faria ESAL, Cenci MS, Moraes RR (2015) A biofilm cariogenic challenge model for dentin demineralization and dentin

bonding analysis. Clinical oral investigations 19 (5):1047-1053. doi:10.1007/s00784-014-1331-1

32. Sung YH, Son HH, Yi K, Chang J (2016) Elemental analysis of caries-affected root dentin and artificially demineralized dentin. Restorative dentistry & endodontics 41 (4):255-261. doi:10.5395/rde.2016.41.4.255

33. Shumi W, Lim J, Nam S-W, Lee K, Kim SH, Kim MH, Cho K-S, Park S (2010) Environmental factors that affect Streptococcus mutans biofilm formation in a microfluidic device mimicking teeth. BioChip 4:257–263. doi:10.1007/ s13206-010-4401-8

34. Xu C, Wang Y (2011) Cross-linked demineralized dentin maintains its mechanical stability when challenged by bacterial collagenase. Journal of biomedical materials research Part B, Applied biomaterials 96 (2):242-248. doi:10.1002/jbm.b.31759

35. LeGeros RZ (1991) Calcium phosphates in oral biology and medicine. Monographs in oral science 15:1-201

36. Al-Naimi AM, Chakmakch M, Taqa AA (2017) Fourier transform infrared spectroscopy (FTIR) of remaining dentin after caries removal with newly prepared experimental chemomechanical caries removal agent. International Journal of Enhanced Research in Medicines & Dental Care 4 (7):6-11

37. Maltz M, Tenuta LMA, Groisman S, Cury JA (2016) Cariologia: Conceitos Básicos, Diagnóstico e Tratamento Não Restaurador.

38. Pioch T, Golfels D, Staehle HJ (1992) An experimental study of the stability of irradiated teeth in the region of the dentinoenamel junction. Endodontics & dental traumatology 8 (6):241-244

39. Celik EU, Ergucu Z, Turkun LS, Turkun M (2008) Effect of different laser devices on the composition and microhardness of dentin. Operative dentistry 33 (5):496-501. doi:10.2341/07-127

Tables

Table 1 Mean and standard deviation of the integrated area of each vibration mode and ratios (C/M, M/M) analyzed by FTIR from study 1

	Amide I		PO_4^{-3} v_1 e v_3		Amide III		Amide II		CO_3^{-2} v_3, v_4		PO_4^{-3} v_4, v_2		CO_3^{-2} v_2		C/M		M/M	
	Non-irradiated	Irradiated	Non-irradiated	Irradiated	Non-irradiated	Irradiated	Non-irradiated	Irradiated	Non-irradiated	Irradiated	Non-irradiated	Irradiated	Non-irradiated	Irradiated	Non-irradiated	Irradiated	Non-irradiated	Irradiated
Control	1.93 (0.3) Aa	1.98 (0.2) Aa	12.36 (1.1) Ab	11.76 (1.0) Bb	0,26 (0,04) Ab	0.27 (0,05) Ab	0.33 (0.08) Aa	0.33 (0.07) Aa	1,64 (0.2) Aa	1.67 (0.2) Aa	5.93 (0.5) Aa	6.02 (0.6) Aa	0.2 (0.02) Aa	0.18 (0.02) Ab	0.016 (0.00) Aa	0.015 (0.00) Ba	0.33 (0.07) Aa	0.35 (0.09) Aa
Caries affected dentin	1.79 (0.3) Aa	1.90 (0.27) Aa	13.2 (0.6) Aa	12.27 (1.4) Ba	0,41 (0.13) Aa	0,40 (0,10) Aa	0.25 (0.16) Ab	0.23 (0.08) Ab	1.97 (0.4) Aa	1.62 (0.3) Aa	5.04 (0.8) Ab	4.56 (1.0) Ab	0.22 (0.04) Aa	0.17 (0.04) Ab	0.015 (0.02) Ab	0.013 (0.00) Bb	0.35 (0.0) Aa	0.42 (0.11) Aa

Different uppercase letters (analysis in rows) and lowercase letters (analysis in columns) represent significant differences ($p < 0.05$)

Table 2 Mean and standard deviation of the integrated area of each vibration mode and ratios (C/M, M/M) analyzed by FTIR from study 2

	Amide I		PO_4^{-3} v_1 e v_3		Amide III		Amide II		CO_3^{-2} v_3, v_4		PO_4^{-3} v_4, v_2		CO_3^{-2} v_2		C/M		M/M	
	Non-irradiated	Irradiated	Non-irradiated	Irradiated	Non-irradiated	Irradiated	Non-irradiated	Irradiated	Non-irradiated	Irradiated	Non-irradiated	Irradiated	Non-irradiated	Irradiated	Non-irradiated	Irradiated	Non-irradiated	Irradiated
Control	2.17 (0.2) Aa	2.00 (0.3) Aa	10,45 (2.0) Ba	11.37 (1.4) Aa	0.26 (0.03) Aa	0.26 (0.05) Aa	0.31 (0.08) Aa	0.31 (0.07) Aa	1.49 (0.3) Aa	1.51 (0.2) Aa	5.13 (0.7) Aa	5.13 (0.9) Aa	0.17 (0.02) Aa	0.17 (0.03) Aa	0.016 (0.00) Aa	0.015 (0.00) Aa	0.43 (0.0) Aa	0.38 (0.1) Aa
Caries affected dentin	1.95 (0.3) Aa	1.83 (0.3) Aa	9.71 (2.8) Ba	12.7 (2.2) Aa	0.26 (0.08) Ba	0.32 (0.10) Aa	0.12 (0.08) Ab	0.20 (0.13) Ab	1.31 (0.4) Aa	1.46 (0.2) Aa	3.98 (1.2) Ab	4.36 (0.8) Ab	0.13 (0.05) Ab	0.15 (0.04) Ab	0.013 (0.00) Ab	0.012 (0.00) Ab	0.54 (0.21) Aa	0.43 (0.1) Aa

Different uppercase letters (analysis in rows) and lowercase letters (analysis in columns) represent significant differences ($p < 0.05$)

Figures

Fig. 1 Absorbance spectra for the sound non-irradiated dentin (purple line), caries affected non-irradiated dentin (red line), sound irradiated dentin (blue line) and caries affected irradiated dentin (orange line) from study 1

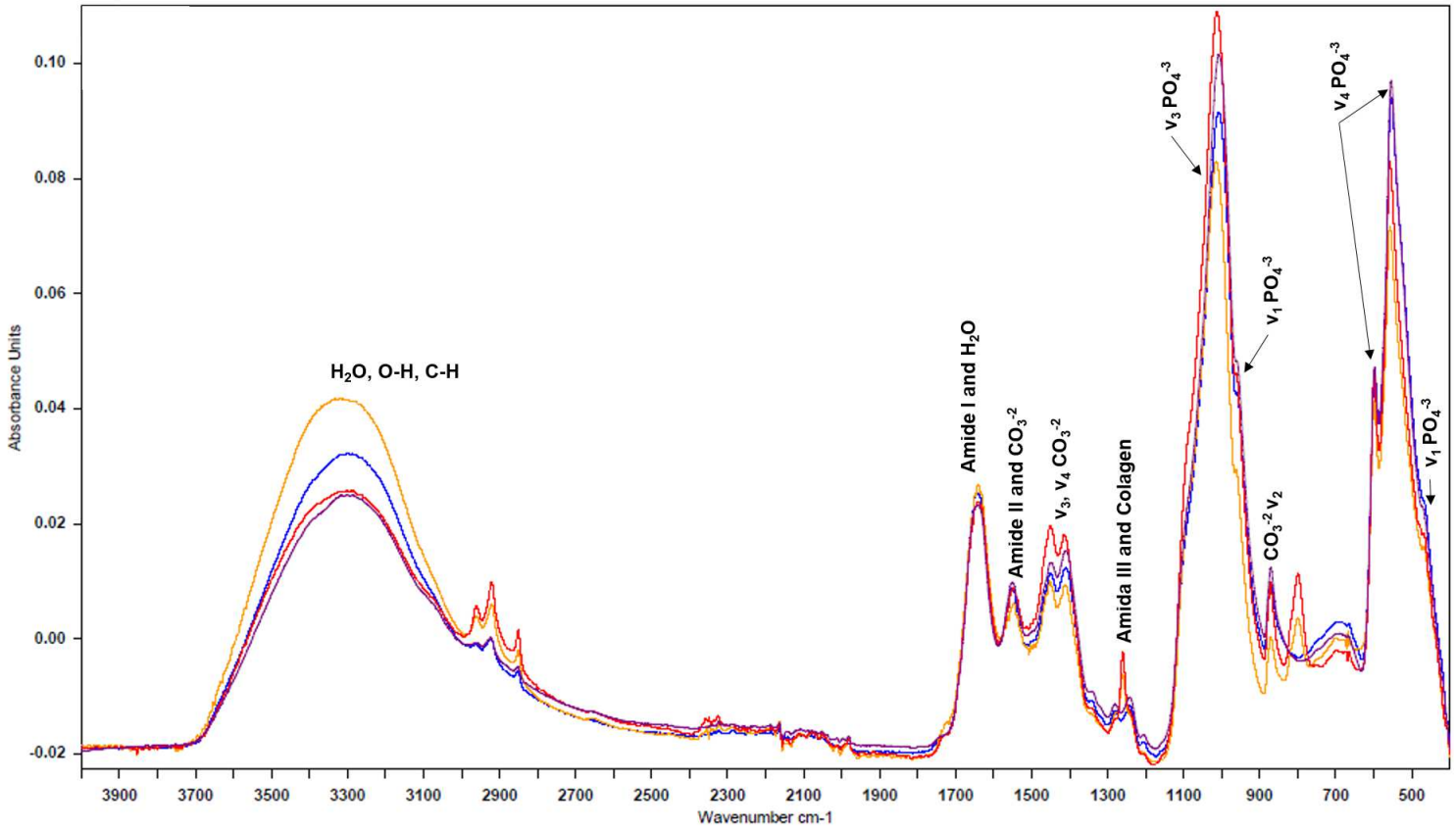

Fig. 2 Mineral density in different groups (*p<0.05).

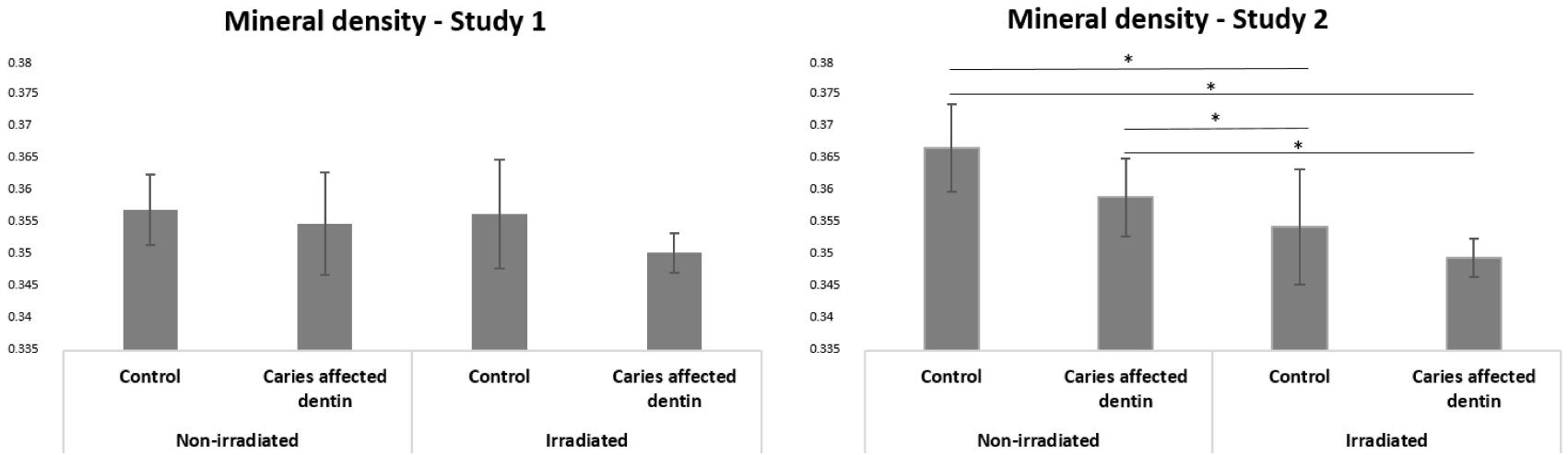

Fig. 3 Absorbance spectra for the sound non-irradiated dentin (purple line), caries affected non-irradiated dentin (red line), sound irradiated dentin (blue line) and caries affected irradiated dentin (orange line) from study 2

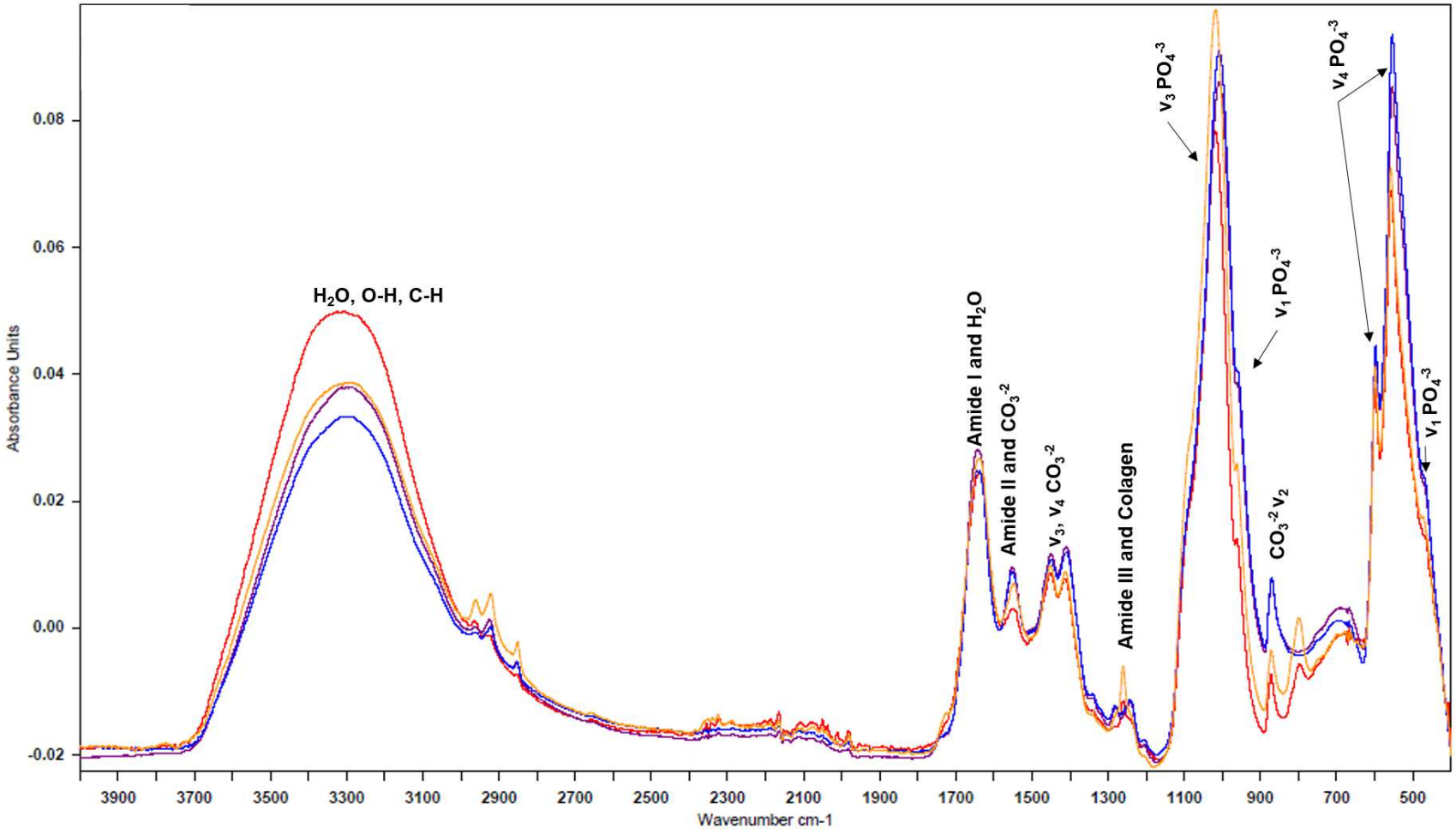

3.3 - Capítulo 3

Chemical and morphological characterization of radiation related caries

Artigo a ser submetido para o periódico PLOS One

Chemical and morphological characterization of radiation-related caries

Characterization of radiation-related caries

Abstract

The aim of this study was to compare sound to caries affected dentin of non-irradiated patients and of patients submitted to radiotherapy due to head and neck cancer. Ten premolars with carious lesions were carefully selected, of which 5 were from non-irradiated patients and the other 5 were from irradiated patients in the head and neck region. Sound and caries affected dentin were evaluated by means of Fourier transform infrared spectroscopy (FTIR) and Energy-dispersive X-ray (EDS and light microscopy). The parameters analyzed by FTIR were: mineral/matrix ratio, carbonate/mineral ratio, amide I/amide III ratio. From EDS, the Ca, P and Ca/P ratio was calculated. A decreased mineral/ organic matrix ratio was found for caries affected dentin ($p<0.001$) and irradiation ($p=0.012$). For carbonate/mineral ratio, only the interaction between the study factors was significant ($p=0.035$). There was a decrease of C/M ratio from non-irradiated to irradiated group and still from sound dentin to caries affected dentin in the irradiated group. Caries affected dentin showed a greater amide I/amide III ratio than sound dentin ($p=0.005$). Lower values of Ca and P was found for caries affected non-irradiated dentin and a lower Ca/P ratio was registered for irradiated dentin compared to non-irradiated dentin ($p=0.01$). Radiation related caries presented irregular and more diffuse demineralization pattern than conventional caries. In the present study, it was demonstrated that caries and radiotherapy lead to demineralization of the hydroxiapatite and protein degradation. However, radiation-related caries exhibited the most pronounced changes, with a diffuse demineralization pattern.

Introduction

Patients with head and neck cancer who underwent radiotherapy have a high risk of a highly destructive and progressive form of dental caries, known as radiation-related caries [1]. The radiation-related caries tends to start within the first year and becomes more severe with time. It occurs at cervical, cuspal, and incisal areas, in contrast to the sites of typical lesions of caries [2]. An increase friability of enamel can be seen and sometimes results in partial to total enamel delamination, exposing the underlying dentin [3], and may even culminate with crown amputation, impacting severely on patients' quality of life [4, 5]. Alterations in the translucency and color, through brown/black pigmentation, again is dissimilar from non-irradiated carious lesions [1, 6].

Radiation related caries have a multifactorial etiology. It is related to the indirect effects of hyposalivation and qualitative saliva alterations, decrease in pH, increase in viscosity, reduced buffering capacity, and changed antibacterial system responsible for immunity [7]. Since saliva is dramatically reduced, teeth are more susceptible to demineralization and the remineralization is impaired [8]. Beyond this, pain from mucositis results in difficulty to promote oral hygiene and increase cariogenic diet, that is also due to the difficulty of swallowing [8]. Accompanied by the reduced oral clearance by saliva, changes of the oral flora in patients treated with radiotherapy is seen, with an increase in acidogenic, and cariogenic microorganisms (Streptococcus mutans, Lactobacillus) [7]. In addition to the indirect effects, there are direct effects of ionizing radiation on dental tissues. In vitro studies report changes in microhardness, micromorphological structure, and chemical composition of human teeth [5, 9-13]. It was observed that minimum damage can occur below 30 Gy, but when the tooth level-dose is above 60 Gy the risk of damage is 10 times greater [2]. And once these lesions are

installed, there is a difficulty in their treatment, since the adhesion of restorative materials is negatively affected [14].

Unlike enamel caries, dentine caries are more complex [15]. The complexity of dentin caries is due to its chemical composition of dentin, composed by 20 wt.% of organic content (which corresponds to type-I collagen) and 70 wt.% of inorganic matrix (carbonated hydroxyapatite) [16]. In addition, the dentin has in its structure smaller hydroxyapatite crystals, higher carbonate and magnesium content and a more porous structure [17]. Thus, dentine is more vulnerable to acidic dissolution than enamel because of its higher critical pH for demineralization (6.2 - 6.4) than that of enamel (5.5) [18]. Caries process in dentin starts with mineral dissolution by acids, resulting in organic matrix exposure and further protein degradation [16].

A comprehensive understanding of what leads to the development of radiation related caries, its characteristics from its earliest stages to latter stages and how to prevent and treat, is indispensable for the optimal management of this oral disease. The aim of this study was to compare sound to caries affected dentin of healthy patients and patients submitted to radiotherapy due to head and neck cancer, regarding their chemical composition and morphological characteristics. Our hypothesis was that radiation-related caries is different from conventional caries.

Materials and methods

After approval from the Ethical Committee in Research of Federal University of Uberlândia, Brazil (protocol No. 50329715.6.0000.5152), ten freshly extracted lower and upper premolars with cervical caries lesions were collected after patients signed informed consent and stored in distilled water at 4ºC. Teeth from patients who had head and neck

cancer were extracted because of advanced periodontal disease and were included in this study. Five teeth were from pre-radiotherapy patients (mean age 57 years) and the other five were from post-radiotherapy patients (mean age 63 years). These latter patients were subjected to fractionated X-ray radiation of 1.8 Gy per day totaling 70 Gy. Teeth were located in the radiation field and due to clinical reasons, they were extracted 41.5±19.2 months after irradiation.

According to medical records, all patients enrolled in this study had undergone radiotherapy to treat head and neck carcinomas. The main affected sites among the presented cases were the oral cavity and the total dose of radiation was 72 Gy (Table 1).

Table 1- Main clinic pathological characteristics of head-and-neck cancer patients submitted to radiotherapy.

Patient	Gender	Age, years	Tumor location	Treatment	Total dose of radiation, Gy
1	M	63	Tongue	CRDT + RDY	72
2	F	66	Inferior alveolar ridge	CRDT + RDY	72
3	M	70	Floor of the mouth	RDY	72
4	M	58	Mandible	Surg + RDY	72
5	F	60	Oropharynx	RDY	70

M, male; F, female; Surg, surgery; CRDT, chemoradiotherapy; RDY, radiotherapy

The teeth were radiographed to assess the extension of the carious lesions. Those who had one cervical carious lesion extending at least half of the distance from the external surface of the enamel/cementum to the pulp chamber and the opposite side presenting a sound dentin were selected [19].

Each tooth was axial sectioned through the center of the caries lesions using a water-cooled diamond saw (Isomet; serie 15HC diamond; Buehler Ltd., Lake Bluff, IL, USA) mounted on a precision saw (Isomet 1000, Buehler, Lake Bluff, IL, USA), under constant water irrigation. To confirm the extent of caries lesion, all sections were further evaluated using a stereomicroscope (Leica MS5, Leica Microscopy Systems Ltd; Heerbrugg, Switzerland). The buccal halves were designated for Fourier transform infrared spectroscopy (FTIR) and Energy-dispersive X-ray (EDS). The lingual halves were intended to light microscopy (Fig 1).

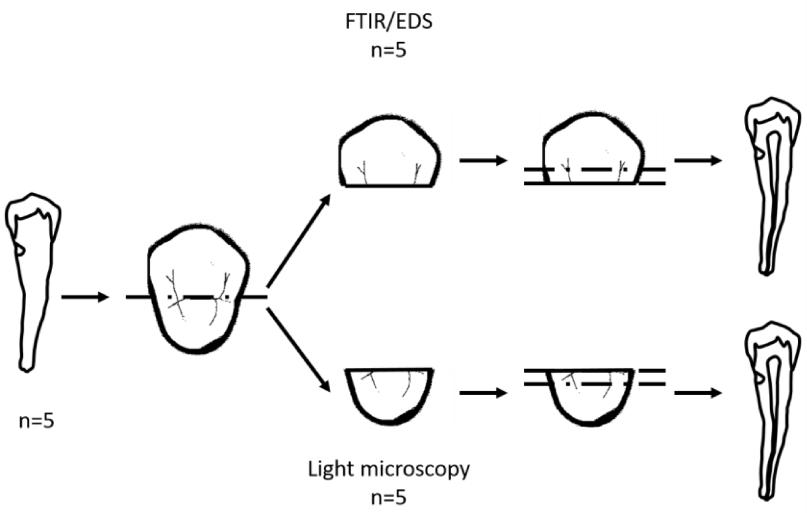

Fig 1. Schematic illustration of specimen preparation and experimental design.

FTIR

Chemical composition of the sound dentin and caries affected dentin was determined using attenuated total reflectance/Fourier transform infrared spectroscopy (ATR/FTIR; Vertex 70, Bruker, Ettlingen, Germany). The testing surfaces were positioned against the diamond crystal of the ATR/FTIR unit and pressed with a force gauge at a constant pressure. Then, the spectra were recorded in the range from 400 to

4,000 cm^{-1} at a 4 cm^{-1} resolution. The sample was scanned 32 times in each FTIR measurement, and the spectrum acquired is the average of all these scans. Spectra were recorded and analyzed by OPUS 6.5 software (Bruker, Ettlingen, Germany). After baseline correction and normalization, the FTIR spectra were analyzed by calculating the integrated areas of specific bands of organic and inorganic dentin content the ν_1 and ν_3 vibration modes of phosphate (PO_4^{-3}) (1300-900 cm^{-1}), amide I (1680-1600 cm^{-1}), amide III (1200-1300 cm^{-1}), the ν_2 vibration mode of carbonate (CO_3^{-2}) (around 870 cm^{-1}). And the following parameters: (1) mineral/ organic matrix ratio - M/M (the band ratio between the ν_1, ν_3 vibration of phosphate ion at 1020 and 960 cm^{-1} to the C=O stretching of collagen amide I at 1660 cm^{-1}); (2) carbonate/mineral ratio - C/M (the ratio of the integrated areas of carbonate ν_2 at 872 cm^{-1} to the phosphate ν_1, ν_3); (3) AI/AIII ratio (the ratio of the integrated areas of amide I to the amide III at 1260 cm^{-1}) [12, 20, 21].

EDS

A semi-quantitative dentin elemental analysis of chemical elements was performed using an EDS (X-act, Oxford Instruments) spectrometer equipped with a rhodium X-ray tube and a liquid nitrogen cooled semiconductor detector (N_2). The voltage in the tube was set to 15 kV. One-half from each tooth was coated with gold and three spectra were collected in the region of the sound dentin and three spectra in the caries affected dentin. The mean concentrations (wT) of each element, as well as the Ca/P ratio of the three spectra were calculated. Atomic (%) values were considered above 1% to allow comparison between groups [22].

Light microscopy

The lingual halves were embedded in methyl methacrylate and one section about 700 μm thick was obtained through the center of the caries lesion with a diamond saw (Isomet, Buehler Ltd., Lake Bluff, USA). Hand-ground polishing was performed using successively finer grade silicon carbide paper to a final thickness of 200 μm. After that, the slice was examined under a light microscope through a 4x magnification (Leica Dental Corp., Wetzlar, Germany), in order to identify the enamel and dentin caries zones, qualitative patterns of demineralization and reactionary dentin. Images were captured by a CCD camera coupled to the light microscopy and analyzed by the LAS EZ (Leica, Wetzlar, Germany) image capture software.

Statistical analysis

FTIR and EDS data were tested for normal distribution (Shapiro-Wilk) and equality of variances (Levene's test). Two-way repeated measures analysis of variance (RM ANOVA) was performed, considering the study factors irradiation (non-irradiated and irradiated) and type of dentine (sound and caries affected dentin), followed by Tukey post-hoc test. Sigma Plot statistical package (version 12.0, Systat Software, Inc., San Jose, CA, USA) was used for analysis and a nominal level of significance of 0.05. Descriptive analysis was used for images from light microscopy.

Results

FTIR

The spectra for the studied groups are shown in Fig 2. The mean values and standard deviation for the vibration modes and chemical parameters obtained by ATR/FTIR are shown in Table 2 and 3, respectively. For M/M ratio, two-way ANOVA showed statistical

significance for radiation (p=0.012), and caries (p<0.001). Lower values of the ratio was found for caries affected dentin and irradiation. For carbonate/mineral ratio, only the interaction between the study factors (radiation and caries) was significant (p=0.035). Tukey's post hoc test revealed higher C/M ratio values for the non-irradiated group and there was a decrease from sound dentin to caries affected dentin in the irradiated group. Amide I/amide III ratio showed significant difference only for caries (p=0.005). Caries affected dentin showed a greater ratio than sound dentin.

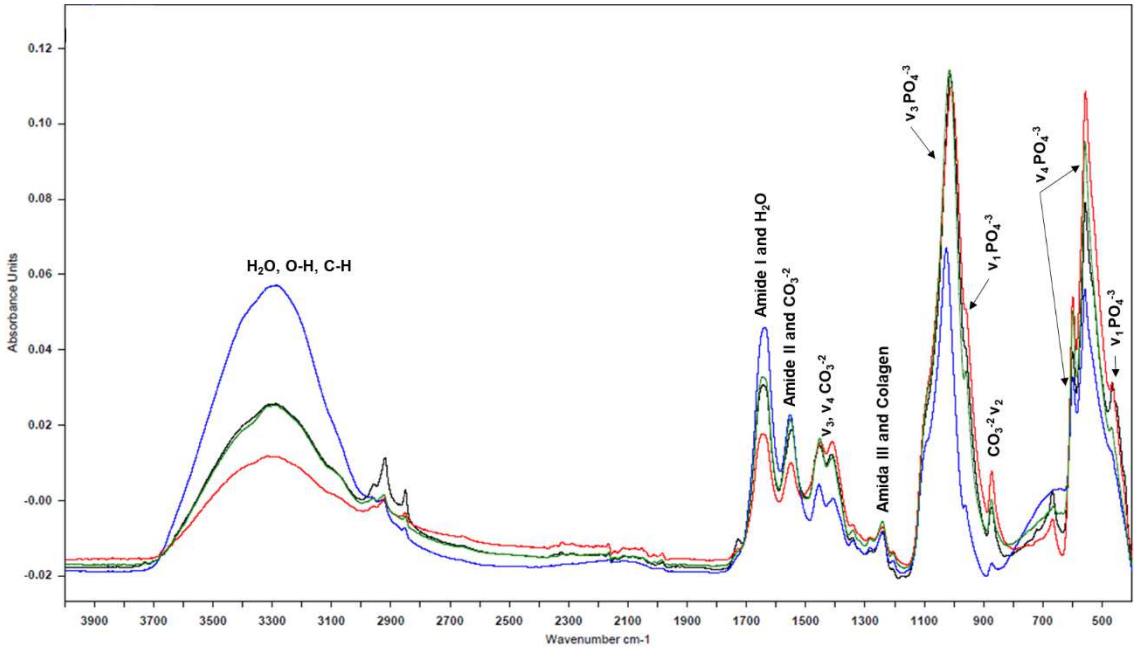

Fig 2. Absorbance spectra for non-irradiated sound dentin (green line), non-irradiated caries affected dentin (black line), irradiated sound dentin (red line) and irradiated caries affected dentin (blue).

Table 2. Mean and standard deviation for the analyzed organic and inorganic vibration modes of the experimental groups in FTIR.

	Amide I		v_1 and v_3 Phosphate		Amide III		v_2 Carbonate	
	Sound dentin	Caries affected dentin	Sound dentin	Caries affected dentin	Sound dentin	Caries affected dentin	Sound dentin	Caries affected dentin
Non-Irradiated	1.30 (0.2)	2.11 (0.5)	13.04 (1.6)	11.27 (2.8)	0.21 (0.0)	0.33 (0.1)	0.25 (0.0)	0.21 (0.0)
Irradiated	1.88 (0.7)	2.85 (0.2)	12.61 (1.5)	8.44 (1.1)	0.29 (0.1)	0.35 (0.1)	0.16 (0.0)	0.06 (0.0)

Table 3. Mean and standard deviation of M/M, C/M and AI/AIII ratios for the experimental groups in FTIR.

	M/M		C/M		AI/AIII	
	Sound dentin	Caries affected dentin	Sound dentin	Caries affected dentin	Sound dentin	Caries affected dentin
Non-Irradiated	10.18 (1.3) Aa	5.84 (2.7) Ab	0.015 (0.01) Aa	0.015 (0.01) Aa	6.38 (1.17) Ab	7.71 (1.29) Aa
Irradiated	7.40 (2.7) Ba	2.99 (0.5) Bb	0.013 (0.00) Ba	0.008 (0.00) Bb	5.76 (1.65) Ab	8.87 (2.65) Aa

*Groups identified with different upper case letter (analysis in columns) and lower case letters (analysis in rows) represent statistically significant differences ($p<0.05$).

EDS

Representative FESEM image of the regions where the three spectra were collected from the sound and caries affected dentin is presented in Fig. 3-a, as well as, a representative EDX spectrum of dentin (Fig 3-b). Energy-dispersive X-ray analysis revealed significant

quantities of the chemical elements Ca, P, C, and O on dentin surface. Others, such as F, Si, Na and Mg, appeared as trace elements (< 1%) and not in all specimens. The results of Ca, P and Ca/P ratio for sound dentin and caries affected dentin per group are shown in Table 4. Two-way RM ANOVA of Ca and P values revealed a statistically significant interaction between the studied factors (p=0.036 and p=0.020, respectively), with non-irradiated sound dentin presenting higher values of Ca and P than non-irradiated caries affected dentin. For Ca/P ratio values, two-way RM ANOVA revealed a statistically significant difference between irradiation (p=0.01). However, the factor caries (p=0.252) and the interaction between factors was not statistically significant (p=0.445). Lower values of Ca/P ratio was registered for irradiated dentin compared to non-irradiated dentin. Although not statistically significant, lower Ca/P ratio values were found for caries affected dentin for both groups.

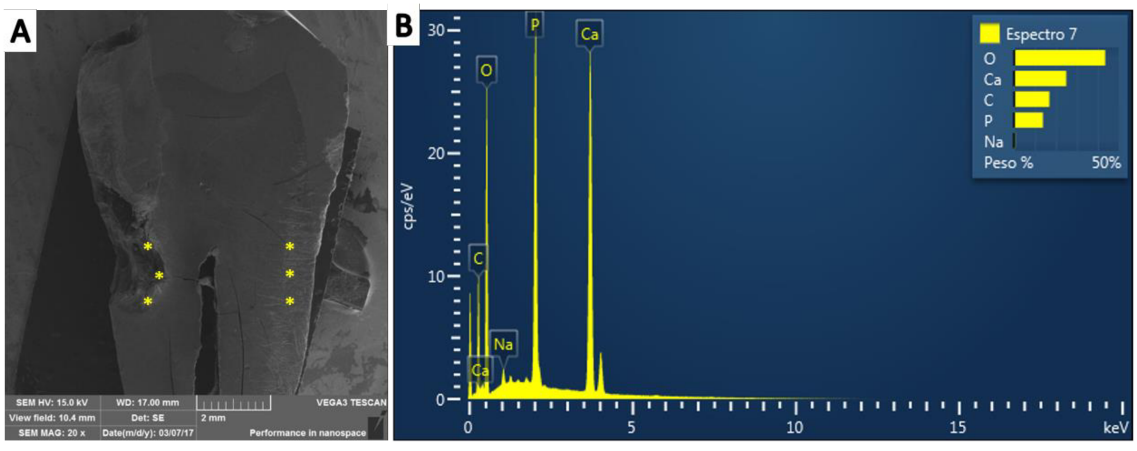

Fig 3. Illustrative FESEM image of the regions where the three spectra were collected from the sound dentin and from the caries affected dentin (A) and a representative EDX spectrum of dentin (B).

Table 4. Mean and standard deviations of Ca/P ratio concerning EDS.

	Ca		P		Ca/P	
	Sound dentin	Caries affected dentin	Sound dentin	Caries affected dentin	Sound dentin	Caries affected dentin
Non-irradiated	17.1 (5.0) Aa	12.7 (3.6) Ab	10.7 (2.0) Aa	8.13 (1.8) Ab	1.6 (0.2) Aa	1.5 (0.2) Aa
Irradiated	11.4 (5.7) Aa	9.67 (7.5) Aa	8.27 (2.6) Aa	7.11 (3.4) Aa	1.2 (0.2) Ba	1.1 (0.1) Ba

*Groups identified with different upper case letter (analysis in columns) and lower case letters (analysis in rows) represent statistically significant differences ($p<0.05$).

Light microscopy

All specimens presented different zones of dentin caries, distinguished between remanescents of softened dentin, demineralized dentin and a translucent zone (Fig 4). Additionally, light microscopy showed a half-moon-like shape of demineralization in cervical dentin caries with the base at the tooth surface and the apex directed to the pulp. The radiation-related caries presented a less circumscribed form (Fig 4-a).

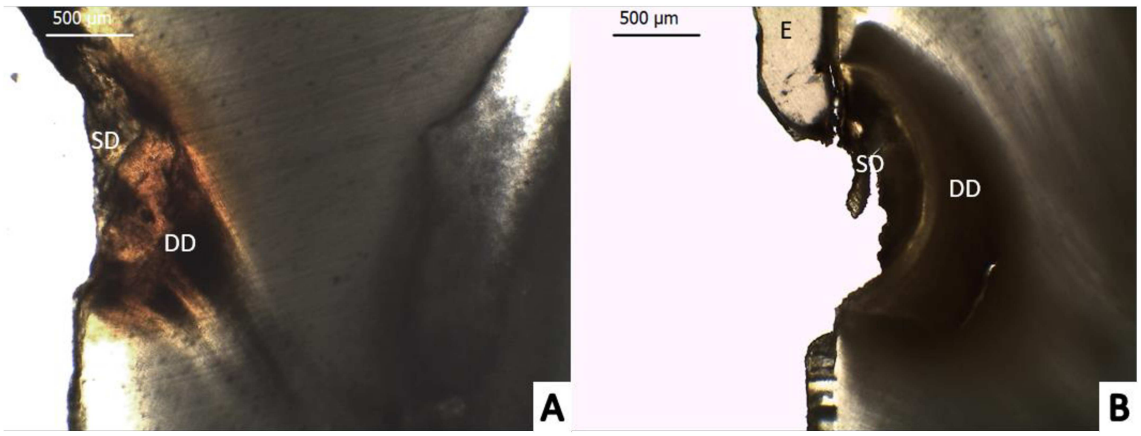

Fig 4. Photomicrographs of root surface caries from an irradiated tooth (A) and from a non-irradiated tooth (B) exhibiting a half-moon-like shape with a semicircular demineralized zone. E = Enamel; DD = demineralized dentin; SD = Softened dentin.

Discussion

The hypothesis tested in this study was accepted. Our results showed that radiation-related dentin caries differed from non-irradiated dentin caries in their chemical composition and morphological characteristics.

Radiation-related caries can be considered a complex and multifactorial disease related to the indirect effects of ionizing radiation in the oral cavity added to the direct effects on teeth [23]. Altered morphological, chemical, and mechanical dentin properties after radiotherapy were reported in some studies [4, 10, 12, 13, 24] and an increasing dentin demineralization in a dose-dependent manner [23, 25], what can partially explain the onset of radiation caries at the cervical areas, at the cement–enamel junction (CEJ) and/or the dentin–enamel junction (DEJ) [26], leading to amputation of crowns and complete loss of dentition.

In this study, teeth with dental caries of patients with head and neck cancer pre-radiotherapy and post radiotherapy were used, since simulating all the oral conditions of these latter patients (salivary flow, pH, diet, microbiota) is extremely difficult. The cancers were located at the tongue, lower alveolar ridge and oropharynx. The standardization of the site of cancer involvement, as well as the total dose of radiotherapy, are very important since the effects on dental structure depends on it [27, 28]. Thus, teeth used in the study were located within the radiation field and the tumor received a total of

72 Gy, in daily increments of 1.8 Gy. And in attempt to obtain the most standardized substrate, the age of patients ranging from in both groups was also similar, since different ages could present differences on microstructural and composition of human dentine [29].

Caries process involves the dynamic phenomenon of de- and remineralization, tilting towards the demineralization [30]. However, this process mainly explains the etiology of enamel caries. Dentin caries, due to the high organic content in dentin, can also be explained by the proteolysis theory [17]. This theory divides what happens in dentin caries in two successive stages [31]. First, acids from the outer surface dissolve the mineral phase, at that time, the demineralized collagen provides a scaffold for bacteria [31]. In a second stage, protein degradation occurs due to proteases activation, such as matrix metalloproteinases and cysteine cathepsins [17].

FTIR spectroscopy measures the wavelength and intensity of the absorption of infrared light by samples with dipole moments [32], thus, most inorganic and organic components in the environment are active in infrared. FTIR analysis of the mineral and organic content of the dentin will reflect the extent of caries process. To the best of our knowledge, this is the first study *ex vivo* conducted with FTIR technique to characterize radiation-related caries.

FTIR analysis of carbonate, phosphate and carbonate/mineral ratio showed lower mineral content for caries affected dentin than sound dentin. This mineral loss was expected since caries biochemical process starts with the dissolution of teeth mineral content by acid. However, in dentin, this process is more critical once dentin hydroxyapatite crystal has smaller size, and high carbonate content. Carbonate presence destabilizes the mineral, making the it more soluble [33]. Thus, during mineral dissolution, these unstable regions rich in carbonate are the first ones to dissolve [34]. A

252 marked reduction of the carbonate/mineral ratio occurred in the irradiated group. In
253 irradiated patients because of low salivary flow, a more pronounced drop in pH occurs
254 once food is ingested, leading to a higher solubility of dentin mineral. In addition, the
255 high exposure to fermentable sugars by these patients has a direct effect on the dissolution
256 of minerals in the dental structure, modifying the ecology of the biofilm and making it
257 metabolically more active [18].

258 In the current study, lower mineral/matrix ratio was found for the caries affected
259 dentin and for the irradiated group. Consecutively to demineralization, exposed collagen
260 fibrils degradation take place by collagenases, present in the bacterial biofilm or even by
261 latent enzyme in the dentin, such as matrix metalloproteinases (MMPs) and cysteine
262 cathepsins, which are activated in acidic environments [17]. The collagenases would
263 break down the telopeptide region of the collagen molecules [16]. In collagen fibril, the
264 five collagen molecules that make up the microfibril each have N- and C-terminal non-
265 helical telopeptides. Hydrolysis of the C- and N-terminal telopeptide (containing the
266 carboxy- and amino terminal cross-links, respectively) [35] results in the loss of terminal
267 ends of the collagen molecule [16] and formation of additional carbonyl groups (C=O).
268 Culminating in the decrease in the mineral/matrix ratio and in the increase of peak area
269 centered at 1665 cm^{-1} , relative to the amide I, the most intense absorption band in proteins
270 and primary governed by the stretching vibrations of the C=O (70–85%) and C–N groups
271 (10–20%) [33].

272 With ionizing radiation, the organic matrix is altered in a similar way, once
273 radiation interacts with water, free radicals of hydrogen and hydrogen peroxide are
274 released and they will oxidize and denature the organic components of dental structure

[36]. These collagen disorganization leads to an altered collagen with different characteristics, which could impair the adhesion of restorative materials [13, 37].

The last parameter analyzed by the FTIR was AI/AIII ratio, and it is related to the organization of collagen [38]. Specifically, the amide III band refers to the C−N stretching and N−H in-plane bending. The AI/AIII ratio shall increase with demineralization, being the organic matrix more detectable and change if collagen is degraded [39], which could be observed with caries affected dentin.

Hydroxyapatites properties are strongly dependent on their stoichiometry, which controls their crystalline structure, the reactivity of their surface and their biological behavior [40]. The stoichiometric hydroxyapatite, with the formula Ca_{10} $(PO_4)_6$ $(OH)_2$, presents Ca / P molar ratio of 1.67. However, the dental hydroxyapatite has contaminants such as magnesium carbonate and fluoride, so its Ca / P ratio is reduced. The Ca/P ratio found for non-irradiated sound dentin was 1.6, which may be assumed to be alike a carbonated apatite [41]. Although there was no statistical difference between sound and caries affected dentin for both groups, sound dentin showed higher values of Ca/P ratio. This might be explained by the fact that during the demineralization cycles, inorganic ions of calcium and phosphorus moves out, altering tissue composition [42]. Furthermore, smaller Ca/P ratio was found for the irradiated group, regardless of the type of dentin evaluated. This suggests a possible demineralization after radiation therapy), as shown by previous studies [23, 25].

Different zones of dentin caries were found between radiation-related caries and conventional caries. Enamel crack formations and residues of softened dentin were visualized over the demineralized dentin from both groups, being in accordance to Silva

et al. [43]. Although, diffuse brown discolorations were seen in radiation-related caries although, this might necessitate further investigations.

With respect to the findings of the study, we suggest that radiation-related caries are more destructive than conventional caries, being due to changes in the tooth structure and to salivary, dietary, and microbiological changes. Thus, new studies are necessary to create and validate methods for prevention of radiation direct effects on tooth and effective methods in the remineralization of the early stages of radiation-related caries. Caries prevention in the post radiation head and neck patient should be multifaceted and comprise maintenance of good oral hygiene, daily fluoride use, dietary counseling and frequent visits to the dentist.

Conclusions

In the present study, it was demonstrated that caries and radiotherapy lead to demineralization of the hydroxiapatite and protein degradation. However, radiation-related caries exhibited the most pronounced changes, with a diffuse demineralization pattern.

Acknowledgments

The authors acknowledge the financial support given by FAPEMIG, CAPES and CNPq.

References

1. Aguiar GP, Jham BC, Magalhaes CS, Sensi LG, Freire AR. A review of the biological and clinical aspects of radiation caries. The journal of contemporary dental practice. 2009;10(4):83-9. PubMed PMID: 19575058.
2. Walker MP, Wichman B, Cheng AL, Coster J, Williams KB. Impact of Radiotherapy Dose on Dentition Breakdown in Head and Neck Cancer Patients. Practical radiation oncology. 2011;1(3):142-8. doi: 10.1016/j.prro.2011.03.003. PubMed PMID: 21857887; PubMed Central PMCID: PMC3156461.

3. Jansma J, Vissink A, Jongebloed WL, Retief DH, Johannes 's-Gravenmade E. Natural and induced radiation caries: A SEM study. American journal of dentistry. 1993;6(3):130-6. PubMed PMID: 8240774.
4. Kielbassa AM, Schendera A, Schulte-Monting J. Microradiographic and microscopic studies on in situ induced initial caries in irradiated and nonirradiated dental enamel. Caries research. 2000;34(1):41-7. doi: 10.1159/000016568. PubMed PMID: 10601783.
5. Kielbassa AM, Hinkelbein W, Hellwig E, Meyer-Luckel H. Radiation-related damage to dentition. The Lancet Oncology. 2006;7(4):326-35. doi: 10.1016/S1470-2045(06)70658-1. PubMed PMID: 16574548.
6. Vissink A, Jansma J, Spijkervet FK, Burlage FR, Coppes RP. Oral sequelae of head and neck radiotherapy. Critical reviews in oral biology and medicine : an official publication of the American Association of Oral Biologists. 2003;14(3):199-212. PubMed PMID: 12799323.
7. Deng J, Jackson L, Epstein JB, Migliorati CA, Murphy BA. Dental demineralization and caries in patients with head and neck cancer. Oral oncology. 2015;51(9):824-31. doi: 10.1016/j.oraloncology.2015.06.009. PubMed PMID: 26198979.
8. Gupta N, Pal M, Rawat S, Grewal MS, Garg H, Chauhan D, et al. Radiation-induced dental caries, prevention and treatment - A systematic review. National journal of maxillofacial surgery. 2015;6(2):160-6. doi: 10.4103/0975-5950.183870. PubMed PMID: 27390489; PubMed Central PMCID: PMC4922225.
9. de Siqueira Mellara T, Palma-Dibb RG, de Oliveira HF, Garcia Paula-Silva FW, Nelson-Filho P, da Silva RA, et al. The effect of radiation therapy on the mechanical and morphological properties of the enamel and dentin of deciduous teeth--an in vitro study. Radiation oncology. 2014;9:30. doi: 10.1186/1748-717X-9-30. PubMed PMID: 24450404; PubMed Central PMCID: PMC3905913.
10. Goncalves LM, Palma-Dibb RG, Paula-Silva FW, Oliveira HF, Nelson-Filho P, Silva LA, et al. Radiation therapy alters microhardness and microstructure of enamel and dentin of permanent human teeth. Journal of dentistry. 2014;42(8):986-92. doi: 10.1016/j.jdent.2014.05.011. PubMed PMID: 24887361.
11. Reed R, Xu C, Liu Y, Gorski JP, Wang Y, Walker MP. Radiotherapy effect on nano-mechanical properties and chemical composition of enamel and dentine. Archives of oral biology. 2015;60(5):690-7. doi: 10.1016/j.archoralbio.2015.02.020. PubMed PMID: 25766468; PubMed Central PMCID: PMC4369427.
12. de Miranda RR, Silva ACA, Dantas NO, Soares CJ, Novais VR. Chemical analysis of in vivo-irradiated dentine of head and neck cancer patients by ATR-FTIR and Raman spectroscopy. Clinical oral investigations. 2018. doi: 10.1007/s00784-018-2758-6. PubMed PMID: 30515577.
13. Rodrigues RB, Soares CJ, Junior PCS, Lara VC, Arana-Chavez VE, Novais VR. Influence of radiotherapy on the dentin properties and bond strength. Clinical oral investigations. 2018;22(2):875-83. doi: 10.1007/s00784-017-2165-4. PubMed PMID: 28776096.
14. Soares CJ, Castro CG, Neiva NA, Soares PV, Santos-Filho PC, Naves LZ, et al. Effect of gamma irradiation on ultimate tensile strength of enamel and dentin. Journal of dental research. 2010;89(2):159-64. doi: 10.1177/0022034509351251. PubMed PMID: 20042736.

15. Yu OY, Zhao IS, Mei ML, Lo ECM, Chu CH. Caries-arresting effects of silver diamine fluoride and sodium fluoride on dentine caries lesions. Journal of dentistry. 2018;78:65-71. doi: 10.1016/j.jdent.2018.08.007. PubMed PMID: 30114443.
16. Tjaderhane L, Buzalaf MA, Carrilho M, Chaussain C. Matrix metalloproteinases and other matrix proteinases in relation to cariology: the era of 'dentin degradomics'. Caries research. 2015;49(3):193-208. doi: 10.1159/000363582. PubMed PMID: 25661522.
17. Takahashi N, Nyvad B. Ecological Hypothesis of Dentin and Root dentin caries. Caries research. 2016;50(4):422-31. doi: 10.1159/000447309. PubMed PMID: 27458979.
18. Correia MF, Tenuta LM, Del Bel Cury AA, Cury JA. Mineral ions in the fluid of biofilms formed on enamel and dentine shortly after sugar challenge. Caries research. 2012;46(4):408-12. doi: 10.1159/000339376. PubMed PMID: 22710251.
19. Toledano M, Aguilera FS, Osorio E, Cabello I, Toledano-Osorio M, Osorio R. Mechanical and chemical characterisation of demineralised human dentine after amalgam restorations. Journal of the mechanical behavior of biomedical materials. 2015;47:65-76. doi: 10.1016/j.jmbbm.2015.03.012. PubMed PMID: 25846265.
20. Zezell DM, Benetti C, Veloso MN, Castroa PAA, Anab PA. FTIR Spectroscopy Revealing the Effects of Laser and Ionizing Radiation on Biological Hard Tissues. J Braz Chem Soc. 2015;26(12):2571-82. doi: 10.5935/0103-5053.20150246.
21. Lopes CCA, Limirio PHJO, Novais VR, Dechichi P. Fourier transform infrared spectroscopy (FTIR) application chemical characterization of enamel, dentin and bone. Applied Spectroscopy Reviews. 2018;53(9):747-69. doi: 10.1080/05704928.2018.1431923.
22. Favretto CO, Delbem ACB, Moraes JCS, Camargo ER, de Toledo PTA, Pedrini D. Dentinal tubule obliteration using toothpastes containing sodium trimetaphosphate microparticles or nanoparticles. Clinical oral investigations. 2018;22(9):3021-9. doi: 10.1007/s00784-018-2384-3. PubMed PMID: 29464359.
23. Abdalla R, Omar A, Eid K. Detecting demineralization of enamel and cementum after gamma irradiation using radiographic densitometry. Radiation and environmental biophysics. 2018;57(3):293-9. doi: 10.1007/s00411-018-0749-2. PubMed PMID: 29948141.
24. Kielbassa AM, Beetz I, Schendera A, Hellwig E. Irradiation effects on microhardness of fluoridated and non-fluoridated bovine dentin. European journal of oral sciences. 1997;105(5 Pt 1):444-7. PubMed PMID: 9395106.
25. Bekes K, Francke U, Schaller HG, Kuhnt T, Gerlach R, Vordermark D, et al. The influence of different irradiation doses and desensitizer application on demineralization of human dentin. Oral oncology. 2009;45(9):e80-4. doi: 10.1016/j.oraloncology.2009.03.005. PubMed PMID: 19442566.
26. Lieshout HF, Bots CP. The effect of radiotherapy on dental hard tissue--a systematic review. Clinical oral investigations. 2014;18(1):17-24. doi: 10.1007/s00784-013-1034-z. PubMed PMID: 23873320.
27. de Barros da Cunha SR, Fonseca FP, Ramos P, Haddad CMK, Fregnani ER, Aranha ACC. Effects of different radiation doses on the microhardness, superficial morphology, and mineral components of human enamel. Archives of oral biology. 2017;80:130-5. doi: 10.1016/j.archoralbio.2017.04.007. PubMed PMID: 28414987.
28. Fregnani ER, Parahyba CJ, Morais-Faria K, Fonseca FP, Ramos PA, de Moraes FY, et al. IMRT delivers lower radiation doses to dental structures than 3DRT in head

and neck cancer patients. Radiation oncology. 2016;11(1):116. doi: 10.1186/s13014-016-0694-7. PubMed PMID: \27604995; PubMed Central PMCID: PMC5015339.
29. Duke ES, Lindemuth J. Variability of clinical dentin substrates. American journal of dentistry. 1991;4(5):241-6. PubMed PMID: 1810335.
30. Takahashi N, Nyvad B. Caries ecology revisited: microbial dynamics and the caries process. Caries research. 2008;42(6):409-18. doi: 10.1159/000159604. PubMed PMID: 18832827.
31. Nyvad B, Fejerskov O. An ultrastructural study of bacterial invasion and tissue breakdown in human experimental root-surface caries. Journal of dental research. 1990;69(5):1118-25. doi: 10.1177/00220345900690050101. PubMed PMID: 2335644.
32. Griffiths PR, de Haseth JA. Fourier Transform Infrared Spectrometry. New York, NY, USA2007.
33. Xu C, Reed R, Gorski JP, Wang Y, Walker MP. The Distribution of Carbonate in Enamel and its Correlation with Structure and Mechanical Properties. Journal of materials science. 2012;47(23):8035-43. doi: 10.1007/s10853-012-6693-7. PubMed PMID: 25221352; PubMed Central PMCID: PMC4160314.
34. Orrego S, Romberg E, Arola D. Synergistic degradation of dentin by cyclic stress and buffer agitation. Journal of the mechanical behavior of biomedical materials. 2015;44:121-32. doi: 10.1016/j.jmbbm.2015.01.006. PubMed PMID: 25637823; PubMed Central PMCID: PMC4499057.
35. Orgel JP, Wess TJ, Miller A. The in situ conformation and axial location of the intermolecular cross-linked non-helical telopeptides of type I collagen. Structure. 2000;8(2):137-42. PubMed PMID: 10673433.
36. Pioch T, Golfels D, Staehle HJ. An experimental study of the stability of irradiated teeth in the region of the dentinoenamel junction. Endodontics & dental traumatology. 1992;8(6):241-4. PubMed PMID: 1302687.
37. Soares CJ, Neiva NA, Soares PB, Dechichi P, Novais VR, Naves LZ, et al. Effects of chlorhexidine and fluoride on irradiated enamel and dentin. Journal of dental research. 2011;90(5):659-64. doi: 10.1177/0022034511398272. PubMed PMID: 21335538.
38. Toledano M, Aguilera FS, Osorio E, Cabello I, Toledano-Osorio M, Osorio R. Functional and molecular structural analysis of dentine interfaces promoted by a Zn-doped self-etching adhesive and an in vitro load cycling model. Journal of the mechanical behavior of biomedical materials. 2015;50:131-49. doi: 10.1016/j.jmbbm.2015.05.026. PubMed PMID: 26122790.
39. Wang Y, Yao X. Morphological/chemical imaging of demineralized dentin layer in its natural, wet state. Dental materials : official publication of the Academy of Dental Materials. 2010;26(5):433-42. doi: 10.1016/j.dental.2010.01.002. PubMed PMID: 20138658; PubMed Central PMCID: PMC2844914.
40. Raynaud S, Champion E, Bernache-Assollant D, Thomas P. Calcium phosphate apatites with variable Ca/P atomic ratio I. Synthesis, characterisation and thermal stability of powders. Biomaterials. 2002;23(4):1065-72. PubMed PMID: 11791909.
41. Dorozhkin SV. Amorphous calcium (ortho)phosphates. Acta biomaterialia. 2010;6(12):4457-75. doi: 10.1016/j.actbio.2010.06.031. PubMed PMID: 20609395.
42. Michalaki M, Oulis CJ, Pandis N, Eliades G. Histochemical changes of occlusal surface enamel of permanent teeth, where dental caries is questionable vs sound enamel surfaces. European archives of paediatric dentistry : official journal of the European Academy of Paediatric Dentistry. 2016;17(6):445-54. doi: 10.1007/s40368-016-0252-x. PubMed PMID: 27866328.

467 43. Silva AR, Alves FA, Antunes A, Goes MF, Lopes MA. Patterns of
468 demineralization and dentin reactions in radiation-related caries. Caries research.
469 2009;43(1):43-9. doi: 10.1159/000192799. PubMed PMID: 19151554.

REFERÊNCIAS

5. REFERÊNCIAS

1. Instituto Nacional de Câncer José Alencar Gomes da Silva (INCA). Estimativa 2018: incidência de câncer no Brasi [acesso em 15 jan 2019]. Disponível em: https://www.inca.gov.br/tipos-de-cancer/cancer-de-boca

2. Jemal A, Siegel R, Ward E, Hao Y, Xu J, Murray T, et al. Cancer statistics, 2008. CA Cancer J Clin. 2008;58(2):71-96. https://doi.org/10.3322/CA.2007.0010

3. Warnakulasuriya S. Global epidemiology of oral and oropharyngeal cancer. Oral Oncol. 2009;45(4-5):309-16. https://doi.org/10.1016/j.oraloncology.2008.06.002

4. Tribius S, Bergelt C. Intensity-modulated radiotherapy versus conventional and 3D conformal radiotherapy in patients with head and neck cancer: is there a worthwhile quality of life gain? Cancer Treat Rev. 2011;37(7):511-9. https://doi.org/10.1016/j.ctrv.2011.01.004

5. Marur S, Forastiere AA. Head and Neck Squamous Cell Carcinoma: Update on Epidemiology, Diagnosis, and Treatment. Mayo Clin Proc. 2016;91(3):386-96. https://doi.org/10.1016/j.mayocp.2015.12.017

6. De Felice F, Polimeni A, Valentini V, Brugnoletti O, Cassoni A, Greco A, et al. Radiotherapy Controversies and Prospective in Head and Neck Cancer: A Literature-Based Critical Review. Neoplasia. 2018;20(3):227-32. https://doi.org/10.1016/j.neo.2018.01.002

7. Lazarus CL, Husaini H, Falciglia D, DeLacure M, Branski RC, Kraus D, et al. Effects of exercise on swallowing and tongue strength in patients with oral and oropharyngeal cancer treated with primary radiotherapy with or without chemotherapy. Int J Oral Maxillofac Surg. 2014;43(5):523-30. https://doi.org/10.1016/j.ijom.2013.10.023

8. Jham BC, da Silva Freire AR. Oral complications of radiotherapy in the head and neck. Braz J Otorhinolaryngol. 2006;72(5):704-8. https://doi.org/10.1016/S1808-8694(15)31029-6

9. Epstein JB, Thariat J, Bensadoun RJ, Barasch A, Murphy BA, Kolnick L, et al. Oral complications of cancer and cancer therapy: from cancer treatment to survivorship. CA Cancer J Clin. 2012;62(6):400-22. https://doi.org/10.3322/caac.21157

* De acordo com a Norma da FOUFU, baseado nas Normas de Vancouver. Abreviaturas dos periódicos com conformidade com Medline (Pubmed).

10. Buglione M, Cavagnini R, Di Rosario F, Sottocornola L, Maddalo M, Vassalli L, et al. Oral toxicity management in head and neck cancer patients treated with chemotherapy and radiation: Dental pathologies and osteoradionecrosis (Part 1) [1]literature review and consensus statement. Crit Rev Oncol Hematol. 2016;97:131-42. https://doi.org/10.1016/j.critrevonc.2015.08.010

11. Ray-Chaudhuri A, Shah K, Porter RJ. The oral management of patients who have received radiotherapy to the head and neck region. Br Dent J. 2013;214(8):387-93. https://doi.org/10.1038/sj.bdj.2013.380

12. Tolentino Ede S, Centurion BS, Ferreira LH, Souza AP, Damante JH, Rubira-Bullen IR. Oral adverse effects of head and neck radiotherapy: literature review and suggestion of a clinical oral care guideline for irradiated patients. J Appl Oral Sci. 2011;19(5):448-54.

13. Jawad H, Hodson NA, Nixon PJ. A review of dental treatment of head and neck cancer patients, before, during and after radiotherapy: part 1. Br Dent J. 2015;218(2):65-8. https://doi.org/10.1038/sj.bdj.2015.28

14. Hong CH, Napenas JJ, Hodgson BD, Stokman MA, Mathers-Stauffer V, Elting LS, et al. A systematic review of dental disease in patients undergoing cancer therapy. Support Care Cancer. 2010;18(8):1007-21. https://doi.org/10.1007/s00520-010-0873-2

15. Beech N, Robinson S, Porceddu S, Batstone M. Dental management of patients irradiated for head and neck cancer. Aust Dent J. 2014;59(1):20-8. https://doi.org/10.1111/adj.12134

16. Devi S, Singh N. Dental care during and after radiotherapy in head and neck cancer. Natl J Maxillofac Surg. 2014;5(2):117-25. https://doi.org/10.4103/0975-5950.154812

17. Liang X, Zhang JY, Cheng IK, Li JY. Effect of high energy X-ray irradiation on the nano-mechanical properties of human enamel and dentine. Braz Oral Res. 2016;30. https://doi.org/10.1590/1807-3107BOR-2016.vol30.0009

18. Thiagarajan G, Vizcarra B, Bodapudi V, Reed R, Seyedmahmoud R, Wang Y, et al. Stress analysis of irradiated human tooth enamel using finite element methods. Comput Methods Biomech Biomed Engin. 2017;20(14):1533-42. https://doi.org/10.1080/10255842.2017.1383401

* De acordo com a Norma da FOUFU, baseado nas Normas de Vancouver. Abreviaturas dos periódicos com conformidade com Medline (Pubmed).

19. Campi LB, Lopes FC, Soares LES, de Queiroz AM, de Oliveira HF, Saquy PC, et al. Effect of radiotherapy on the chemical composition of root dentin. Head Neck. 2019;41(1):162-9. https://doi.org/10.1002/hed.25493.

20. Queiroz AM, Bonilla CMC, Palma-Dibb RG, Oliveira HF, Nelson-Filho P, Silva LAB, et al. Radiotherapy Activates and Protease Inhibitors Inactivate Matrix Metalloproteinases in the Dentinoenamel Junction of Permanent Teeth. Caries Res. 2018;53(3):253-9. https://doi.org/10.1159/000492081

21. Seyedmahmoud R, Wang Y, Thiagarajan G, Gorski JP, Reed Edwards R, McGuire JD, et al. Oral cancer radiotherapy affects enamel microhardness and associated indentation pattern morphology. Clin Oral Investig. 2018;22(4):1795-803. https://doi.org/10.1007/s00784-017-2275-z

22. Goncalves LM, Palma-Dibb RG, Paula-Silva FW, Oliveira HF, Nelson-Filho P, Silva LA, et al. Radiation therapy alters microhardness and microstructure of enamel and dentin of permanent human teeth. J Dent. 2014;42(8):986-92. https://doi.org/10.1016/j.jdent.2014.05.011

23. Hoppenbrouwers PM, Driessens FC, Borggreven JM. The demineralization of human dental roots in the presence of fluoride. J Dent Res. 1987;66(8):1370-4. https://doi.org/10.1177/00220345870660081701

24. Nanci A. Ten Cate histologia oral: desenvolvimento, estrutura e função. Rio de Janeiro: Elsevier; 2013.

25. Markitziu A, Gedalia I, Rajstein J, Grajover R, Yarshanski O, Weshler Z. In vitro irradiation effects on hardness and solubility of human enamel and dentin pretreated with fluoride. Clin Prev Dent. 1986;8(4):4-7.

26. Franzel W, Gerlach R, Hein HJ, Schaller HG. Effect of tumor therapeutic irradiation on the mechanical properties of teeth tissue. Z Med Phys. 2006;16(2):148-54. https://doi.org/10.1078/0939-3889-00307

27. Grotz KA, Duschner H, Kutzner J, Thelen M, Wagner W. [New evidence for the etiology of so-called radiation caries. Proof for directed radiogenic damage od the enamel-dentin junction]. Strahlenther Onkol. 1997;173(12):668-76.

28. Andrews N, Griffiths C. Dental complications of head and neck radiotherapy: Part 1. Aust Dent J. 2001;46(2):88-94. https://doi.org/10.1111/j.1834-7819.2001.tb00562.x

29. Gaetti-Jardim E, Jr., Jardim ECG, Schweitzer CM, da Silva JCL, Oliveira MM, Masocatto DC, et al. Supragingival and subgingival microbiota from patients with poor oral hygiene submitted to radiotherapy for head and neck cancer treatment. Arch Oral Biol. 2018;90:45-52. https://doi.org/10.1016/j.archoralbio.2018.01.003

30. Hu JY, Chen XC, Li YQ, Smales RJ, Yip KH. Radiation-induced root surface caries restored with glass-ionomer cement placed in conventional and ART cavity preparations: results at two years. Aust Dent J. 2005;50(3):186-90. https://doi.org/10.1111/j.1834-7819.2005.tb00359.x

31. Naves LZ, Novais VR, Armstrong SR, Correr-Sobrinho L, Soares CJ. Effect of gamma radiation on bonding to human enamel and dentin. Support Care Cancer. 2012;20(11):2873-8. https://doi.org/10.1007/s00520-012-1414-y

32. Jansma J, Vissink A, Gravenmade EJ, Visch LL, Fidler V, Retief DH. In vivo study on the prevention of postradiation caries. Caries Res. 1989;23(3):172-8. https://doi.org/10.1159/000261173

* De acordo com a Norma da FOUFU, baseado nas Normas de Vancouver. Abreviaturas dos periódicos com conformidade com Medline (Pubmed).

RELEASE PARA A IMPRENSA

O câncer de cabeça e pescoço (cavidade oral, faringe e laringe) tem sido reconhecido como um dos cânceres com mais alta taxa de prevalência, sendo a sexta causa de morte por câncer em todo o mundo. Os fatores de risco mais comuns para o desenvolvimento de cânceres de cabeça e pescoço são uso de cigarro e o álcool e, no caso dos cânceres orofaríngeos, a infecção pelo papiloma vírus humano. O câncer de cabeça e pescoço é frequentemente tratado com radioterapia, que leva a morte das células cancerígenas. A localização e o tipo e a extensão do tumor que determinam como o tratamento é conduzido, se a radiação é usada isoladamente ou em combinação com outras modalidades de tratamento, bem como a dose de radiação necessária. Apesar de ser um tratamento altamente eficaz para o controle do tumor, a radioterapia provoca muitas reações adversas que afetam significativamente a qualidade de vida dos pacientes. Algumas dessas reações adversas ocorrem durante as sessões de radioterapia, entre elas estão dor ou desconforto na gengiva, dificuldade em comer e deglutir, infecções na boca por fungos. Outras consequências têm um caráter mais permanente e podem ou não ocorrer. Entre elas estão: limitação na abertura bucal, redução da saliva, sensação de boca seca, alterações nos dentes deixando eles mais susceptíveis a cárie e necrose no osso após extrações de dentes ou machucados de próteses. Por isso, é tão importante e necessário o acompanhamento clínico odontológico de pacientes submetidos à radioterapia na região de cabeça e pescoço antes, durante e após o tratamento. A cárie em paciente após radioterapia é chamada de cárie relacionada à radiação e ela é resultante das alterações que ocorrem nos dentes após a radioterapia, da diminuição na produção de saliva (uma vez que ela tem papel fundamental na remineralização do dente), do consumo de alimentos ricos em carboidratos e da falta de escovação dos dentes e do uso de fio dental. Ela se difere da cárie convencional por se desenvolver rapidamente e ser altamente destrutiva, levando a perda dos dentes. Este tipo de cárie representa um desafio para o dentista, que precisa entender os efeitos da radioterapia no paciente, para assim poder atender melhor essas pessoas. O melhor seria um acompanhamento de perto desses pacientes, para evitar que a cárie apareça. Para isso, o paciente precisa ir no consultório odontológico regularmente de 3 em 3 meses, ou dependendo da necessidade, não podendo ser muito espaçado. Nessas visitas, o cirurgião dentista deve realizar exame de toda a cavidade bucal, uma limpeza nos dentes, aplicação de flúor e estar atento a qualquer alteração da normalidade. Quanto ao exame dos dentes, sempre procurar por indícios de

início de cárie. É sempre melhor a prevenção destas, do que o tratamento restaurador, já que muitas vezes as restaurações realizadas se soltam, pois, o material não adere de forma ideal ao dente. Assim, algumas medidas são recomendadas: higiene bucal rigorosa; auto-aplicação diária tópica de gel de fluoreto de sódio neutro a 1% com o auxílio da escova de dente ou cotonete ou então bochechos com solução fluoretada, sob supervisão do profissional; limitação de alimentos cariogênicos. Neste contexto, mais estudos científicos devem ser realizados na tentativa de elucidar porque esta cárie é diferente da cárie convencional, qual é o melhor método para a sua prevenção e seu tratamento.